

PERMANENT MAGNET ALTERNATOR
CONTROL BY MEANS OF
MAGNETIC SATURATION

WILLIAM L. AITKENHEAD
AND
FRANK C. ANDERSON

1953

Library
U. S. Naval Postgraduate School
Monterey, California



PERMANENT MAGNET ALTERNATOR CONTROL BY MEANS OF MAGNETIC
SATURATION

by

William L. Aitkenhead, Lieutenant, U. S. Coast Guard
B. S., U. S. Coast Guard Academy, 1946

Frank C. Anderson, Lieutenant, U. S. Coast Guard
B. S., U. S. Coast Guard Academy, 1945

Submitted in Partial Fulfillment
of the Requirements for the
Degree of Naval Engineer
from the
Massachusetts Institute of Technology
1953

PERMANENT MAGNET ALTERNATOR CONTROL BY MEANS OF MAGNETIC SATURATION

by

William L. Aitkenhead, Lieutenant, U. S. Coast Guard
Frank C. Anderson, Lieutenant, U. S. Coast Guard

Submitted to the Department of Naval Architecture and Marine Engineering on 25 May, 1953 in partial fulfillment of the requirements for the degree of Naval Engineer.

ABSTRACT

The permanent magnet alternator as a source of power has been impractical until comparatively recent times. The advent of powerful new magnetic materials similar to the "Alnico" types has made such machines more practical, and has caused renewed interest in their development and use.

One serious limitation of a permanent magnet alternator is the lack of control over the output voltage. If voltage control by means of a simple electrical means could be developed, the usefulness of the machine would be vastly increased. The purpose of the present investigation is twofold: (1) to analyze the magnetic circuit in a permanent magnet alternator when the stator becomes saturated from an independent source of magnetomotive force, and (2) to devise a means of voltage control for this type of machine.

If the stator of an alternator is visualized as a toroid and a continuous winding of many turns is wound thereon, it is possible to induce within the toroid, a continuous unidirectional flux by means of a direct current in the winding. When a permanent magnet rotor is inserted in the stator, it also tends to send flux lines through the iron of the stator. However, in portions of the stator the flux from these two separate sources tend to flow in the same direction and in portions they tend to oppose. Analysis of the magnetic circuit under these conditions shows that the air gap flux is reduced because of the overall increase in the reluctance of the flux paths facing the permanent magnet. At constant speed, the voltage is proportional to the flux in the air gap and hence if the air gap flux can be controlled the output voltage can be controlled by toroidal saturation. Furthermore the analysis and experimental verification show that the percent of voltage control by means of magnetic saturation may be increased by building into the machine additional leakage paths for the flux, although the magnitude of the voltage output is thereby reduced. The saturation of the stator appears to have no serious effects upon the waveform of a properly designed machine, or on machine heating.

William H. Rouse, Jr., U.S. Coast Guard
Frank J. Anderson, U.S. Coast Guard

Submitted to the Department of Naval Architecture and Marine
Engineering, Massachusetts Institute of Technology, in partial fulfillment of the
requirements for a degree of Master of Science in Engineering

ABSTRACT

The permanent magnet motor as a source of power has been investigated and compared with the conventional motor. The advantages of power in the permanent magnet motor are similar to the "Aircraft" type and such machines were produced, and has caused renewed interest in their development and use.

One serious limitation of a permanent magnet motor is the lack of control over the output voltage. If voltage control by means of a simple electrical means could be developed, the usefulness of the machine would be greatly increased. The purpose of the present investigation is to develop a simple electrical circuit in a permanent magnet motor which will cause the motor to operate from an independent source of magnetomotive force, and (2) to devise a means of voltage control for this type of machine.

It is known that a permanent magnet motor is a motor and a generator. In many forms it is found in the form of a motor with a permanent magnet, a continuous unit. It is possible to have a motor with a permanent magnet and a generator. The purpose of the present investigation is to develop a simple electrical circuit in a permanent magnet motor which will cause the motor to operate from an independent source of magnetomotive force, and (2) to devise a means of voltage control for this type of machine.

Analysis of the magnetic circuit of the permanent magnet motor shows that the air gap flux is proportional to the overall increase in the magnetomotive force. The voltage is proportional to the flux in the air gap and hence the air gap flux can be controlled by controlling the magnetomotive force. The analysis and experimental verification show that the voltage can be controlled by building into the machine additional magnetic paths for the flux, although the magnitude of the voltage which is thereby reduced. The saturation of the magnetic paths will have no serious effect upon the waveform of the voltage, as in the case of the generator.

The power expended to achieve voltage control by this method is nominal within limits, although by no means compares with the control afforded by the wound-rotor type installation. The machine tested was found to maintain constant voltage for a variable load of from 190 to 21 watts (or variation of 89%) with an expenditure of direct current power in the control winding of 23.7 watts, or 11.9% of the initial ac output power. Furthermore, the power expended for control in this device is greatest when the load power is least, making an automatic voltage regulation system using a feedback loop practical.

Two practical methods of designing more efficient control systems based on the principle of toroidal saturation are (1) develop permanent magnet materials with a higher incremental permeability (the slope of the "recovery line"), and (2) design the alternator with the maximum leakage possible consistent with the magnitude of the voltage output required.

The theoretical analysis of the magnetic circuitry is supported by the experimental results to within the accuracy of the various assumptions.

Thesis Supervisor: Professor D. C. White
Title: Assistant Professor of Electrical
 Engineering

The power expended to achieve voltage control of this motor is constant within limits, although by no means compares with the small amount afforded by the wound-rotor type induction. The winding tested was found to maintain constant voltage for a variable load of from 150 to 1000 (or variation of 80%) with an expenditure of electric energy of 10 to 15 watts, or 1/10 to 1/20 of the power in the control winding of 75 watts. The power expended in the output motor, however, was expended in the control in this device is greatest when the load power is least, making an automatic voltage regulation system using a feedback loop practical.

Two practical methods of designing more efficient control systems based on the principle of toroidal induction are (1) develop permanent magnet materials with a higher inductance per ampere (the slope of the "recovery line") and (2) design the circuit with the maximum leakage possible consistent with the magnitude of the voltage output required.

The theoretical analysis of the magnetic circuitry is supported by the experimental results to within the accuracy of the various measurements.

This Supervisor: Professor D. G. White
 Title: Assistant Professor of Electrical Engineering

Cambridge, Massachusetts
May 25, 1953

Professor E. B. Millard
Secretary of the Faculty
Massachusetts Institute of Technology
Cambridge, Massachusetts

Dear Sir:

In accordance with the requirements for the Degree of
Naval Engineer, we submit herewith a thesis entitled
"Permanent Magnet Alternator Control by means of
Magnetic Saturation".

ACKNOWLEDGMENTS

The authors wish to express their appreciation to Professor David C. White for his advice and encouragement; and to Professor Charles Kingsley, Jr. for his helpful suggestions on magnetic circuitry.

ACKNOWLEDGEMENT

The author wishes to express his appreciation to
Professor David C. White for his advice and encouragement;
and to Professor Charles K. Hays for his helpful
suggestions on matters of detail.

TABLE OF CONTENTS

	Page
I. INTRODUCTION	1
II. PROCEDURE	5
III. RESULTS	29
IV. DISCUSSION OF RESULTS	31
V. CONCLUSIONS AND RECOMMENDATIONS	40
VI. APPENDIX	
A. DETAILS OF PROCEDURE	42
B. DETAILS OF CALCULATED DATA	57
C. SUMMARY OF DATA AND CALCULATIONS	65
D. EXPERIMENTAL DATA	78
E. BIBLIOGRAPHY	104

TABLE OF CONTENTS

Page

I.	INTRODUCTION	1
II.	PROCEDURE	2
III.	RESULTS	29
IV.	DISCUSSION OF RESULTS	31
V.	CONCLUSIONS AND RECOMMENDATIONS	40
VI.	APPENDIX	
A.	DETAILS OF PROCEDURE	42
B.	DETAILS OF CALCULATED DATA	51
C.	SUMMARY OF DATA AND CALCULATIONS	62
D.	EXPERIMENTAL DATA	78
E.	BIBLIOGRAPHY	101

I. INTRODUCTION

A permanent magnet alternator is a synchronous generator which has a permanent magnet for its source of magnetomotive force instead of the wound rotor electromagnet used in the conventional alternators. As recently as 1940, permanent magnet generators were impractical because suitable magnetic materials were not available. With the advent of magnets which can better withstand the effects of temperature, demagnetizing fields, and vibration, the permanent magnet alternator is now being used in applications where a compact source of small amounts of power is required.

Permanent magnet alternators have an inherent disadvantage compared to machines excited by direct-current. Because the flux from the permanent magnet is an intrinsic quantity, there is no direct way to maintain a constant terminal voltage under varying conditions of loading and speed.

Although the characteristics of the permanent magnet cannot be altered, it is possible to regulate the output voltage of a permanent magnet alternator by establishing control over the circuit traversed by the lines of magnetic flux from the permanent magnet.

The magnetic circuit between each pair of poles of a permanent magnet rotor consists of two air gaps and a path in the iron of the stator, all in series. Control of this magnetic circuit can be obtained by either controlling the length of the air gaps or the reluctance of the path in the stator iron.

1. INTRODUCTION

A permanent magnet alternator is a synchronous generator which has a permanent magnet for its rotor. It is used in the conventional alternator. As recently as 1940, permanent magnet generators were considered because suitable magnetic materials were not available. The advent of magnets which can be used without the effects of temperature, demagnetizing fields, and vibration, the permanent magnet alternator is now being used in applications where a compact source of small amounts of power is required. Permanent magnet alternators have an inherent disadvantage compared to machines excited by direct-current. Because the flux from the permanent magnet is an intrinsic quantity, there is no direct way to maintain a constant terminal voltage under varying conditions of loading and speed. Although the characteristics of the permanent magnet cannot be altered, it is possible to regulate the output voltage of a permanent magnet alternator by establishing control over the circuit traversed by the lines of magnetic flux from the permanent magnet. The magnetic circuit between each pair of poles of a permanent magnet rotor consists of two air gaps and a path in the form of a closed circuit. Control of this magnetic circuit is obtained by either controlling the length of the air gap or the reluctance of the path in the air gap.

In a rotary device such as an alternator, the mechanical system necessary for adjusting the air gap length would be complex, and, in the case of a permanent magnet alternator, would nullify its chief advantage of simplicity.

The alternative method, which consists of controlling the reluctance of the stator iron, is more feasible because such control can be obtained by purely electrical means. If a coil of toroidal form were wound around the hollow cylindrical form of the stator, and a direct current were introduced in this coil, the stator iron would readily be saturated. The effect of saturating the stator iron on the reluctance of the magnetic circuit is not immediately apparent because the flux from the rotor travels in both clockwise and counter-clockwise directions in the stator between adjacent pole faces, whereas the saturation caused by the toroidal winding on the stator is due to flux traveling in but one direction in the stator.

This investigation consists of analysis and experimental verification of the results obtained by toroidal saturation of the stator iron of a permanent magnet alternator. The method of analysis and general results are applicable to all permanent magnet machines, but in order to show to what extent the output voltage can be controlled at various loads and speeds, experimental data for the particular alternator tested was used.

The alternator upon which the analysis and experimental verification were performed is shown in Fig. I. This

In a primary design study as of this date, the following
 system necessary to adjusting the gap length, which is
 complex, and, in the case of a permanent magnet alternator
 would nullify its stated advantages of simplicity.
 The alternative method, which consists of controlling
 the reluctance of the rotor, is more feasible as there
 such control can be obtained in purely electrical means. It
 is felt that considerable work would be required to follow
 cylindrical form of the stator, and a direct current wire
 introduced in this wall, the stator iron would readily be
 saturated. The effect of saturating the stator iron on the
 reluctance of the magnetic circuit is not immediately apparent
 because the flux from the rotor travels in both clockwise and
 counter-clockwise directions in the stator between adjacent
 pole faces, whereas the saturation caused by the cylindrical
 winding on the stator is due to flux traveling in but one
 direction in the stator.
 This investigation consists of analysis and experimental
 verification of the results obtained by cylindrical saturation
 of the stator iron of a permanent magnet alternator. The
 method of analysis and general results are applicable to
 all permanent magnet machines, but it is noted that where
 extent the output voltage can be controlled at various loads
 and speeds, experimental data for the particular alternator
 tested was used.
 The alternator upon which the analysis and experimental
 verification were performed is shown in Fig. 1. This

FIGURE 1
ALTERNATOR ASSEMBLY



alternator is a four-pole, three-phase, Y-connected machine. Its normal speed is 12,000 RPM corresponding to a frequency of 400 cycles per second. The permanent magnet rotor is of ALNICO VI. Two stators, one of USS Electrical Grade Steel, and one of HIPERNIK, were wound and tested. The stators had shallow slots milled in the outer periphery, one slot opposite each of the eighteen inner slots to admit the toroidal winding, allowing clearance for the stator to be inserted in the housing. The toroidal winding lies in the bottom of the main slots, and the generator windings are placed over the toroidal windings.

Experimental data was obtained from the machine under various conditions of saturation, loading, and speed in order to determine the effects of toroidal saturation upon the output voltage.

alternator is a four-pole, three-phase, Y-connected machine. Its normal speed is 18,000 RPM corresponding to a frequency of 400 cycles per second. The permanent magnet rotor is of ALNICO VI. Two stators, one of USS Electrical Grade Steel,

and one of HIPERNIK, were wound and tested. The stator had shallow slots milled in the outer periphery, one slot

opposite each of the eighteen inner slots to admit the toroidal winding, allowing clearance for the stator to be inserted in the housing. The toroidal winding lies in the bottom of the main slots, and the generator windings are placed over the toroidal windings.

Experimental data was obtained from the machine under

various conditions of saturation, loading, and speed in order to determine the effects of toroidal saturation upon the output voltage.

II. PROCEDURE

The procedure followed has been divided into two separate, but mutually supporting techniques. The first consists of an analytical solution derived from a consideration of magnetic circuit theory as applied to the peculiar magnetic circuit involved. The second procedure consists of experimental determinations of the behavior of a permanent magnet alternator when subjected to the specified conditions of magnetic saturation.

A. Analytical Procedure

The procedure used to solve the problem of the effect of saturation in the stator iron on the air-gap flux of the permanent magnet in a permanent magnet alternator is graphical in nature. The solution consists of solving two simultaneous equations in which the graphical representation of the flux versus magnetomotive characteristic of the permanent magnet provides one equation, and the flux versus mmf characteristic of the air gaps and stator iron in the magnetic circuit seen by the permanent magnet provides a second equation. The magnetizing force and flux of the permanent magnet must equal the mmf drop and the flux in the external circuit including leakage flux. For the following analysis, hysteresis is neglected so that flux versus mmf characteristics may be represented by single lines.

Determination of Rotor Characteristic

The characteristics of permanent magnets are represented by a demagnetization curve which is the second

II. PROCEDURE

The procedure followed has been divided into two separate, but mutually supporting techniques. The first consists of an analytical solution derived from a consideration of magnetic circuit theory as applied to the peculiar magnetic circuit involved. The second procedure consists of experimental determination of the behavior of a permanent magnet alternator when subjected to the specified conditions of magnetic saturation.

A. Analytical Procedure

The procedure used to solve the problem of the effect of saturation in the stator iron on the air-gap flux of the permanent magnet in a permanent magnet alternator is graphical in nature. The solution consists of solving two simultaneous equations in which the graphical representation of the flux versus magnetomotive characteristic of the permanent magnet provides one equation, and the flux versus mmf characteristic of the air frame and stator iron in the magnetic circuit seen by the permanent magnet provides a second equation. The magnetizing force and flux of the permanent magnet must equal the mmf drop and the flux in the external circuit including leakage flux. For the following analysis, intervals is defined so that flux versus mmf characteristics may be represented by straight lines.

Determination of Motor Characteristics

The characteristics of permanent magnets are represented by a demagnetization curve which is the second

quadrant of the material's hysteresis loop between B_r , the retentivity, and H_c , the coercive force as shown in Fig. II. The point B_r represents the flux density of the magnet when it is magnetically short-circuited; when the magnet is subjected to a demagnetizing force such as an air-gap line Oa , the point representing the operating condition moves along the demagnetization curve from B_r to point a , and B_a is the flux density in the air gap. If the air gap is increased in length until the air-gap line becomes Ob , the operating point will move down the ^{de}magnetization curve from a to b , and the resulting flux density will then be B_b . If the gap is decreased, the operating point will not return along the demagnetization curve, but will travel along a minor hysteresis loop such as bd . For example, if the air-gap line is again Oa , the operating point will become point d , and the flux density becomes B_d . [1]

In order to determine the characteristics of the permanent magnet rotor, it is necessary to determine the slope of the minor hysteresis loop, otherwise known as the "recovery line", and the position on the demagnetization curve where the recovery line originates. The origin of the recovery line does not necessarily represent the point on the demagnetization curve where the magnetic open-circuit air-gap line intersects the demagnetization curve because the magnet may have been subjected to a demagnetization force in excess of the open-circuit air-gap condition. This would put the open-circuit operating point on the

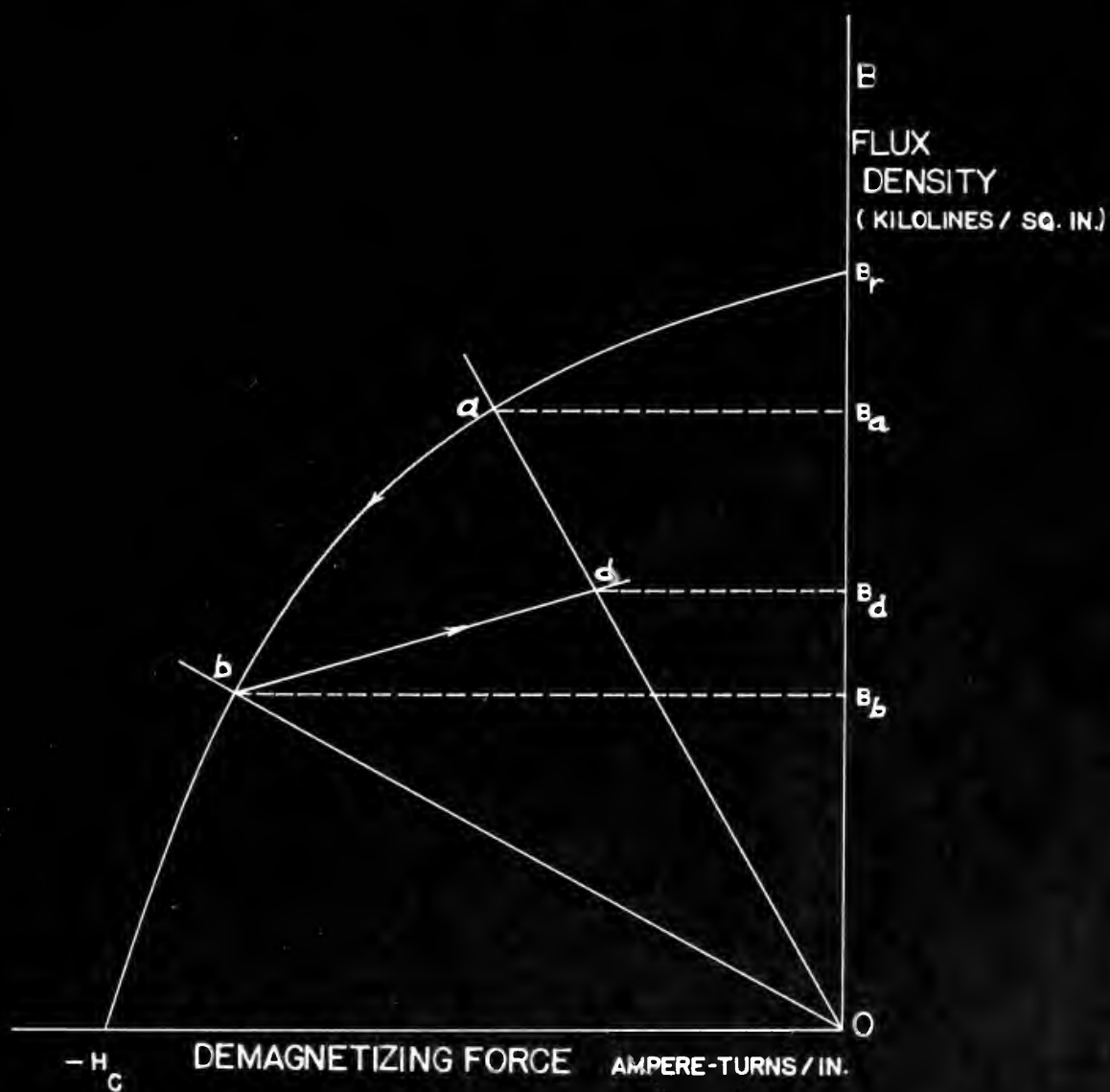
gradient of the material's hysteretic loop between H_1 and H_2 . The point B_1 represents the flux density of the magnet when it is magnetically short-circuited when the magnet is subjected to a demagnetizing force such as an air-gap line OB_1 , the point representing the operating condition moves along the demagnetization curve from B_1 to point a , and H_2 is the flux density in the air gap. If the air gap is increased in length until the air-gap line becomes OB_2 , the operating point will move down the demagnetization curve from a to b , and the resulting flux density will then be H_2 . If the gap is decreased, the operating point will not return along the demagnetization curve, but will travel along a minor hysteretic loop such as cd . For example, if the air-gap line is again OB_1 , the operating point will become point d .

and the flux density becomes H_1 . [1]

In order to determine the characteristics of the permanent magnet motor, it is necessary to determine the slope of the minor hysteretic loop, otherwise known as the "recovery line", and the position on the demagnetization curve where the recovery line originates. The origin of the recovery line does not necessarily represent the point on the demagnetization curve where the magnetic open-circuit air-gap line intersects the demagnetization curve because the magnet may have been subjected to a demagnetization force in excess of the open-circuit air-gap condition. This would put the open-circuit operating point on the

FIGURE II

PERMANENT MAGNET BEHAVIOR



intersection of the open-circuit air-gap line and a recovery line whose origin is closer to H_c on the demagnetization curve (Fig. II). A point on the recovery line of the permanent magnet rotor can be determined by measuring the open-circuit flux per pole with a fluxmeter and plotting this value of flux on the open-circuit air-gap line.

Methods have been devised [2] to determine the open-circuit air-gap line for magnets which do not have a well defined air gap. Scott [3] found that a definite relation exists between the ratio of length-to-diameter of round bar magnets and the flux in the air between poles. This relationship is expressed by a curve of B/H versus l/d (Fig. III) where B/H is the slope of the open-circuit air-gap line, also called the "permeance coefficient", and l/d is the length-to-diameter ratio of the bar magnet. The relationship holds within a fair degree of accuracy to magnets other than round bar magnets provided that, if the magnet is curved, the poles are not too close together. To apply Scott's bar magnet theory to the multipolar shape of a permanent magnet rotor, an equivalent bar magnet is assumed by estimating the length of the mean flux path between adjacent pole faces to provide the dimension, l (Fig. IV); an equivalent diameter is established by assuming the pole face of the magnet has the diameter of a circle of the same area as the pole face [3] :

$$d = \sqrt{\frac{4A}{\pi}} \quad (1)$$

investigation of the open circuit line and a

recovery line whose origin is R_0 on the

determination curve (Fig. III) is determined.

line of the permanent magnet curve can be determined.

measuring the open circuit line for a given

and plotting this value of R_0 on a graph of R_0 vs.

gap line.

Methods have been devised [2] for determining the open

circuit air-gap line for magnets with a gap g will

defined air gap. Scott [3] found that a definite relation

exists between the ratio of length-to-diameter of round

bar magnets and the flux in the air between poles. This

relationship is expressed by a curve of R_0 vs. g (Fig.

(Fig. III) where R_0 is the slope of the open-circuit air

gap line, also called the "performance coefficient", and g is

is the length-to-diameter ratio of the bar magnet. The

relationship holds within a fair degree of accuracy for

magnets other than round bar magnets provided that if the

magnet is curved, the poles are not too close together.

To apply Scott's bar magnet theory to the multipole design

of a permanent magnet rotor, an equivalent bar magnet is

assumed by estimating the length of the magnet from the

between adjacent pole faces to provide the dimension,

l (Fig. IV); an equivalent diameter is calculated by

measuring the pole face of the magnet and the diameter of

a circle of the same area as the pole face [4].

$$D = \sqrt{\frac{4A}{\pi}}$$

FIGURE III

PERMEANCE COEFFICIENTS
OF
EQUIVALENT BAR MAGNETS

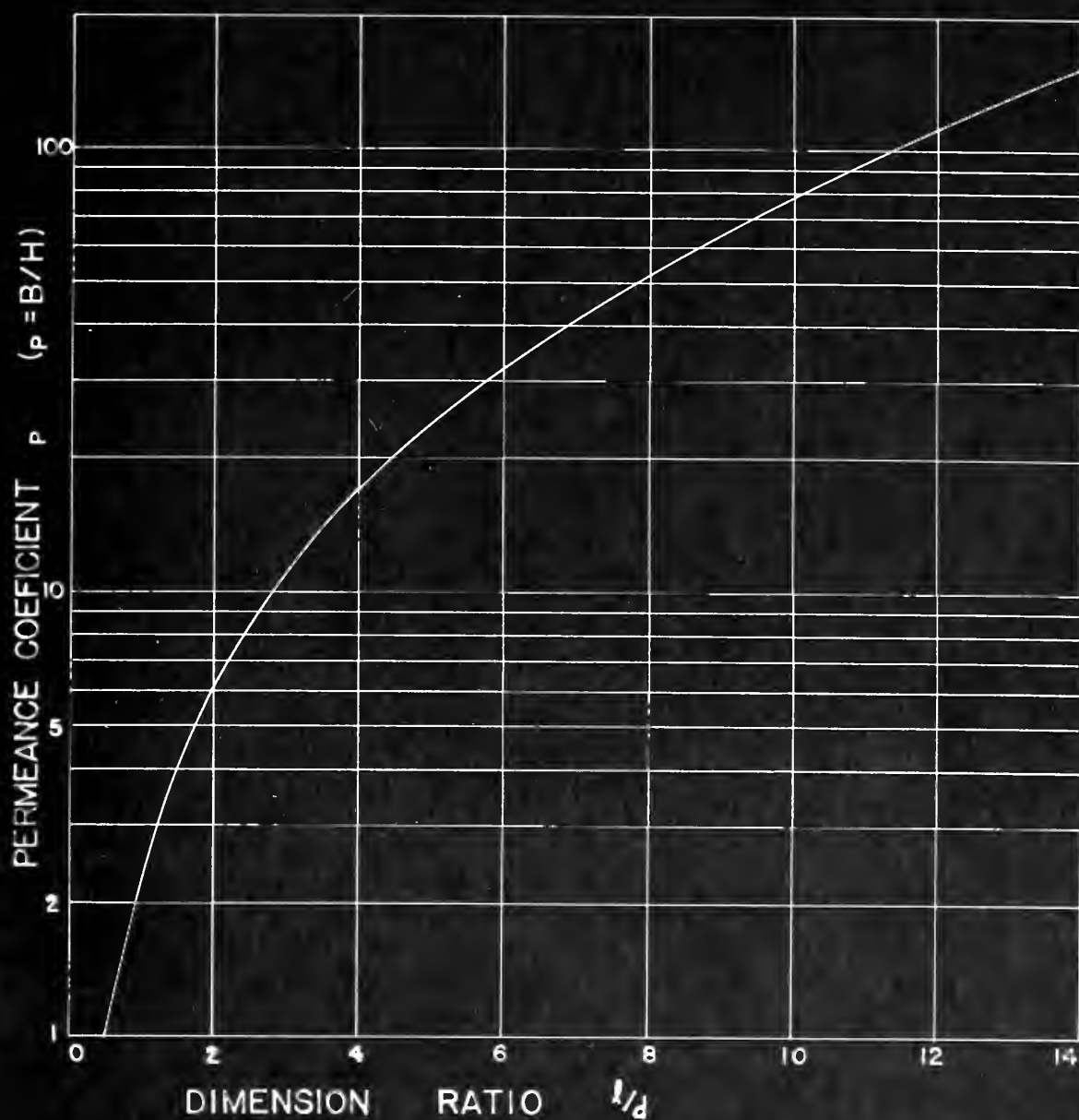


FIGURE IV

FLUX PATHS IN ROTOR



Having assumed an equivalent l/d , enter the curve of Fig. III and determine the slope of the open-circuit air-gap line, B/H . This value of B/H in conjunction with the measured flux of the magnet establishes the open-circuit operating point of the permanent magnet.

The slope of the recovery line, called the "incremental permeability", can be obtained from manufacturer's literature [4], where the slope of the recovery line is given in the form of a graph of incremental permeability versus the flux density at point of reversal for various magnetic materials. Knowing that the recovery line must pass through the operating point on the open-circuit air-gap line, the slope of the recovery line is determined.

An estimate of the flux versus mmf characteristic for the permanent magnet rotor has now been established. When the rotor is inserted in the stator, the operating point of the magnet will lie on this recovery line. Fig. V shows this flux versus mmf characteristic.

Determination of Stator Characteristic

To visualize the approach used to determine the stator characteristic, consider the rotor inserted in the stator. The lines of flux from a magnet pole will cross the air gap and split into two parallel paths in the stator iron and close on themselves through adjacent pole faces. Leakage flux from the permanent magnet will also exist, but this flux does not appear in the stator magnetic circuit and can be considered separately.

Having assumed an equivalent $\frac{1}{2}$, where the curve of Fig. 1.1 and determine the slope of the open-circuit air-gap line, B/H . This value of B/H is conjunction with the measured flux of the magnet establishes the open-circuit operating point of the permanent magnet.

The slope of the recovery line, called the "incremental

permeability", can be obtained from manufacturer's literature [4], where the slope of the recovery line is given in the form of a graph of incremental permeability versus the flux density at point of reversal for various magnetic materials. Knowing that the recovery line must pass through the operating point on the open-circuit air-gap line, the slope of the recovery line is determined.

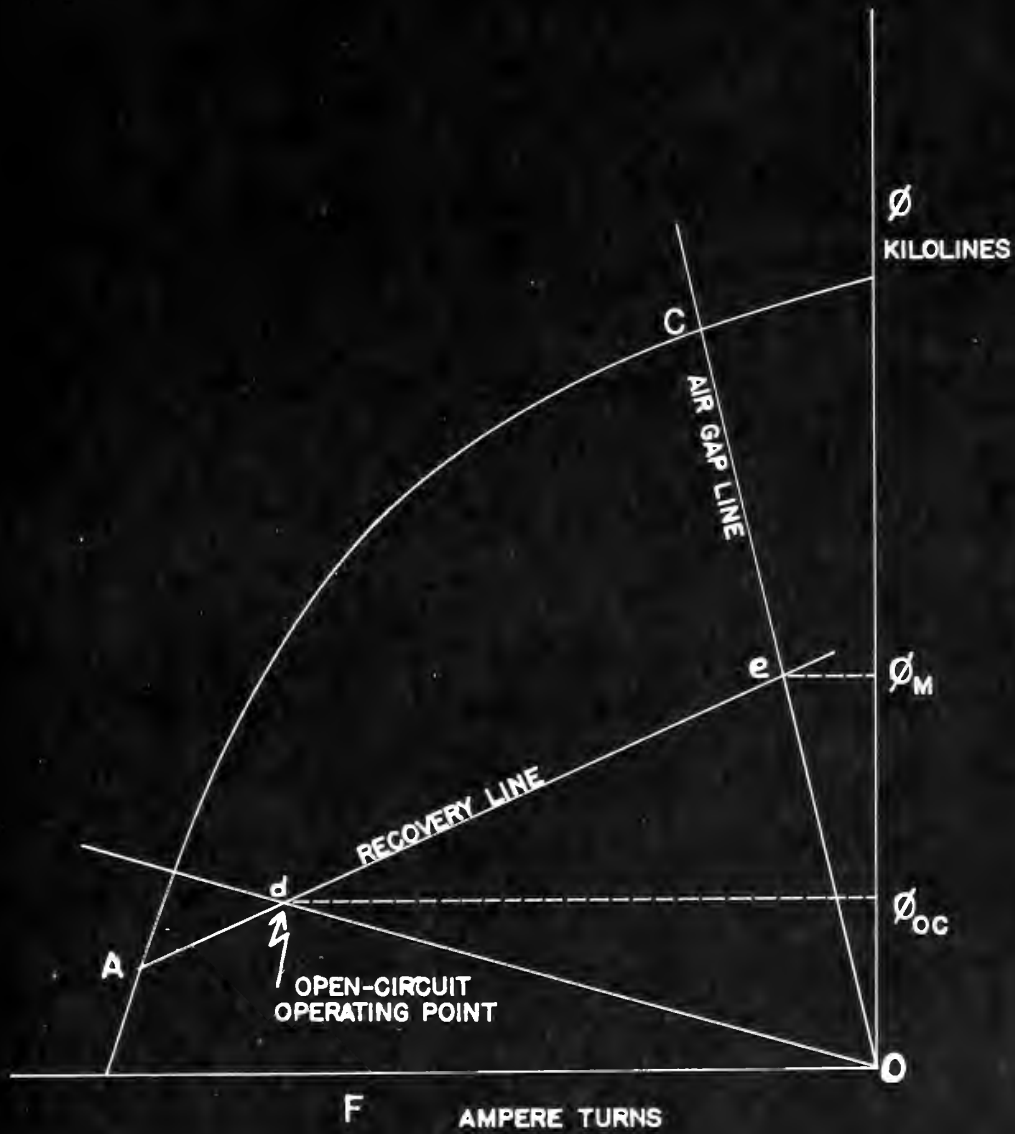
An estimate of the flux versus magnet characteristic for the permanent magnet rotor has now been established. When the rotor is inserted in the stator, the operating point of the magnet will lie on this recovery line. Fig. 5 shows this flux versus magnet characteristic.

Determination of Stator Characteristic

To visualize the approach used to determine the stator characteristic, consider the rotor inserted in the stator. The lines of flux from a magnet pole will cross the air gap and split into two parallel paths in the stator iron and close on themselves through adjacent pole faces. Leakage flux from the permanent magnet will also exist, but this flux does not appear in the stator magnetic circuit and can be considered separately.

FIGURE V

DETERMINATION OF RECOVERY LINE



Using an electric circuit analogy in which reluctance is analogous to resistance, flux to current, and magnetomotive force to voltage, the magnetic circuit is represented in Fig. VI. The effect of $R_{\text{(air gap)}}$ can be represented by an air-gap line in the stator characteristic. The effect of R_1 and R_2 , the reluctances of the stator iron paths which are to be saturated by the toroidal winding, can be analyzed separately and added graphically to the air-gap line to obtain the overall magnetic characteristic of the magnetic circuit external to the rotor. Temporarily neglecting the air gap and leakage paths, we now have the analogous circuit shown in Fig. VII. It is to be emphasized that electric circuit analogies are for illustrative purposes only, and that the equations resulting therefrom must always require a graphical solution because of the non-linear nature of reluctance.

Now consider the stator, without the permanent magnet rotor, as a toroid with a continuous winding around it as shown by Fig. VIII. A direct current in the toroidal winding will cause a magnetomotive force between points a and b

$$F_c = F_{ab} = \oint_l R_{ab} \quad (2)$$

where R is the reluctance and F_c is the ampere turns in half the toroid. The electric circuit analogy may be represented by Fig. IX.

If the circuit of Fig. IX were cut in half at line

Using an electric circuit analogy in which reluctance is analogous to resistance, flux to current, and magnetomotive force to voltage, the magnetic circuit is represented in Fig. VI. The effect of B (air gap) is represented by an air-gap line in the stator characteristic. The effect of F_1 and F_2 , the reluctances of the stator iron paths which are to be saturated by the toroidal winding, can be analyzed separately and added graphically to the air-gap line to obtain the overall magnetic characteristic of the magnetic circuit external to the rotor. Temporarily neglecting the air gap and leakage paths, we now have the analogous circuit shown in Fig. VII. It is to be emphasized that electric circuit analogies are for illustrative purposes only, and that the equations resulting therefrom must always require a graphical solution because of the non-linear nature of reluctance.

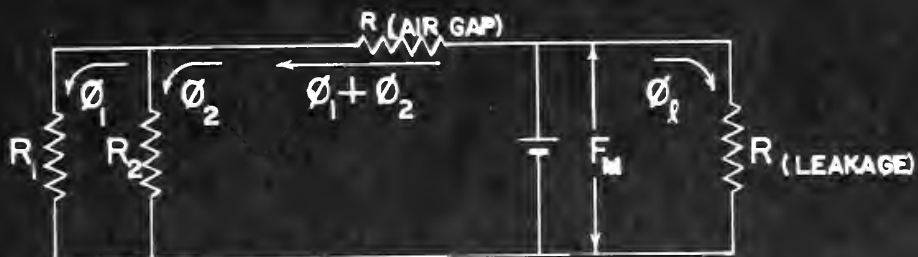
Now consider the stator, without the permanent magnet rotor, as a toroid with a continuous winding around it as shown by Fig. VIII. A direct current in the toroidal winding will cause a magnetomotive force between points a and b

$$(9) \quad F_c = F_{ab} = \frac{B_c^2}{2\mu_0} \cdot \frac{V_c}{B_c}$$

where F is the reluctance and V is the ampere turns in half the toroid. The electric circuit analogy may be represented by Fig. IX.

If the circuit of Fig. IX were cut in half at line

FIGURE VI
ELECTRIC CIRCUIT ANALOGY



NOTE: R_1 AND R_2 REPRESENT THE RELUCTANCE IN EACH PATH OF THE STATOR IRON

FIGURE VII
ELECTRIC CIRCUIT ANALOGY OF STATOR
AIR GAP AND LEAKAGE NEGLECTED

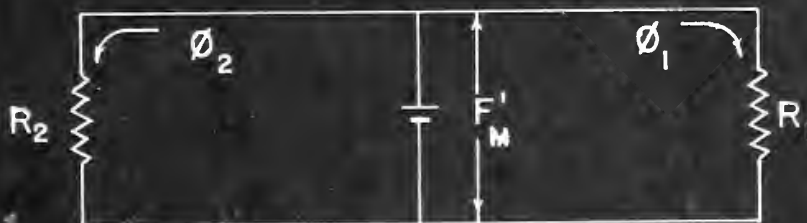


FIGURE VIII

TOROIDAL WINDING

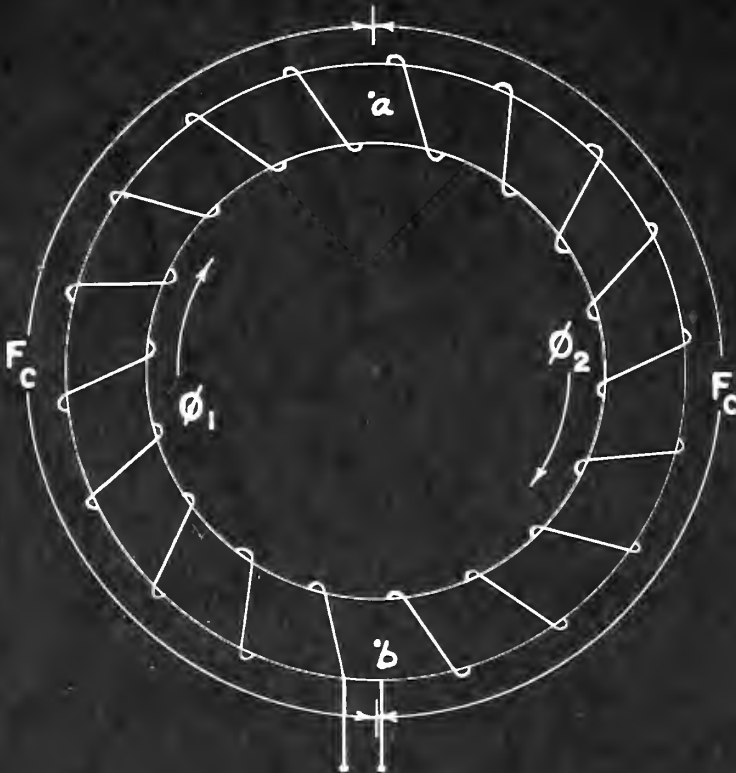
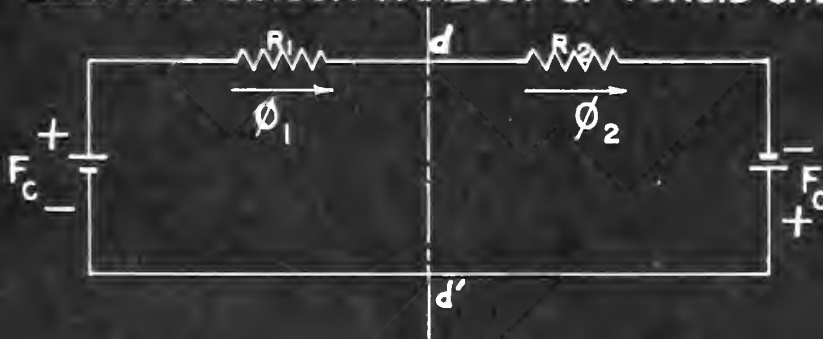


FIGURE IX

ELECTRIC CIRCUIT ANALOGY OF TOROID ONLY



NOTE:

$$F_c = \phi R$$

d-d' by a magnetic short-circuit, the flux in each side would be unchanged:

Half of circuit shorted:

$$(1) \quad F_c = \phi_1 R ; \phi_1 = F_c / R ; \text{ shown in Fig. X} \quad (3)$$

Both halves of circuit in series:

$$(2) \quad 2F_c = \phi_1 (2R) ; \phi_1 = F_c / R \text{ as before.} \quad (4)$$

The above case is not to be confused with the case of the curve of ϕ versus H , where doubling H (amperes turns per inch) would give, in effect, $2F$ acting to produce ϕ .

Having established the circuit behavior with no magnet inserted, we can now proceed to find the effect of adding the permanent magnet rotor. For simplicity of illustration, a two-pole magnet is used, but the same conclusions will be valid for multipolar rotors. The effects of the air gap and leakage are still temporarily neglected.

The resulting electric circuit analogy is illustrated by Fig. XI.

The following equations apply:

In left half of the circuit A:

$$(F_c - F_m') = R_a (\phi_1 - \phi_{m1}') = R_a \phi_A \quad (5)$$

In right half of the circuit B:

$$(F_c + F_m') = R_b (\phi_1 + \phi_{m2}') = R_b \phi_B \quad (6)$$

and

$$\phi_m' = (\phi_{m1}' + \phi_{m2}')$$

by a magnetic flux density, the flux in each side

would be unchanged:

Half of circuit shorted:

$$(1) \quad F_c = F_1 = F_2 = F_0 \sqrt{2} \quad \text{as shown in Fig. 7}$$

Both halves of circuit in series:

$$(2) \quad F_c = F_1(2F) ; F_2 = F_0 \sqrt{2} \quad \text{as before}$$

The above case is not to be confused with the case of the

curve of ϕ versus H , where doubling H (amperes turns per

inch) would give, in effect, $2F$ acting to produce ϕ .

Having established the circuit behavior with no magnet

inserted, we can now proceed to find the effect of adding

the permanent magnet rotor. For simplicity of illustration,

a two-pole magnet is used, but the same conclusions will be

valid for multipole rotors. The effects of the air gap

and leakage are still temporarily neglected.

The resulting electric circuit analogy is illustrated

by Fig. XI.

The following equations apply:

In left half of the circuit A:

$$(3) \quad (F_c - F_m) = F_1(Q_1) = F_2(Q_2) = F_0 \sqrt{2}$$

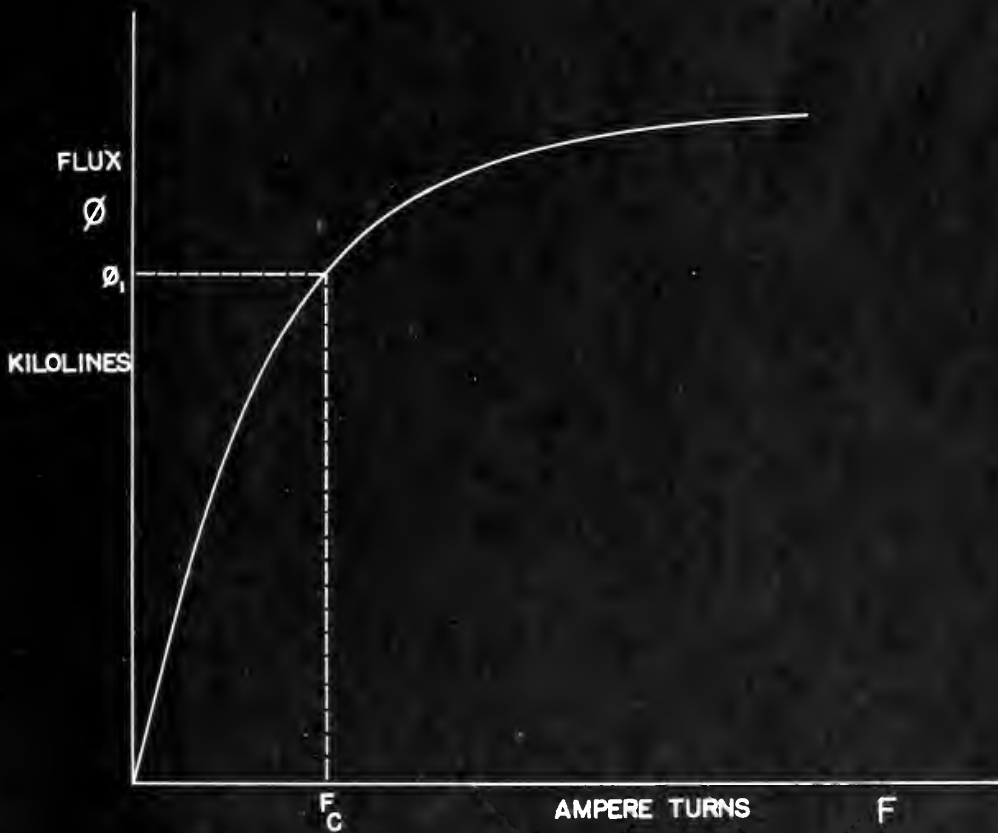
In right half of the circuit B:

$$(4) \quad (F_c + F_m) = F_1(Q_1) + F_2(Q_2) = F_0 \sqrt{2}$$

$$F_m = (Q_1 + Q_2)$$

and

FIGURE X
DC MAGNETIZATION CURVE —
IN TERMS OF FLUX AND MAGNETOMOTIVE FORCE



It is also obvious that $\phi_B - \phi_A = \phi_m'$ (7)

since $(\phi_1 + \phi_{m1}') - (\phi_1 - \phi_{m2}') = \phi_m' = \text{Flux}$ (8)
 through the permanent magnet
 (neglecting leakage effects)

For the actual solution the graphical representation of reluctance (i.e.: the magnetization curve) must be used as shown in Fig. XII.

It now becomes desirable to develop a simple graphical method of expressing ϕ_m' versus F_m' . In Fig. XIII, consider the point P on the demagnetization curve at F_c to be the "operating point". Then for each value of F_m' (the mmf imposed between points ab by the permanent magnet) (see Fig. VIII), add the ordinates $[(\phi_1 + \phi_{m2}') - \phi_1]$ and $[\phi_1 - (\phi_1 - \phi_{m1}')] = \phi_{m1}'$ to give the ordinate ϕ_m' . If a new curve is now plotted with the origin taken at P, the result will give a curve of ϕ_m' versus F_m' as shown in Fig. XIV.

Figure XIV may now be reversed and plotted directly on the demagnetization quadrant of the rotor, sheared* into the air gap line†, and corrected for leakage‡. The correction for air gap and leakage will yield a curve of F versus ϕ_m , the same coordinate system as the recovery line. Therefore the point of intersection of these two curves represents the flux through the permanent magnet

* See "Details of Shearing" Appendix A

† See "Calculation of Air Gap Line" Appendix A

‡ See "Estimate of Flux Leakage" Appendix A

• 7. 12

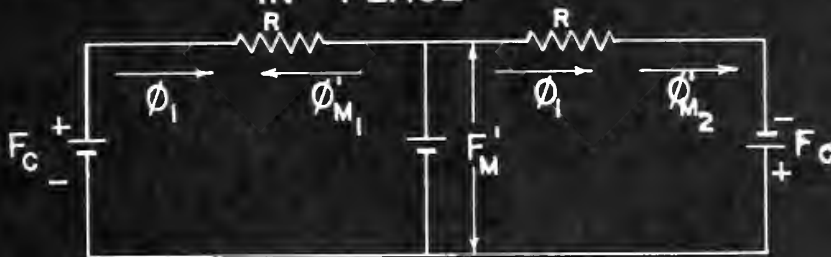
715 1000 01 07:00 00

1990-1991

1. The first group of people who are not in the labor force are those who are not in the labor force because they are not in the labor force.

FIGURE XI

ELECTRIC CIRCUIT ANALOGY WITH ROTOR IN PLACE



NOTE: F_M' IS THE MMF IMPOSED BETWEEN THE POINTS
 $a-b$ OF THE STATOR

FIGURE XII GRAPHICAL SOLUTION FOR ϕ_M'

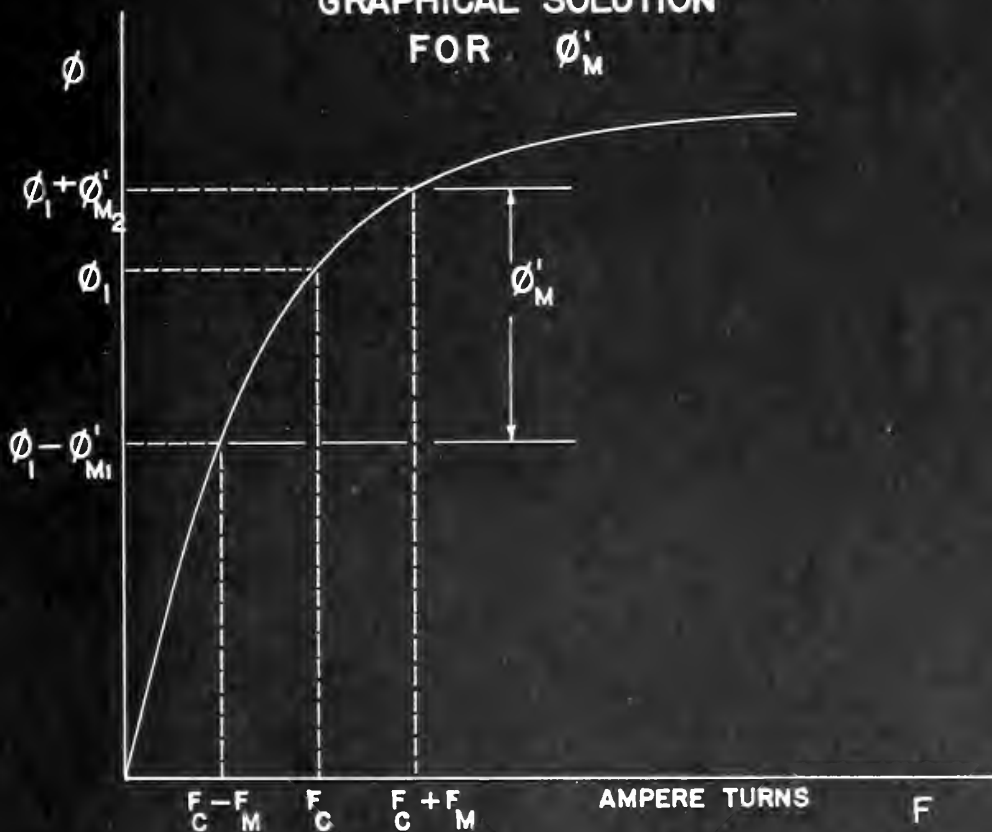


FIGURE XIII
GRAPHICAL SOLUTION

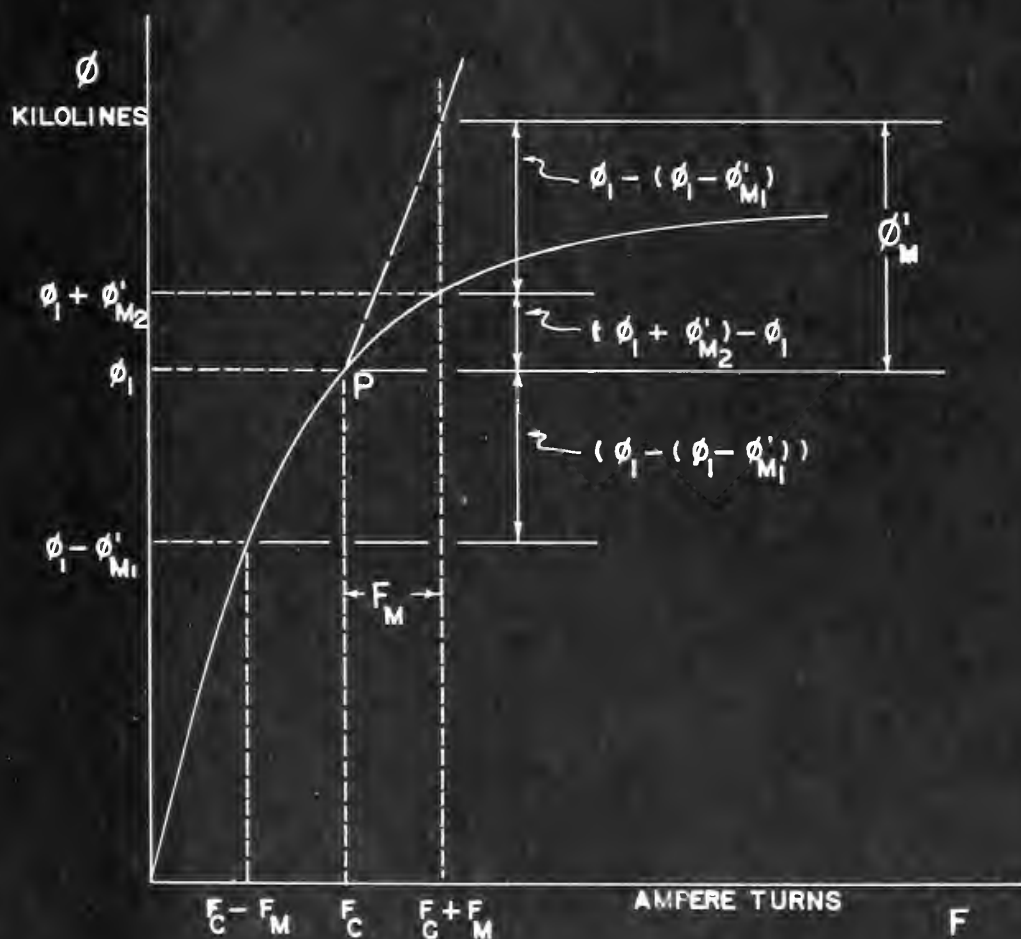
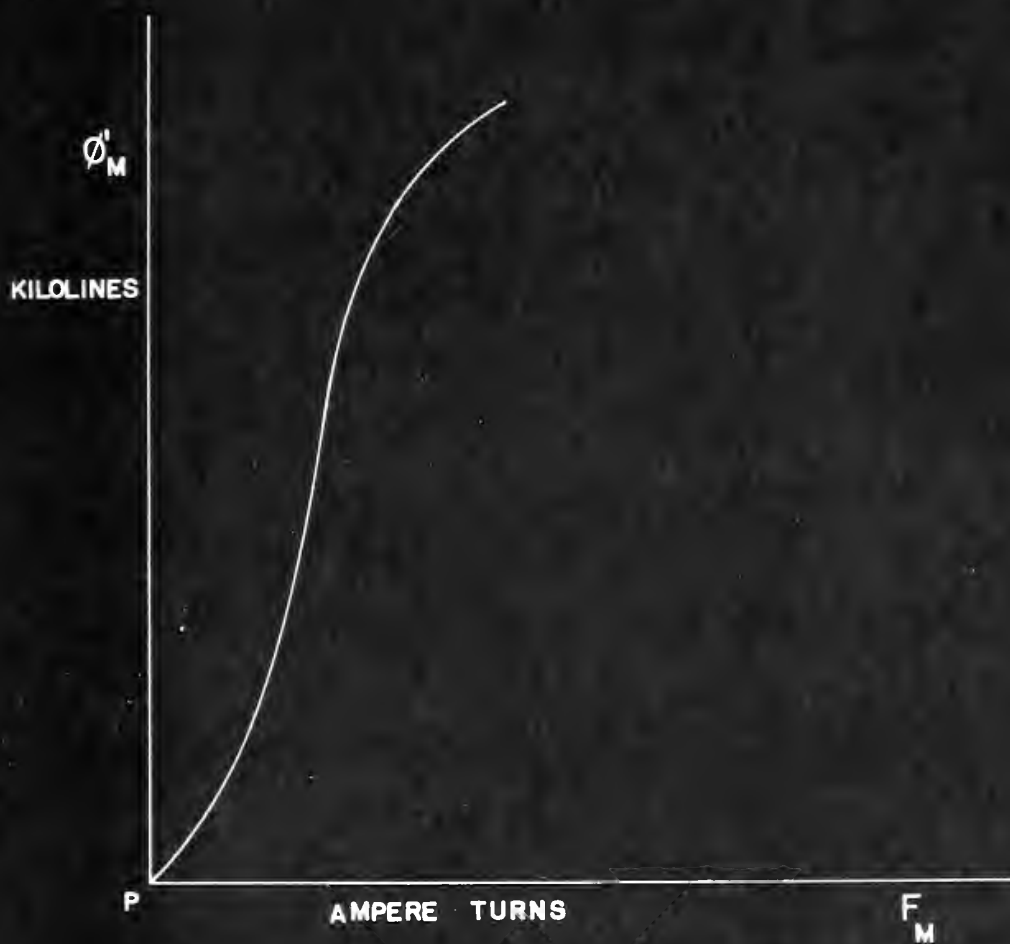


FIGURE XIV

ϕ'_M VS. F_M CURVE



under existing conditions. Because of the nearly vertical slope of the ϕ_m' curve, the leakage correction is small and negligible error is introduced, percentage wise, by neglecting it. Therefore the ϕ_m' versus F_m curve may be used for the solution of the simultaneous (graphical) equations of the magnetic circuit.

The leakage is estimated as a function of magnetic potential drop in the circuit, and is assumed to be linear*. It is shown as line OL on Fig. XV. The effect of this leakage is to reduce the useful flux, and therefore at any value of F or U (magnetic potential drop in ampere turns), the leakage flux must be subtracted from the magnet flux, to give the useful flux. This can be shown as having the same effect as a change in the slope of the recovery line of the magnet would have, and the results may be shown as a "virtual recovery line" on Fig. XV. The intersection of the reversed ϕ_m versus F_m curve with the "virtual recovery line" will now provide a solution for the state of useful flux in the air gap.

Furthermore it is readily seen that as the direct current in the toroidal winding is varied, (F_c is varied), the shape of the ϕ_m versus F_m curve changes as shown in Fig. XVI.

Hence when these curves are reversed and plotted on the demagnetization curve as before, and corrected for the air

* See "Estimate of Flux Leakage" Appendix A

under existing conditions. Because of the nearly vertical slope of the Φ_m curve, the leakage current is small and negligible error is introduced, but leakage will be neglected in the derivation of the Φ_m curve may be used for the solution of the simultaneous (graphical) equations of the magnetic circuit.

The leakage is estimated as a function of magnetic potential drop in the circuit, and is assumed to be linear*. It is shown as line OL on Fig. XV. The effect of this leakage is to reduce the useful flux, and therefore to give a value of H or B (magnetic potential drop in ampere turns), the leakage flux must be subtracted from the magnet flux, to give the useful flux. This can be shown as having the same effect as a change in the slope of the recovery line of the magnet would have, and the results may be shown as a "virtual recovery line" on Fig. XV. The intersection of the reversed Φ_m curve with the "virtual recovery line" will now provide a solution for the state of useful flux in the air gap.

Furthermore it is readily seen that as the direct current in the toroidal winding is varied, (H_0 is varied), the shape of the Φ_m versus Φ_m curve changes as shown in Fig. XVI.

Hence when these curves are reversed and plotted on the demagnetization curve as before, and corrected for the air

FIGURE XV

CIRCUIT CHARACTERISTICS PLOTTED ON MAGNET CHARACTERISTICS

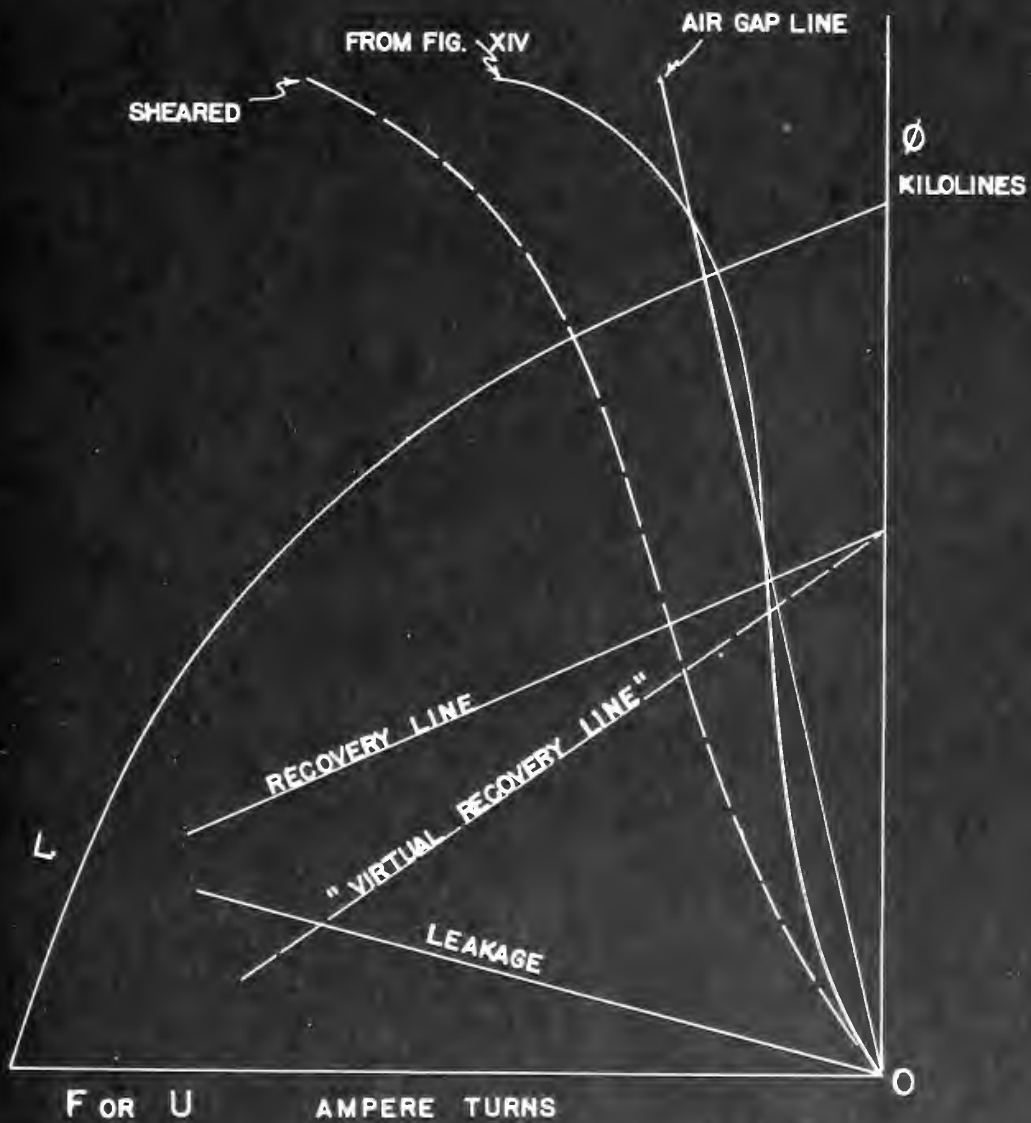
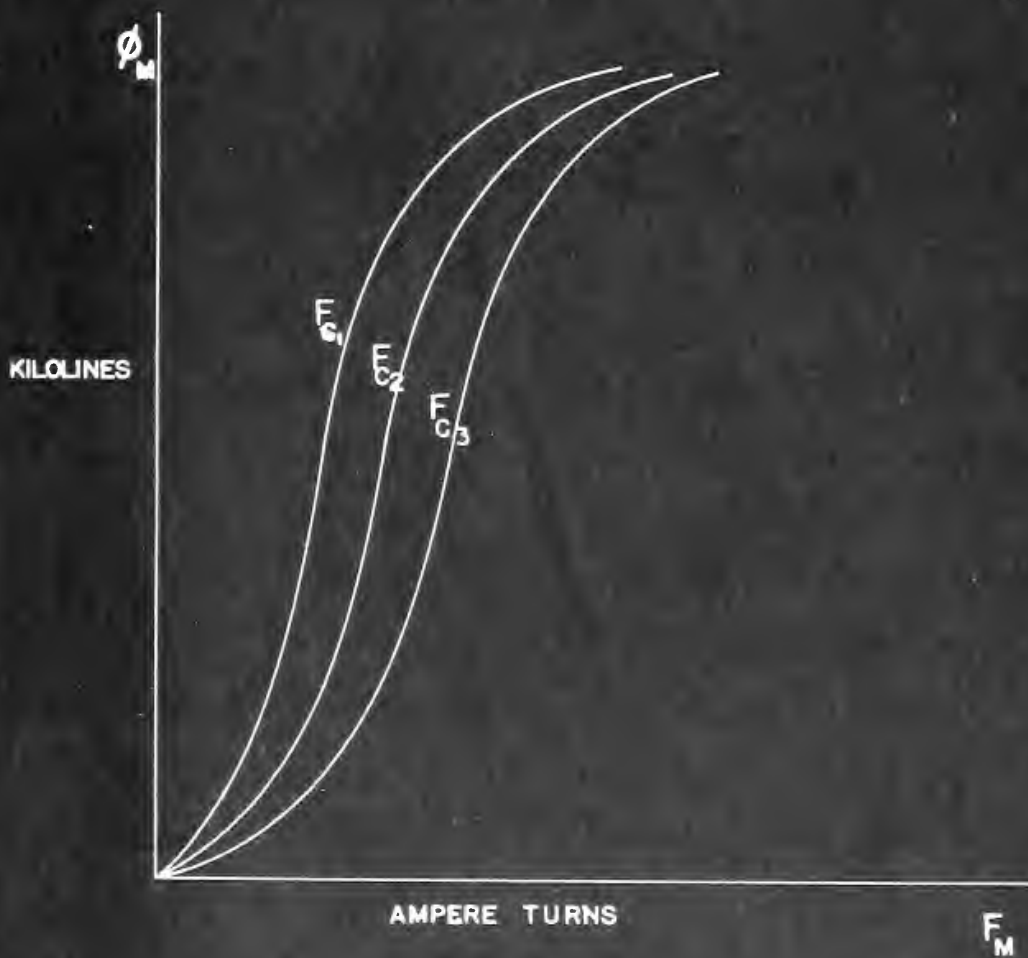


FIGURE XVI

EFFECT OF F_C ON THE ϕ'_M VS. F_M CURVE



gap, the intersection with the "virtual recovery line" moves progressively toward the left, as shown in Fig. XVII, and the effective air gap flux ϕ_g is thereby decreased.

If the alternator is running at constant speed, a common occurrence in synchronous machines, the voltage output will be directly proportional to the useful gap flux ϕ_g , and we have therefore established a method of control over the output voltage of a permanent magnet alternator.

B. Experimental Procedure

In order to verify the effectiveness of controlling a permanent magnet alternator by saturation of the stator iron, two stators, one of USS Electrical Grade Steel, and one of HIPERNIK were wound with coils of toroidal form, in addition to the normal three-phase winding. Tests of performance were made under varying conditions of saturation, loading and speed. The data obtained was correlated in a series of graphs illustrating the characteristics of this type of voltage control.

The load circuit used for testing the permanent magnet alternator consisted of a three-phase, y-connected, balanced load.

A Ward-Leonard system prime mover driving the alternator through a 1.5:10 V-belt drive was found to be the most effective means for maintaining constant alternator speeds. No synchronous drive of usable size was available; moreover, a synchronous drive would limit the test frequency to but one value.

gap, the intersection with the "virtual recovery line" moves progressively toward the left, as shown in Figs. 1, 2, 3, and the effective air gap δ_{eff} is thereby decreased. If the alternator is running at constant speed, a

common occurrence in synchronous machines, the voltage output will be directly proportional to the useful gap δ_{eff} , and we have therefore established a method of control over the output voltage of a permanent magnet alternator.

5. Experimental Procedure

In order to verify the effectiveness of controlling a permanent magnet alternator by saturation of the rotor, two alternators, one of USSR Electrical Grade Steel, and one of HIPERNIK were wound with coils of toroidal form, in

addition to the normal three-phase winding. Tests of

performance were made under varying conditions of

saturation, loading and speed. The data obtained was

correlated in a series of graphs illustrating the

characteristics of this type of voltage control.

The load circuit used for testing the permanent magnet

alternator consisted of a three-phase, Y-connected, balanced

load.

A Ward-Leonard system prime mover driving the alternator

through a 1:5:10 V belt drive was found to be the most

effective means for maintaining constant alternator speeds

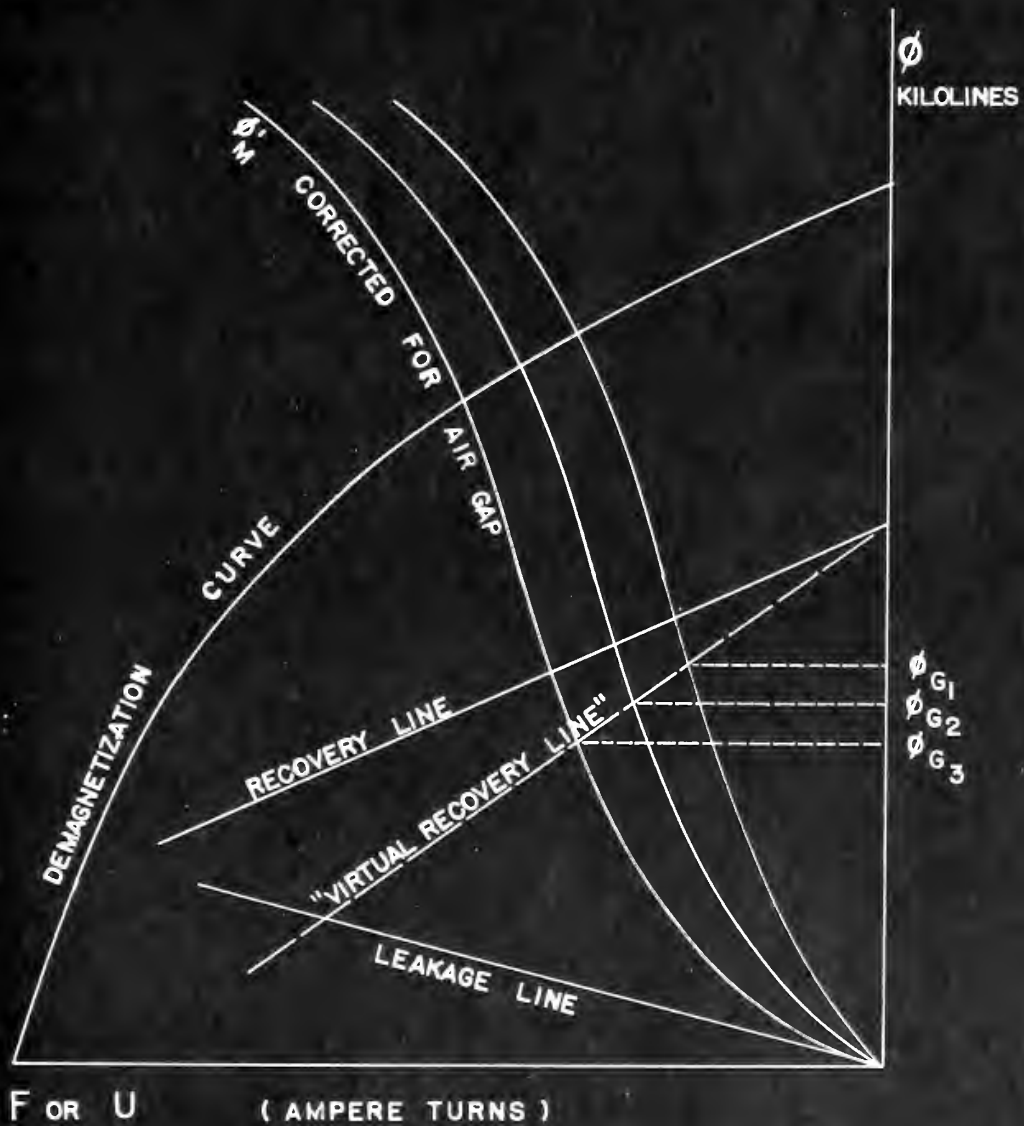
No synchronous drive of variable size was available;

moreover, a synchronous drive would limit the test frequency

to but one value.

FIGURE XVII

EFFECT OF F_c ON AIR GAP FLUX



The frequency for each test was set by maintaining a Lissajou pattern on an oscilloscope, an oscillator being used to measure the frequency.

The load resistance were slide-wire rheostats which were balanced at various values of resistance with a calibrated ohmmeter. In the tests where an inductive load was used, standard 100 millihenry inductances were connected in series with slide-wire rheostats so that the resistive part of the load could be balanced also.

Data was taken at given constant frequencies and load resistances. Control current was varied from 0 to 8 amperes in one ampere steps; at each value of control current, the generator load current and terminal voltage were read on rms-reading thermocouple instruments. The data recorded was direct-current control current, alternating-current terminal voltage, and alternating-current load current.

From the load current measured, the alternating-current real power was computed by the equation:

$$P = 3I^2R_L \quad (9)$$

Otherwise, the data taken was used directly in plotting the curves showing the results.

The results obtained from tests on the USS Electrical Grade stator are of limited value because it was found that the toroidal control winding developed multiple grounds when the stator was inserted in the stator housing. Because

The frequency of each test was 100 cycles per second.

Excitation pattern on an oscilloscope in order to obtain a
used to measure the frequency.

The load resistance was varied with a potentiometer which

was balanced at various values of resistance with a

calibrated ohmmeter. In the test were an inductive load

was used, standard 100 millihenry inductances were connected

in series with slide-wire potentiometer to test the relative

part of the load could be balanced also.

Data was taken at given constant frequencies and load

resistances. Control current was varied from 0 to 8

amperes in one ampere steps; at each value of control

current, the generator load current and terminal voltage

were read on two reading thermocouple instruments. The

data recorded was direct-current control current, alternating-

current terminal voltage, and alternating-current load

current.

From the load current measured, the alternating-current

real power was computed by the equation:

$$(9) \quad P = I_a I_f \cos \phi$$

Otherwise, the data taken was used directly to plotting the

curves showing the results.

The results obtained from tests on the two electrical

grade motor are of limited value because it was found that

the electrical control winding developed multiple grounds

when the motor was started in the motor rooming. Because

of these grounds, the ampere-turns of control mwf could not be established and no control current-terminal voltage relationship could be established. Nevertheless, current in the control winding had a definite effect on the generator terminal voltage.

Usable results were obtained from the HIPERNIK stator.

A summary of the test conditions for the tests on the HIPERNIK stator are as follows:

Frequency (cycles per second)	400	350	300
Load Resistance (ohms per phase)	open circuit 46.5 93.0 139.5	open circuit 46.5 93.0 139.5	open circuit 46.5 93.0 139.5
Inductive Load (per phase)	100 mh + 100 ohms	100 mh + 100 ohms	100 mh + 100 ohms

Tests on the HIPERNIK stator with an auxiliary flux leakage path were made. The auxiliary leakage path consisted of HIPERNIK discs clamped to each end of the rotor, but separated from the rotor by non-magnetic TEFLON spacers:

No. of 0.01" TEFLON spacers	2	2	2
No. of 0.014" HIPERNIK discs	1	2	2
Frequency in cps	400	400	350
Load in ohms/phase	open circuit 100	open circuit 100	open circuit 100

of these grounds, the upper limits of a motor load would not be established and no control current-forming voltage relationship could be established. However, current in the control winding had a definite effect on the generator terminal voltage.

Useful results were obtained from the HERNIMAN test. A summary of the test conditions for the tests on the

HERNIMAN motor are as follows:

Frequency (cycles per second)		100		150		200	
Inductive Load (per phase)		100 ohms + 100 mH		100 ohms + 100 mH		100 ohms + 100 mH	
Load Resistance (ohms per phase)		100		100		100	
open circuit		100		100		100	
open circuit		100		100		100	
open circuit		100		100		100	

Tests on the HERNIMAN motor with an auxiliary flux leakage path were made. The auxiliary leakage path consisted of HERNIMAN discs clamped to each end of the motor and separated from the rotor by non-magnetic THIN sheets.

No. of 0.01" THIN sheets		1		2		3	
No. of 0.01" HERNIMAN discs		1		2		3	
Frequency in cps		400		400		400	
Load in ohms/phase		100		100		100	
open circuit		100		100		100	
open circuit		100		100		100	

III. RESULTS

Experiment and analysis establish the following results:

1. The generator terminal voltage can be reduced, by means of the control winding, to a smaller value than the terminal voltage before control current is applied to the control winding. This reduction is caused in part by an actual reduction in flux from the magnet, and in part by an increase in the portion of magnet flux that traverses the leakage paths.
2. The percent of voltage control is directly dependent on the flux leakage path seen by the permanent magnet rotor.
3. The percent voltage reduction of item (1) is independent of the generator load current and power factor of the current, although the magnitude of voltage reduction is proportional to the initial voltage.
4. The relation between control current and terminal voltage is linear, provided the leakage paths do not saturate:

$$E = E_1 - KI_{dc} \quad \text{or} \quad \phi = \phi_1 - KI_{dc} \quad (10)$$

5. The wave shape of the terminal voltage is not affected, except in amplitude, by the saturation of the stator iron by the control current, provided the stator is designed so that harmonics are negligible. In the USS Electrical stator, which was designed with a slot skew, no harmonics were noticeable on the oscilloscope and the wave shape was not noticeably affected by saturation. In the

Experimental and Analytical Investigation of the Effect of the

1. The generator terminal voltage was reduced by means of the control winding, to a certain value. The terminal voltage before control current is applied to the control winding. This reduction is caused in part by an actual reduction in flux from the magnet, and in part by an increase in the position of magnet flux lines traversing the leakage paths.

2. The current of voltage control is directly dependent on the flux leakage seen by the permanent magnet rotor.

3. The percent voltage reduction of item (1) is independent of the generator load current and power factor of the circuit, although the magnitude of voltage reduction is proportional to the initial voltage.

4. The relation between control current and terminal voltage is linear, provided the leakage paths do not saturate.

$$(10) \quad E = E_0 - K I_c \quad \text{or} \quad E = E_0 - K I_c \quad \text{or} \quad E = E_0 - K I_c$$

5. The wave shape of the terminal voltage is not affected, except in small degree by the saturation of the magnet iron by the control current, provided the latter is designed so that harmonics are negligible. In the UPS Electrical Section a test was designed with a flux magnet, in which the wave shape was not really affected by saturation. In the

HIPERNIK stator which, for reasons of economy, was constructed with straight slots, some effects on harmonics due to stator saturation were noticed.

6. The magnetic material of the stator has negligible effect on voltage control providing the material is magnetically soft and is unsaturated when no control current is applied.

7. There is no net voltage induced in the toroidal winding by the air gap flux.

dedicated, new, machine to process, with special HIGH/IN
with special, some effects on materials due to stress
action were noticed.

6. The magnetic material of the motor was negligible

effect on voltage control providing the material is
magnetically soft and is unexcited when no control current
is applied.

7. There is no net voltage induced in the toroidal

winding by the air gap flux.

IV. DISCUSSION OF RESULTS

The two stators were wound and tested in order to determine the effect of different magnetic materials on the regulation of the generator output voltage when controlled by a direct-current toroidal winding. The four-pole Alnico VI permanent magnet rotor, the cast aluminum stator housing, and the two stators are illustrated in Fig. I. The detailed drawings of the stator and rotor appear in Fig. XX.

The generator prime mover consisted of a direct current motor, supplied from a direct current motor-generator set with field control. Frequency of alternator voltage was continuously checked by means of an oscilloscope.

Tests were performed under balanced resistive loads from no load to heavy loads, and one test was performed under a lagging reactive load of 0.37 power factor. Tests were conducted at 400, 350, and 300 cycles per second.

The first stator tested was of USS Electrical Grade Steel with a direct-current toroidal control winding of 162 turns of 24 gauge wire. This stator had a slot skew of one slot pitch. However this stator was found to have multiple grounds in the toroidal winding, and therefore the data must be considered of limited value. The second stator was of HIPERNIK with a toroidal winding of 198 turns of 24 gauge wire. Appendix A gives the details of the generating windings, and the magnetic properties of USS Electrical Grade Steel and HIPERNIK are given in Appendix B.

For the particular HIPERNIK stator tested, it was found

IV. DISCUSSION OF RESULTS

The two stators were wound and tested in order to determine the effect of different magnetic materials on the regulation of the generator output voltage when controlled by a direct-current toroidal winding. The four-pole Aialo VI permanent magnet motor, the test aluminum stator housing, and the two stators are illustrated in Fig. 1. The detailed drawings of the stator and motor appear in Fig. XX. The generator prime mover consisted of a direct current motor, supplied from a direct current motor-generator set with field control. Frequency of alternator voltage was continuously checked by means of an oscilloscope. Tests were performed under balanced resistive loads from no load to heavy loads, and one test was performed under a lagging reactive load of 0.57 power factor. Tests were conducted at 400, 500, and 550 cycles per second. The first stator tested was of HRS Electrical Grade Steel with a direct-current toroidal control winding of 105 turns of 24 gauge wire. This stator had a slot size of one slot pitch. However this stator was found to have multiple grounds in the toroidal winding, and therefore the data must be considered of limited value. The second stator was of HIRNIX with a toroidal winding of 105 turns of 24 gauge wire. Appendix A gives the details of the generating windings, and the magnetic properties of HRS Electrical Grade Steel and HIRNIX are given in Appendix B. For the particular HIRNIX stator tested, it was found

that the generator terminal voltage for a given load could be reduced to 63 per cent of its initial value by applying direct current to the toroidal control winding. Further control could have been obtained by applying larger amounts of control current at the expense of increased I^2R losses in the control winding. The final limitation on the amount of control is that the permanent magnet rotor should not be subjected to a knockdown lower than the existing knockdown point on its demagnetization curve.

Considering the expression for generated voltage:

$$E = K \phi n \quad (11)$$

and assuming the terminal voltage of the generator at a given load is to be held constant, then:

$$\phi n = K' \quad (12)$$

and the relation between ϕ and n must be a hyperbola. The speed of the generator can vary along the hyperbola within certain limits, determined by the amount ϕ can be changed by the control winding, and yet maintain a constant terminal voltage.

The relation between the control current I_c and the effective air gap flux ϕ is nearly a straight line with negative slope. (See Fig. XXVIII). Within a limited range, the flux may be considered to vary inversely with a control current.

$$\phi = \frac{K}{I_c} \quad (13)$$

that the generator terminal voltage E is given by the equation

$$E = I_a R_a + V_t$$

where I_a is the armature current and V_t is the terminal voltage. The terminal voltage V_t is the voltage across the load and is the voltage that is available to the load. The terminal voltage V_t is the voltage that is available to the load and is the voltage that is available to the load.

(11)
$$E = I_a R_a + V_t$$

and assuming the terminal voltage of the generator as a constant, then

(12)
$$E = I_a R_a + V_t$$

and the relation between E and I_a must be a straight line. The speed of the generator is constant and the terminal voltage V_t is constant. The terminal voltage V_t is constant and the terminal voltage V_t is constant.

The relation between the terminal voltage V_t and the terminal voltage V_t is given by the equation

$$V_t = E - I_a R_a$$

where I_a is the armature current and R_a is the armature resistance. The terminal voltage V_t is the voltage across the load and is the voltage that is available to the load.

(13)
$$V_t = E - I_a R_a$$

Therefore at constant terminal voltage,

$$\phi_n = K'' \quad (14)$$

$$\frac{n}{I_c} = K''' \quad (15)$$

$$\text{or } n = K'''' I_c \quad (16)$$

and the relation between speed (or frequency) and control current may be seen to be a straight line. This is borne out by the experimental results. (See Fig. XXXVIII).

Since ϕ decreases linearly with control current, and the power dissipated in the control winding increases as the square of the control current, it is seen that the range of voltage control obtained is limited by increased power consumption in the control winding.

The linear relation between control current and terminal voltage can be explained by consideration of the graphical solution of the problem. It is found that control current moves the characteristic of the stator, (ϕ'_m in Figure XIV), an equal amount to the right for each unit increase in control current. Since the point of intersection of the ϕ'_m curve and the permanent magnet recovery line occurs in the linear region of the ϕ'_m curve, the point of intersection follows a linear relation.

Analytically it can be seen by expressing the linear portion of the ϕ'_m curve as:

$$\phi'_m = aF - b I_{dc} \quad (17)$$

Therefore as constant terminal voltage,

$$(14) \quad \dot{E}_m = K_1$$

$$(15) \quad \frac{E}{I_a} = K_2$$

$$(16) \quad \text{or } E = E'' I_a$$

and the relation between speed (or frequency) and control current may be seen to be a straight line. It is shown by the experimental results. (See Fig. XXXVIII). Since \dot{E} decreases linearly with control current, and the power dissipated in the control winding increases as the square of the control current, it is seen that the range of voltage control obtained is limited by increased power consumption in the control winding.

The linear relation between control current and terminal voltage can be explained by consideration of the graphical solution of the problem. It is found that control current moves the characteristics of the motor (\dot{E}_m in Figure XIV), an equal amount to the right for each unit increase in control current. Since the point of intersection of the \dot{E}_m curve and the permanent magnet recovery line occurs in the linear region of the \dot{E}_m curve, the point of intersection follows a linear relation. Analytically it can be seen by expressing the linear

portion of the \dot{E}_m curve as:

$$(17) \quad \dot{E}_m' = E_0 + K_3 I_a$$

The "virtual" permanent magnet recovery line may be expressed as:

$$\phi_{\text{gap}} = C - dF \quad (18)$$

Figure XVIII shows these expressions in graphical form plotted on conventional coordinates.

Solving for ϕ_g :

$$\phi_g = A - B I_{\text{dc}} \quad \text{or} \quad \phi_g = \phi_1 - k I_{\text{dc}} \quad (19)$$

For any initial value of ϕ_1 for a given load, the above expression for ϕ_g holds, thus the per cent reduction of the initial voltage is independent of the load current drawn.

If the generator were driven by a constant speed drive, it is possible to maintain a constant terminal voltage from no load to full load by means of the control winding.

Moreover, if the power for the control winding were to be obtained from the generated output, the control power would be least when the power demand on the generator were the greatest. (See Fig. XXXVI). That the amounts of control power required for certain applications is practical is indicated by Figs. XXXVI and XXXVII, in which the control winding is used to maintain constant terminal voltage for (1) variable power consumption by the load, and (2) variable generator speed from 9,000 RPM to 12,000 RPM.

The control of terminal voltage under all load conditions, and with variations in prime mover speed appears

expressed as

$$(11) \quad \frac{d\theta}{dt} = \omega - \omega_0$$

Figure XVII shows these expressions in graphical form

plotted on conventional co-ordinates.

Solving for θ

$$(12) \quad \theta = \frac{1}{\omega_0} \left(\omega - \omega_0 \right) t + \theta_0$$

For any initial value of θ_0 for a given load, the

above expression for θ holds, thus the per cent reduction

of the initial voltage is independent of the load current

drawn.

If the generator were driven by a constant speed drive,

it is possible to maintain a constant terminal voltage from

no load to full load by means of the control winding.

Moreover, if the power for the control winding were to be

obtained from the generated output, the control power would

be less than the power drawn on the generator were the

generator. (See Fig. XXVI). Thus the amount of control

power required for certain applications is practical in

indicated by Figs. XXVI and XXVII, in which the control

winding is used to maintain constant terminal voltage for

(1) variable power consumption by the load, and (2)

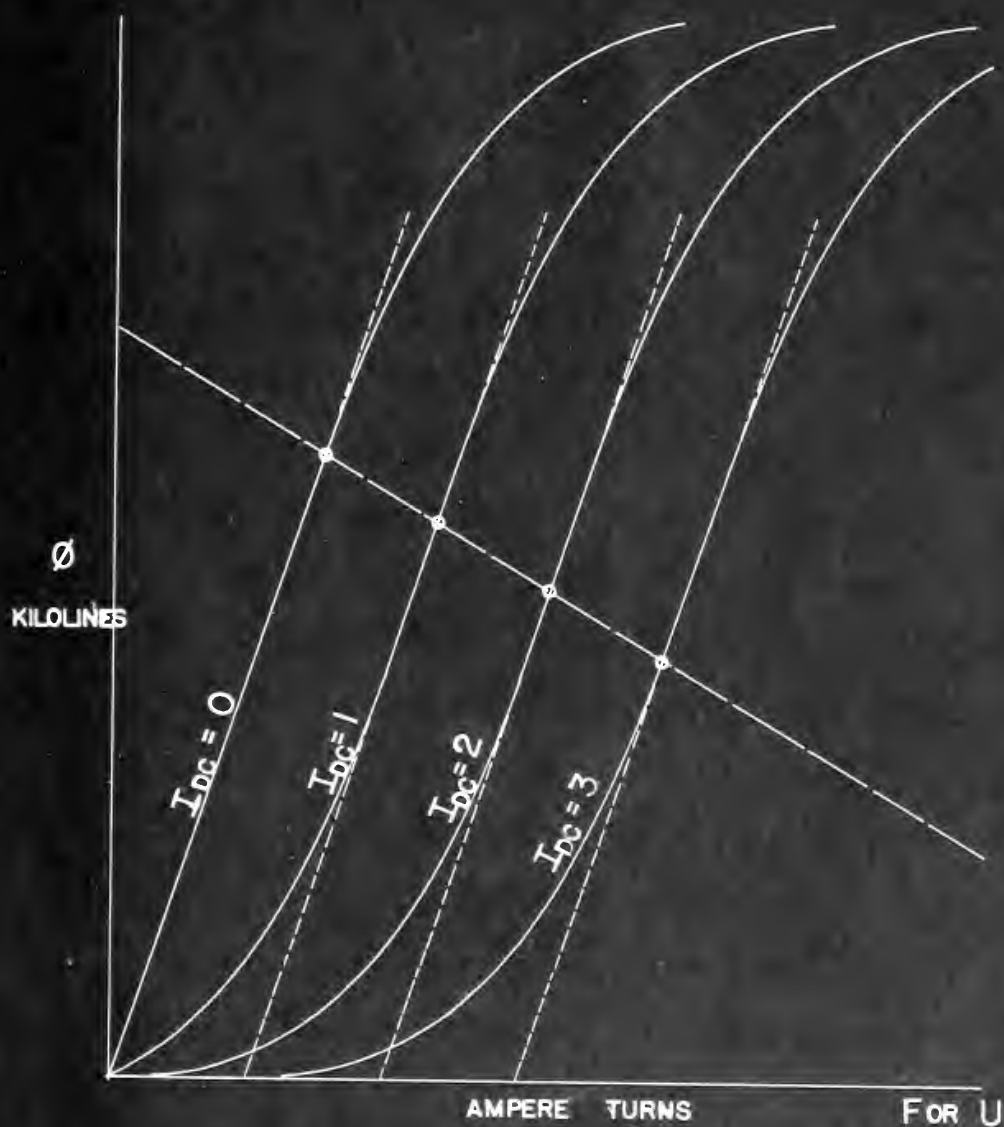
variable generator speed from 5,000 RPM to 12,000 RPM.

The control of terminal voltage under all load

conditions, and the variation in drive motor speed systems

FIGURE XVIII

GRAPHICAL SOLUTION





to be a highly valuable feature and should find wide application in systems which can use permanent magnet generators to advantage. Since the control is by purely electrical means, automatic voltage regulation is feasible.

The wave shape of the terminal voltage of a properly designed stator appears to remain constant, except in amplitude, throughout the range of control current used. Observations were made on an oscilloscope so minor changes in shape may not have been discerned. The saturation of the stator by control current does not have any effect on the stator teeth since all flux induced by the toroidal control winding must be contained within the toroid; thus, the condition of the iron in the stator teeth immediately opposite the permanent magnet poles is unchanged by control current. The air gap in the generator was only 0.007" so little air gap flux redistribution results as the control current increases. For these reasons, the effect of saturation of the stator iron will not have as much effect on the voltage wave shape as might first be suspected. On a machine with a larger air gap, some variation in the output voltage wave shape might well be observed.

Analysis and experiment both indicate that the stator magnetic material has little effect on the voltage control. This is because the point of intersection of the stator magnetic characteristic curve and the permanent magnet characteristic in the graphical solution occurs in the non-saturated region of the stator characteristic. That is,

to be a slight voltage across the brush and commutator
 application in systems which use permanent magnets
 generators is advantageous. Since the control is by purely
 electrical means, automatic voltage regulation is feasible.
 The wave shape of the terminal voltage of a generator
 designed as a motor appears to remain constant, except in
 amplitude, throughout the range of current output used.
 Observations were made on an oscilloscope as minor changes
 in shape may not have been discerned. The assumption of the
 stator by control current does not have any effect on the
 stator teeth since all flux induced by the stator control
 winding must be contained within the stator; thus, the
 condition of the iron in the stator teeth immediately
 opposite the permanent magnet poles is unchanged by stator
 current. The air gap in the generator was only 0.007" as
 little air gap flux redistribution results as the control
 current increases. For these reasons, the effect of
 saturation of the stator iron will not have as much effect
 on the voltage wave shape as might first be supposed. On
 a machine with a larger air gap, some variation in the output
 voltage wave shape might well be observed.
 Analysis and experiment have indicated that the stator
 magnetic material has little effect on the voltage control.
 This is because the point of saturation of the stator
 magnetic characteristic curve and the permanent magnet
 characteristic in the graph are well separated. Thus, in
 non-saturated region of the stator characteristic, there is

the stator is not saturated due to the flux from the permanent magnet. Since the magnetic characteristics of materials suitable for use in generator stators are practically the same in the unsaturated condition, the graphical solution of the problem does not change.

Had the stator been saturated by the flux from the permanent magnet, the type of magnetic material would have marked effect on the initial voltage and the voltage control. The regulation obtained when the stator is originally saturated is marginal until the control current is increased enough to cause the stator to operate in an unsaturated condition. Figure XIX illustrates this effect.

The leakage path seen by the permanent magnet rotor has an effect of major importance on the reduction of air gap flux. The permanent magnet flux solved for as shown in Fig. XV does not represent the air-gap flux which actually induces voltage in the generator windings; leakage flux must be deducted from the permanent magnet flux to obtain air gap flux. The larger the leakage, the more reduction in air-gap flux per unit change in control current can be obtained. That the leakage was underestimated in the calculated results is evident from curve of Fig. XXXI. A method of improving the control obtained is to increase the available flux leakage paths. The effects of decreasing the reluctance of the leakage path facing the magnet is remarkably well demonstrated in Fig. XXXII.

To obtain these curves, several experiments were run

the stator is not saturated due to the flux from the permanent magnet. Since the magnetic characteristics of materials available for use in generator stators are practically the same in the unsaturated condition, the graphical solution of the problem does not change.

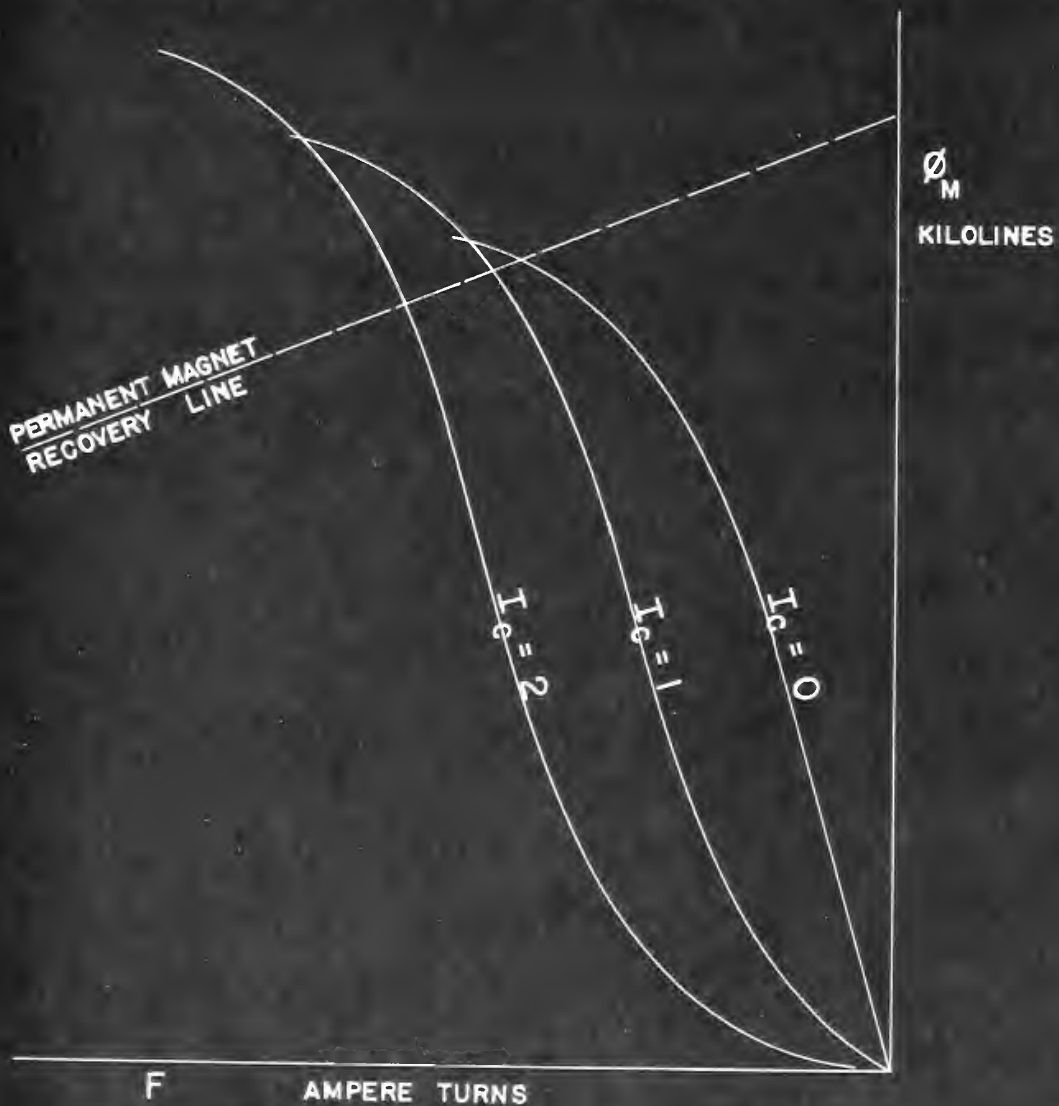
Had the stator been saturated by the flux from the permanent magnet, the type of magnetic material would have marked effect on the initial voltage and the voltage control. The regulation obtained when the stator is originally saturated is marginal until the control current is increased enough to cause the stator to operate in an unsaturated condition. Figure XIX illustrates this effect.

The leakage path seen by the permanent magnet rotor has an effect of major importance on the reduction of air gap flux. The permanent magnet flux solved for as shown in Fig. XV does not represent the air-gap flux which actually induces voltage in the generator windings; leakage flux must be deducted from the permanent magnet flux to obtain air gap flux. The larger the leakage, the more reduction in air-gap flux per unit change in control current can be obtained. That the leakage was underestimated in the calculated results is evident from curve of Fig. XXXI. A method of improving the control obtained is to increase the available line leakage path. The effects of decreasing the reluctance of the leakage path facing the magnet is remarkably well demonstrated in Fig. XXXII.

To obtain these curves, several experiments were run

FIGURE XIX

EFFECT OF SATURATION IN THE STATOR
BEFORE APPLICATION OF CONTROL MMF





with magnetically soft discs separated from the rotor by non-magnetic spacers clamped to both ends of the rotor. It was found that increasing the leakage path by this auxiliary means did increase the per cent voltage regulation. The curves in Fig. XXXII also show that the voltage regulation eventually decreases at higher control currents because the leakage characteristic changes when the discs saturate. No analysis of this phase of the experiment was undertaken because of the uncertain nature of the auxiliary leakage path.

No trouble was encountered due to voltage being induced in the toroidal control winding since the north and south poles of the permanent magnet rotor induced equal and opposite voltages in this continuous winding.

with magnetically soft discs separated from the rotor by
 non magnetic spacers placed at both ends of the rotor. It
 was found that increasing the leakage path by this auxiliary
 means did increase the per cent voltage regulation. The
 curves in Fig. XXXII also show that the voltage regulation
 eventually decreases at higher control currents because
 the leakage characteristics changes when the discs saturate.
 No analysis of this phase of the experiment was undertaken
 because of the uncertain nature of the auxiliary leakage
 path.

No trouble was encountered due to voltage being
 induced in the toroidal control winding since the north and
 south poles of the permanent magnet rotor induced equal and
 opposite voltages in this continuous winding.

V. CONCLUSIONS AND RECOMMENDATIONS

The method of analysis devised for the magnetic circuit under the specified conditions of saturation is sound in principle and leads to an acceptable prediction of resultant effects.

It has further been shown that this method is entirely practical for voltage control of a permanent magnet alternator by electrical means. The amount of control obtainable is limited only by the characteristics of the permanent magnet, the design of the magnetic circuit, and by the power one wishes to expend to obtain this control. One advantage of the permanent magnet alternator has, however, been lost. That is, now a source of direct current must be made available, and to obtain direct current from the output requires some rectifying mechanism or circuit.

The amount of control is greatly affected by the reluctance of the leakage paths, and the most obvious method of improving the control for a given power expenditure is to provide an easy leakage path in the magnetic circuit.

Recommendations for further investigation are as follows:

- (1) Seek to improve the stator design to take advantage of the leakage effects to better advantage.
- (2) Perform a more thorough study of the leakage paths to improve upon the approximations used in this analysis.
- (3) Design a circuit for automatic voltage control of

V. CONCLUSIONS AND RECOMMENDATIONS

The method of analysis devised for the magnetic circuit under the specified conditions of saturation is based in principle and leads to an acceptable prediction of resultant effects.

It has further been shown that this method is entirely practical for voltage control of a permanent magnet alternator by electrical means. The amount of control obtainable is limited only by the characteristics of the permanent magnet. The design of the magnetic circuit, and by the power and means required to obtain this control. One advantage of the permanent magnet alternator has, however, been lost. That is, now a source of direct current must be made available, and to obtain direct current from the output requires some rectifying mechanism or circuit.

The amount of control is greatly affected by the reluctance of the leakage paths, and the most obvious method of improving the control for a given power expenditure is to provide an easy leakage path in the magnetic circuit.

Recommendations for further investigation are as follows:

- (1) Seek to improve the stator design to take advantage of the leakage effects to better advantage.
- (2) Perform a more thorough study of the leakage paths to improve upon the approximations used in this analysis.
- (3) Design a circuit for voltage control of

the device, using rectified power from the output in a feedback loop. The transient characteristics and power characteristics would be of interest.

- (4) Investigate the effects of alternating current at various frequencies applied to the toroidal winding.[6]
- (5) Apply the principles learned herein to other types of machines where they may be of value. For example, poor voltage regulation of a high-speed induction generator is a serious disadvantage [7], [8]. This method of analysis suggests that the effects of toroidal saturation of an induction generator may be of interest.

The device, using regulated power from the
 output in a feedback loop. The transient
 characteristics and power characteristics
 would be of interest.

(4) Investigate the effects of alternating current at

various frequencies applied to the controlled

winding. [5]

(5) Apply the principles learned herein to other

types of machines where they may be of value.

For example, poor voltage regulation of a high-

speed induction generator is a common

disadvantage [6], [7]. This method of analysis

suggests that the effects of controlled saturation

of an induction generator may be of interest.

VI. APPENDIX A

DETAILS OF PROCEDURE

VI. APPENDIX A

DETAILS OF PROCEDURE

DETAILS OF PROCEDURE

Machine Design:

The design is limited by the characteristics of the existing stator. The physical dimensions, the number of slots, and the shape of the laminations were left unchanged, and a three phase "Y" winding was designed which would generate approximately 90 volts per phase, root mean-square.

The peripheral rim was milled to produce 18 additional slots to recess the outside of the toroidal winding so it would clear the casing when the stator and case were assembled. See Fig. XX.

Design of the three-phase armature winding: [9]

The design of this winding is based upon two existing pieces of apparatus: the 18-slot stator and the permanent-magnet rotor.

The flux per pole is determined for the "closed circuit" position of the rotor (i.e.: rotor in place in the magnetic circuit) by the method outlined in Section II "PROCEDURE".

Flux per pole, $\phi_t = 21.7$ kilolines

Assume a field form distribution factor $f_d = 0.666$

Therefore the "hypothetical total flux" [9]:

$$\phi_t = \frac{\phi_p}{f_d} = \frac{21.74 (4)}{0.666} = 130.9 \text{ kilolines} \quad (20)$$

$$B_g = \frac{\phi_t}{\pi DL} = \frac{130,900}{\pi (2.22)(.875)} = 21520 \text{ lines/inch}^2 \quad (21)$$

DETAILS OF PROCEDURE

Machine Design:

The design is limited by the mechanical strength of the existing stator. The physical dimensions, the number of slots, and the shape of the laminations were held unchanged, and a three phase "Y" winding was designed which would generate approximately 90 volts per phase, root mean square. The peripheral rim was killed to produce 18 additional slots to recess the outside of the toroidal winding so it would clear the casing when the stator and case were assembled. See Fig. XX.

Design of the three-phase armature winding [3]

The design of this winding is based upon two existing pieces of apparatus: the 18-slot stator and permanent-magnet motor.

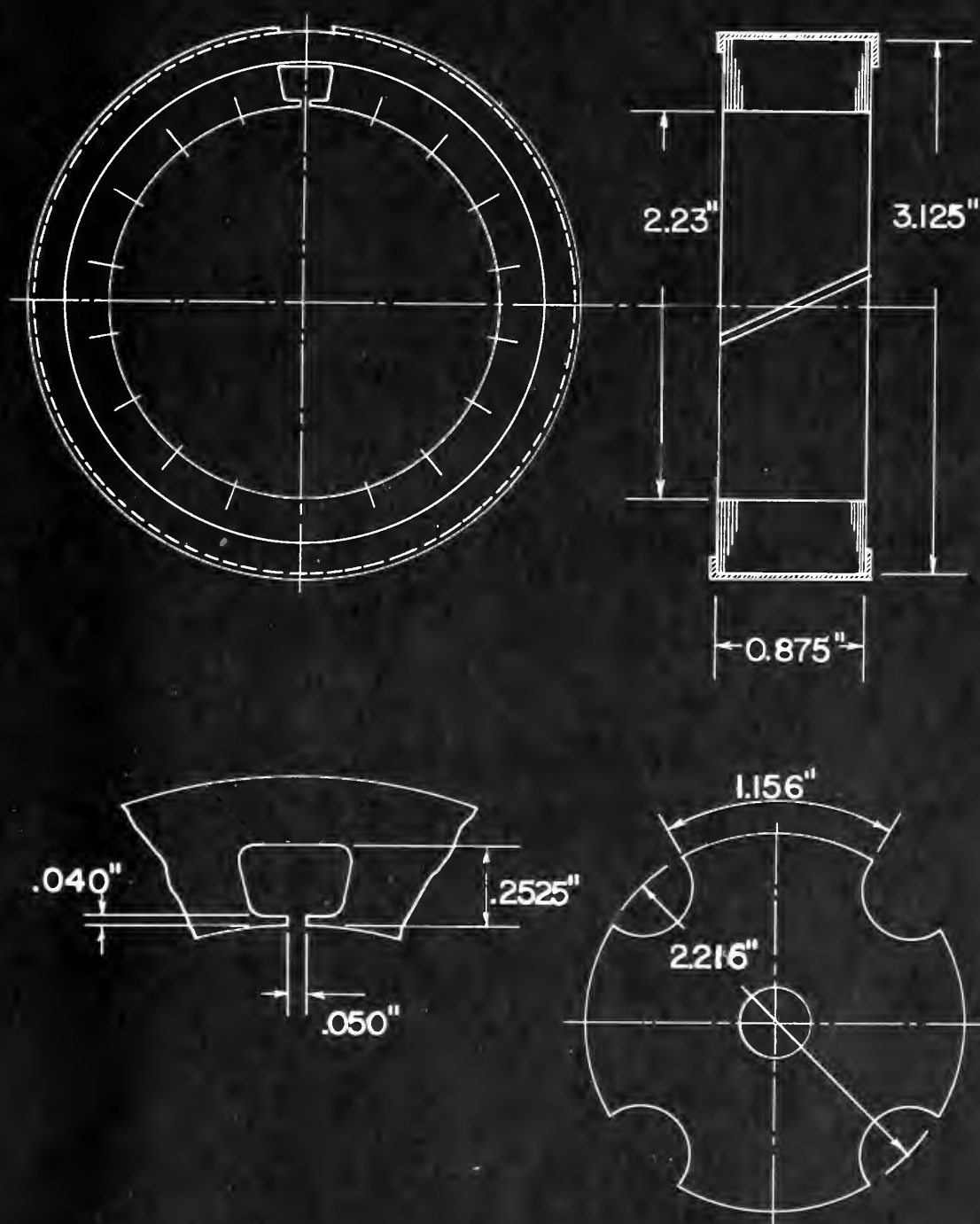
The flux per pole is determined for the "closed circuit" position of the rotor (i.e., rotor in place in the magnetic circuit) by the method outlined in Section II "PROCEDURE".

Flux per pole, $\Phi_p = 21.7$ kilolines
Assume a field form factor $f_g = 0.800$
Therefore the "hypothetical total flux" [3]:

$$\Phi_t = \frac{\Phi_p}{f_g} = \frac{21.7}{0.800} = 27.125 \text{ (4)} = 27.125 \text{ kilolines (5)}$$

$$\Phi_s = \frac{\Phi_t}{2} = \frac{27.125}{2} = 13.5625 \text{ kilolines (6)}$$

FIGURE XX
DETAILS OF STATOR AND ROTOR



DETAILS OF PROCEDURE (cont.)

Assume a winding distribution factor C_w :

$$\begin{aligned}C_w &= f_b \times f_d \times k_d \\&= 1.14 \times 0.666 \times 0.956 \\&= 0.725\end{aligned}\tag{22}$$

Where f_b = form factor,

f_d = flux distribution factor

k_d = winding distribution factor

For a pitch winding, the number of conductors in series per phase N:

$$N = \frac{E \times 60 \times 10^8}{\phi_t \times n \times k_p \times C_w} = \frac{90 \times 60 \times 10^8}{130,900 \times 12,000 \times 1 \times 0.725}\tag{23}$$

= 476 conductors in series per phase

The total number of conductors equals $476 \times 3 = 1428$
for a winding with one circuit per phase.

The number of conductors per slot is N.

$$N = 1428/18 = 79.2\tag{24}$$

However with this stator a pitch coil cannot be used,
since the pitch equals $4\frac{1}{2}$ slots.

Therefore a coil throw of slots 1 to 5 will be
necessary:

$$k_p = \sin \left[\frac{4 \times 90^\circ}{4\frac{1}{2}} \right] = .986\tag{25}$$

DETAILS OF PROPORTION (cont.)

Assume a winding distribution factor k_d

(37)

$$k_d = \frac{1}{p} \times \frac{1}{q} \times \frac{1}{r}$$

$$= 1.17 \times 0.95 \times 0.95$$

$$= 0.785$$

Where k_d = form factor

k_d = flux distribution factor

k_d = winding distribution factor

For a pitch winding, the number of conductors in

series per phase is:

(38)

$$N = \frac{2 \times 60 \times 10^3}{\frac{120,000 \times 12,000 \times 1 \times 0.785}{30 \times 60 \times 10^3}}$$

= 475 conductors in series per phase

The total number of conductors equals $475 \times 3 = 1425$

for a winding with one circuit per phase.

The number of conductors per slot is N .

(39)

$$N = 1425/3 = 475$$

However with 12 slots a pitch of 12 cannot be used.

Since the pitch equals 12 slots

Therefore a full pitch of slots 1 to 12 will be

necessary:

(40)

$$k_p = \frac{1}{p} \times \frac{1}{q} \times \frac{1}{r}$$

DETAILS OF PROCEDURE (cont.)

$$\text{and } N = \frac{476}{.986} = 483 \text{ conductors in series per phase.} \quad (26)$$

$$\text{The total number of conductors} = 483 \times 3 = 1449$$

Therefore we will have $\frac{1449}{18} = 80.3 \approx 80$ conductors per slot, or 40 turns per coil.

Figure XXI shows the wiring diagram for the three-phase winding, and Fig. XXII shows the coil end-connections.

Wire size; and machine rating:

Determination of wire size depends upon space considerations in the slots.

Stator Number 1 (USS Electrical Steel) was limited to 40 turns per coil of Number 26 gauge wire.

S_a = cross sectional area of wire

S_a = .000199 square inches

A_a = allowable current density for short term operation

= 4400 amperes per square inch (twice normal)

I_a = allowable armature current

$$= S_a \times A_a = (.000199) \times (4400) = .875 \text{ amperes.} \quad (27)$$

Machine rating:

$$VA = 3 E I_a = 3 \times 90 \times .875 = 236.2 \text{ volt-amperes.} \quad (28)$$

Stator Number 2 ("HIPERNIK"): In this stator the absence of skew gave more effective slot area, allowing Number 24 gauge wire to be used.

DETAILS OF PROCEDURE (cont.)

(26) and $N = 485$ conductors in series per phase.

The total number of conductors = $485 \times 3 = 1455$

Therefore we will have $\frac{1455}{18} = 80.8 \approx 80$ conductors

per slot, or 40 turns per coil.

Figure XXI shows the winding diagram for the three

phase winding, and Fig. XXII shows the coil end-connections.

Wire size; and machine rating:

Determination of wire size depends upon space

considerations in the slots.

Stator Number 1 (US Steel) was limited to

40 turns per coil of Number 26 gauge wire.

$S_a =$ cross sectional area of wire

$S_a = .000199$ square inches

$A_a =$ allowable current density for short term operation

$= 4400$ amperes per square inch (twice normal)

$I_a =$ allowable ampere current

$= S_a \times A_a = (.000199) \times (4400) = .875$ amperes. (27)

Machine rating:

$VA = 3 \times I_a = 3 \times .875 = 2.625$ volt-amperes. (28)

Stator Number 2 ("KIPWIK"): In this stator the

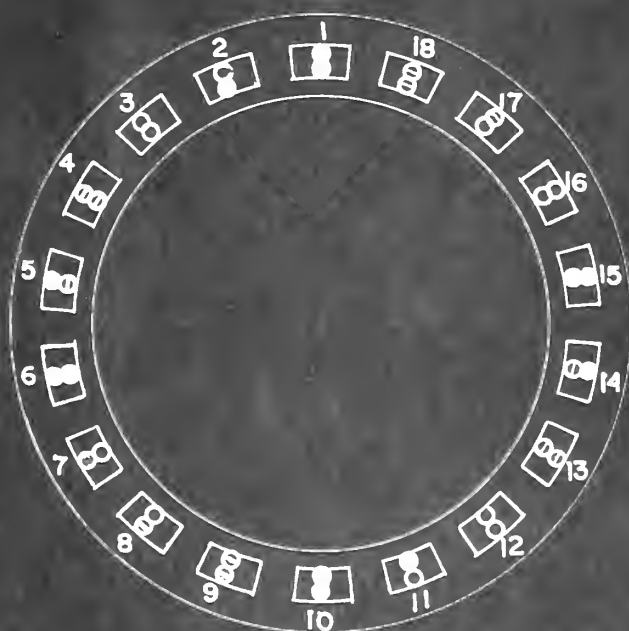
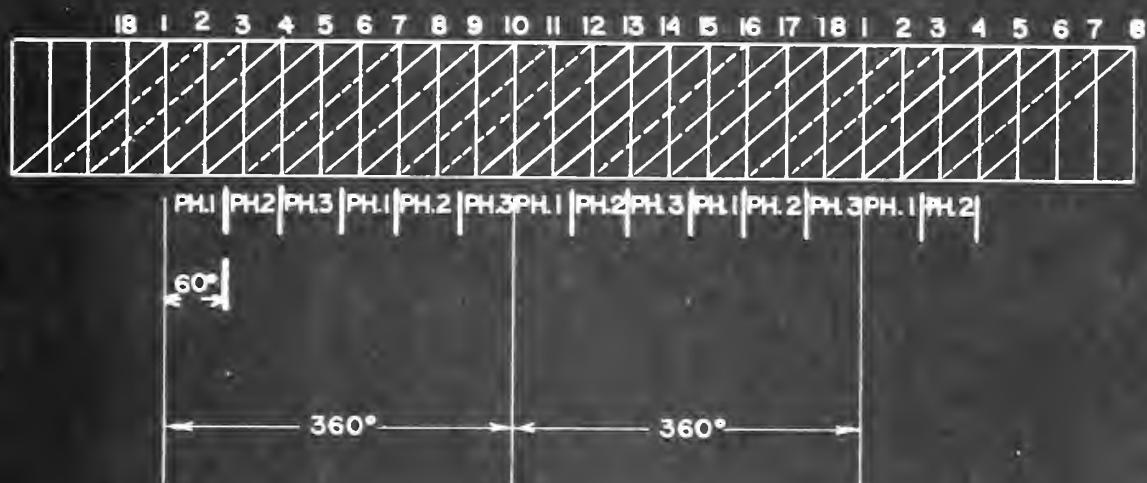
absence of skew gave more effective slot area, allowing

Number 26 gauge wire to be used.

FIGURE XXI

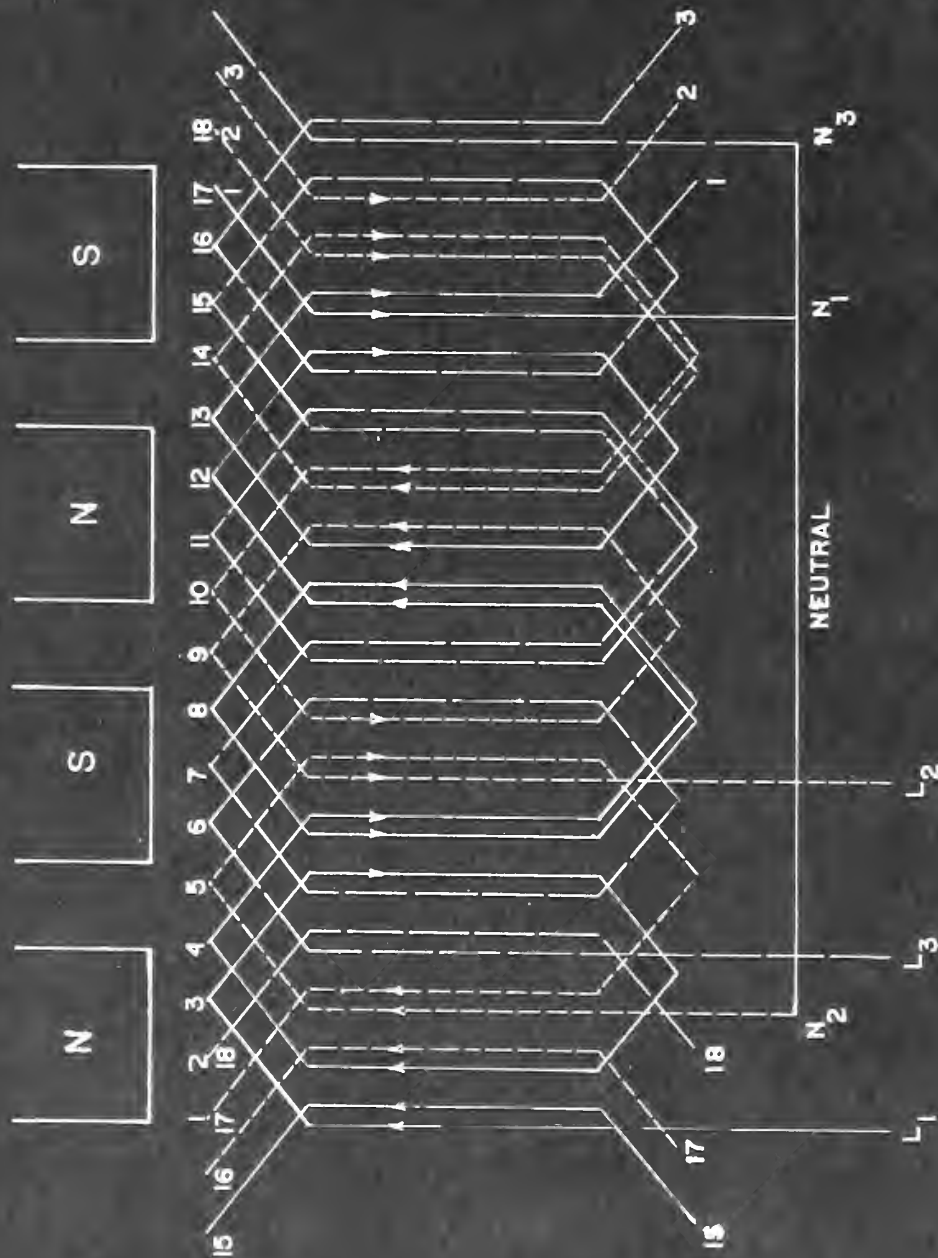
DIAGRAM FOR THREE PHASE WINDING

1 1/2 SLOTS PER POLE PER PHASE



- PH. 1
- ⊖ PH. 2
- PH. 3

FIGURE XXII
GENERATOR COIL END CONNECTIONS
 THREE PHASE - Y CONNECTED



DETAILS OF PROCEDURE (cont.)

$$S_a = .000317 \text{ square inches}$$

$$A_a = 4400 \text{ amperes per square inch}$$

$$I_a = S_a \times A_a = (.000317) \times (4400) = 1.395 \text{ amperes (29)}$$

Machine rating:

$$VA = 3 \times I_a = 3 \times 90 \times 1.395 = 377 \text{ volt-amperes (30)}$$

DETAILS OF PROCEDURE

Step 1: $10000 = 10^4$

Step 2: $10000 = 10^4$

(3) $10000 = 10^4 = (10^4) \times (10^0) = 10^4 \times 1 = 10^4$

Machine test:

(4) $10000 = 10^4 = 10^4 \times 10^0 = 10^4 \times 1 = 10^4$

DETAILS OF PROCEDURE (cont.)

Details of "Shearing": [5]

A method of obtaining the reluctance characteristics of a magnetic path consisting of a ferromagnetic portion plus an air gap in series is as follows: Neglecting leakage, the flux may be assumed constant throughout the magnetic circuit. Then on coordinates of flux versus magnetomotive force (or magnetic potential drop U) we can plot separately the characteristics of the air gap and the rest of the circuit, as shown in Fig. XXIII.

Then, since these two portions of the magnetic circuit are in series, for each value of flux (ϕ) the magnetic potential drop (U) of the entire circuit is the sum of the magnetic potential drops of the two portions. This addition may be done graphically by a process known as "shearing" the characteristic of the ferromagnetic portion into the air-gap line as shown in Fig. XXIV.

DETAILS OF METHOD

Details of "Shearing"

A method of obtaining the relationship between the magnetic field and the air gap in a magnetic circuit is as follows: A magnetic circuit is constructed of two pieces of magnetic material, one of which is a permanent magnet and the other is a soft magnetic material. The two pieces are joined together at one end, forming a closed magnetic circuit. The other end of the circuit is open, forming an air gap. The magnetic field is measured across the air gap, and the relationship between the magnetic field and the air gap is determined. This relationship is then used to determine the magnetic field across the air gap for a given magnetic field across the permanent magnet. This method is known as "shearing".

Then, since these two sections of the magnetic circuit are in series, for each value of the magnetic potential drop (0) of the entire circuit is the sum of the magnetic potential drops of the two portions. This addition may be done graphically by a process known as "shearing", the characteristic of the permanent magnet into the air-gap line as shown in Fig. XIV.

FIGURE XXIII

SAMPLE CHARACTERISTICS OF IRON & AIR GAP

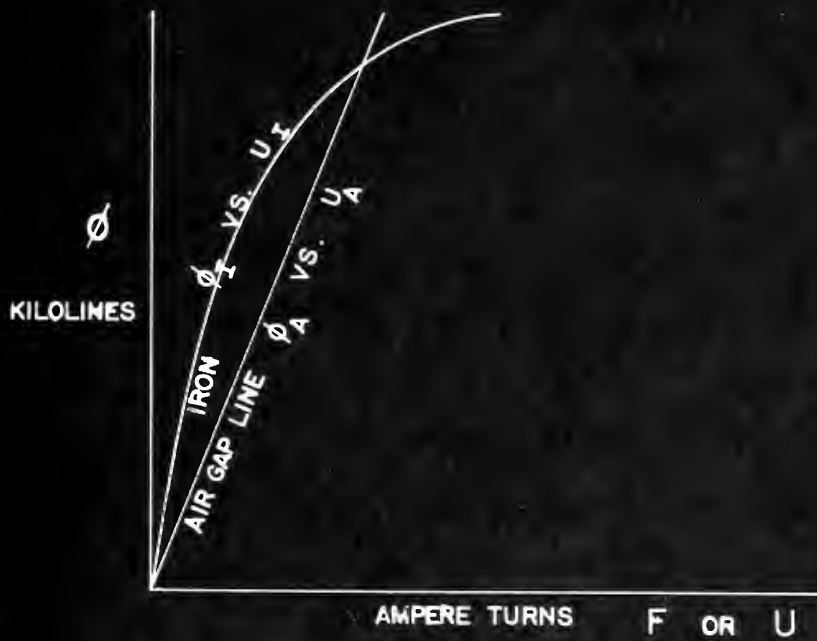
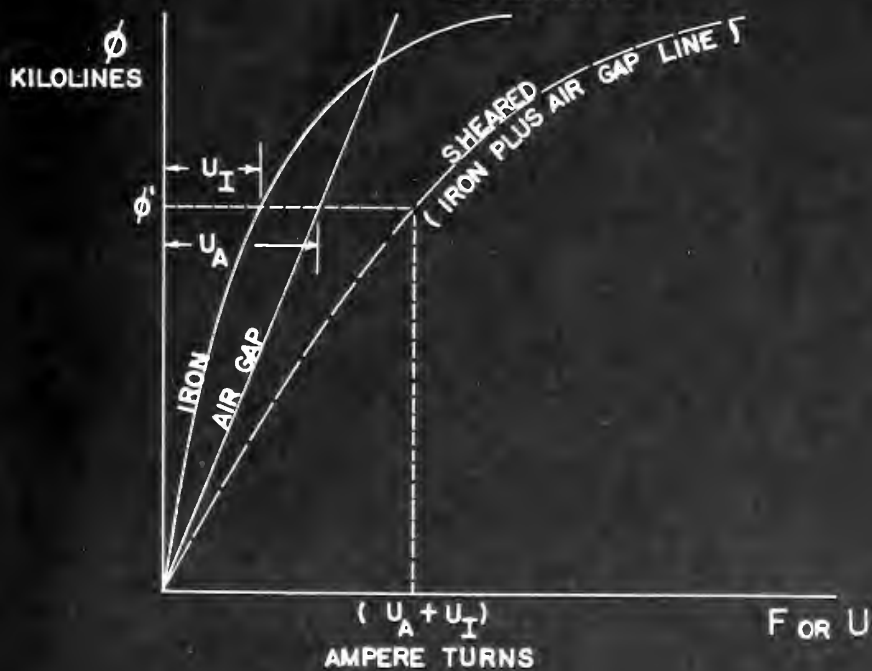


FIGURE XXIV

SHEARING



DETAILS OF PROCEDURE (cont.)

Computation of Air-Gap Line:

The dimensions of the armature iron and permanent magnet rotor are as shown in Fig. XX.

The air gap between pole face and stator teeth is:

$$a-g = r_1 - r_m = 1.115" - 1.108" = 0.007" \quad (31)$$

The true air-gap cannot be used directly for computation of the air-gap line in flux vs. magnetomotive force because of the effect of slot openings in the stator. An approximation of an effective air-gap; that is, a fictitious air-gap which would be required if the inside of the stator were made perfectly smooth and the air-gap adjusted so that the flux from the rotor were not changed, is made by the method of Carter [5].

The method of Carter is based on the assumption of slot openings with straight sides and with infinite depth. In the case of the slots under consideration, the slots are semi-closed, not straight, but the method is used on the assumption that the fringing flux will be about the same whether the slots be open or semi-closed since the depth at the edge of a slot tooth is over five times the air gap. This assumption neglects any saturation in the thin parts of the teeth.

Carter's method is outlined below:

$$\sigma = \frac{2}{\pi} \left\{ \tan^{-1} \frac{s}{2\delta} - \frac{\delta}{s} \ln \left[1 + \left(\frac{s}{2\delta} \right)^2 \right] \right\} \quad (32)$$

$$C = \frac{t + s}{t + s(1 - \sigma)} \quad (33)$$

$$\delta' = C\delta \quad (34)$$

DETAILS OF PROCEDURE (cont.)

where:

- s = width of opening between teeth
- δ = air-gap length
- σ = an intermediate factor
- t = length of tooth face
- C = Carter coefficient, the ratio between effective air-gap and actual air-gap
- δ' = effective air gap

$$\sigma = \frac{2}{\pi} \left\{ \tan^{-1} \frac{0.05}{2 \times 0.007} - \frac{0.007}{0.05} \ln \left[1 + \left(\frac{0.05}{2 \times 0.007} \right)^2 \right] \right\} = 0.594 \quad (35)$$

$$C = \frac{0.34 + 0.05}{0.34 + 0.05 (1 - 0.594)} = 1.082 \quad (36)$$

$$\delta' = 1.082 \times 0.007 = 0.00758" \quad (37)$$

The area of each pole face, corrected for air-gap fringing is:

$$A = (l_m + \delta')(l_f + \delta') = (0.875 + 0.0076)(1.156 + 0.0076) \quad (38)$$

$$= 1.03 \text{ in}^2 \quad (39)$$

The length of two air gaps in series is:

$$2 \times 0.00758 = 0.0152" \quad (40)$$

The slope of the air-gap line is:

$$\frac{\phi}{F} = \frac{\mu_r A}{2 \delta'} \quad (41)$$

where: μ_r = the permeability of free space
= 3.192 in mixed English units

$$\frac{\phi}{F} = \frac{3.192 \times 1.03}{0.0152} = 216 \frac{\text{Lines}}{\text{Amp-Turn}} \quad (42)$$

CHARACTERISTICS OF PHOTOGRAPHIC (CONT.)

where:

- δ = effective air gap
- δ' = effective air-gap and actual air-gap
- C = (scatter coefficient, the ratio between
- γ = length of tooth face
- γ' = an intermediate factor
- β = air-gap length
- α = width of opening between teeth

(25)

$$0.594 = \left\{ \frac{0.05}{2 \times 0.007} \tan^{-1} \frac{0.05}{0.007} - \frac{0.007}{0.05} \ln \left[1 + \left(\frac{0.05}{2 \times 0.007} \right)^2 \right] \right\} \times 0.594$$

(26)

$$C = \frac{0.34 + 0.05}{0.34 + 0.05 (1 - 0.594)} = 1.082$$

(27)

$$\delta' = 1.082 \times 0.007 = 0.00758"$$

The area of each pole face, converted for air-gap

fringing is:

(28)

$$A = (l_m + \delta) \left(\frac{1}{\gamma} + \frac{1}{\gamma'} \right) = (0.875 + 0.00758) (1.156 + 0.00758)$$

(29)

$$= 1.03 \text{ in}^2$$

The length of two air gaps in series is:

(30)

$$2 \times 0.00758 = 0.0152"$$

The slope of the air-gap line is:

(31)

$$\frac{dV}{d\delta} = \frac{A}{2\delta^2}$$

where: V = the permeability of free space
 δ = 2.54 in mixed English units

(32)

$$\frac{dV}{d\delta} = \frac{2.19 \times 10^9}{0.0152^2} = 9.18 \times 10^{10} \text{ lines/amp-turn}$$

DETAILS OF PROCEDURE (cont.)

Estimate of Flux Leakage

Leakage flux can be estimated by several methods [6], but in any case the estimate should be checked by actual experiment. For an approximation of the slope of the leakage line, the reluctance of the stator iron is neglected. The short air-gap between the rotor and stator is neglected because the area of this air gap in series with the leakage path cannot be determined and is small compared to the remainder of the leakage path. Only the reluctance in the air between the edges of the teeth is considered as shown in Fig. XXV.

Assume, due to fringing, the area of the gap between teeth edges is twice the area of the edge of a tooth.

The leakage flux of the USS Electrical Grade stator will not be the same as that of the HIPERNIK stator because the former has a slot skew of one slot pitch between stator ends whereas the latter stator has no skew.

For the skewed stator, referring to the dimensions shown in Fig. XX, the length of a tooth edge is:

$$l = \sqrt{(0.875)^2 + (0.34 + 0.05)^2} = 0.958 \quad (43)$$

The leakage line is:

$$\frac{\phi}{F} = \frac{3.192 \times 0.958 \times 0.04 \times 2}{0.05} = 4.9 \quad \frac{\text{Lines}}{\text{Amp-Turn}} \quad (44)$$

Since the rotor sees two of these paths in parallel, the slopes of the leakage line is:

$$\frac{\phi}{F} = 2 \times 4.9 = 9.8 \quad \frac{\text{Lines}}{\text{Amp-Turn}} \quad (45)$$

DETAILS OF PROCEDURE (cont.)

Estimate of Flux Leakage

Leakage flux can be estimated by several methods [5].

but in any case the estimate should be checked by a test.

experiment. For an approximation of the slope of the

leakage line, the reference of the rotor iron to

neglected. The short air-gap between the rotor and stator is

neglected because the area of this air gap is small compared to

leakage path cannot be determined and is small compared to

the remainder of the leakage path. Only the reference in

the air between the edges of the teeth is considered as

shown in Fig. XIV.

Assume, due to fringing, the area of the gap between

teeth edges is twice the area of the edge of a tooth.

The leakage flux of the USSR Electrical Grade stator

will not be the same as that of the HIPERNIX stator

because the former has a slot skew of one slot pitch

between stator slots whereas the latter stator has no skew.

For the skewed stator, referring to the dimensions

shown in Fig. IX, the length of a tooth edge is:

$$l = \sqrt{(0.875)^2 + (0.35 + 0.00)^2} = 0.928 \quad (47)$$

The leakage line is:

$$\frac{L}{W} = \frac{0.125 \times 0.35 \times 0.00 \times 2}{0.00} = 4 \quad (48)$$

Since the rotor has two of these paths in parallel,

the slope of the leakage line is:

$$\frac{L}{W} = 2 \times 4 = 8 \quad (49)$$

DETAILS OF PROCEDURE (cont.)

In addition to leakage between teeth edges, the skewed stator has another leakage path due to a tooth in the gap between adjacent poles which partially overlaps each of the adjacent pole faces as shown by the shaded areas in Fig. XXVI.

The area of each of the triangular shaped air gaps (which are in series) is:

$$A = \frac{1}{2} \left(\frac{1}{4} t \right) \left(\frac{1}{4} l_i \right) = \frac{1}{32} (0.34) (0.875) = 0.0093 \text{ in}^2 \quad (46)$$

and

$$\frac{\phi}{F} = \frac{3.192 \times 0.0093}{2 \times 0.007} = 2.12 \quad \frac{\text{Lines}}{\text{Amp-Turn}} \quad (47)$$

This leakage path can occur only between one pair of adjacent poles at one time; that is, the value $\frac{\phi}{F} = 2.12$ is not doubled since there is no similar path at the other edge of a pole at any one instant.

The total slope of the leakage line for the skewed stator is

$$\frac{\phi}{F} = 9.8 + 2.12 = 11.92 \quad \frac{\text{Lines}}{\text{Amp-Turn}} \quad (48)$$

since the slopes 2.12 and 9.8 are added as paralleled circuit elements.

For the stator without skew, the slope of the leakage line is considered to be:

$$\frac{\phi}{F} = (2) \frac{3.192 \times 0.875 \times 0.04 \times 2}{0.05} = 8.94 \quad \frac{\text{Lines}}{\text{Amp-Turn}} \quad (49)$$

DETAILS OF THE METHOD

In addition to leakage between each object, the
 showed a set of two adjacent leakage paths due to a total in
 the gap between adjacent poles which partially overlaps
 each of the adjacent pole faces as shown by the shaded
 areas in Fig. XVI.

The area of each of the triangular shaped air gaps
 (which are in series) is:

$$A = \frac{1}{2} \left(\frac{1}{4} + \frac{1}{4} \right) \left(\frac{1}{2} \right) = 0.0025 \text{ in}^2 \quad (46)$$

and

$$\frac{\text{Lines}}{\text{Amp-Turn}} = \frac{2.192 \times 0.0025}{2 \times 0.007} = 0.15 \quad (47)$$

This leakage path can occur only between one pair of
 adjacent poles at one time; that is, the value $\frac{1}{2}$ = 0.15
 is not doubled since there is no similar path at the other
 edge of a pole at any one instant.

The total slope of the leakage line for the shaded
 areas is

$$\frac{\text{Lines}}{\text{Amp-Turn}} = 0.8 + 0.15 = 0.95 \quad (48)$$

since the slopes 0.15 and 0.8 are added as parallel
 circuit elements.
 For the series-wound motor the slope of the leakage

line is considered to be:

$$\frac{\text{Lines}}{\text{Amp-Turn}} = \frac{2.192 \times 0.0025}{0.007} = 0.94 \quad (49)$$

FIGURE XXV
PATH ASSUMED FOR LEAKAGE
COMPUTATIONS

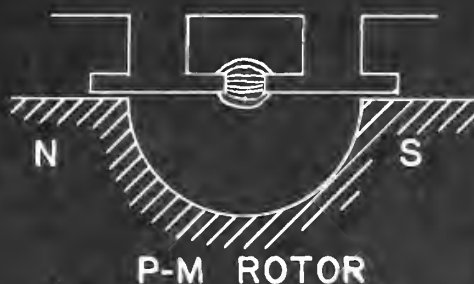
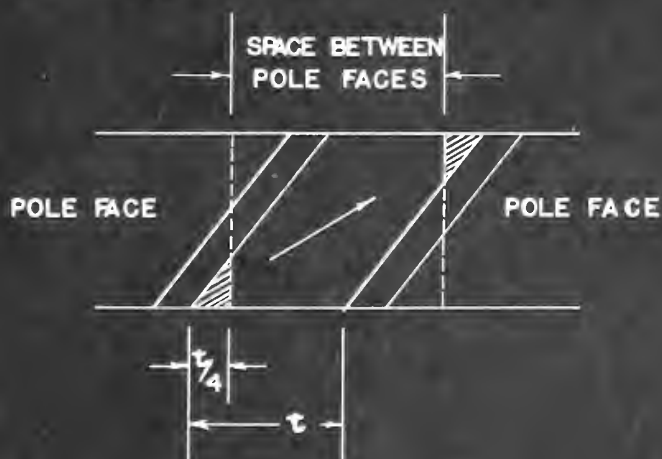


FIGURE XXVI
DEVELOPED SECTION OF STATOR

SHOWING LEAKAGE PATH ALONG LENGTH OF ONE TOOTH
DUE TO SLOT SKEW



VI. APPENDIX B

DETAILS OF CALCULATED DATA

3. KITCHEN . IV

ATACI COTADU' LAC NO SIAATHE

DETAILS OF CALCULATED DATA

TABLE I

Plot of the demagnetization curve of Alnico VI in terms of
Flux and Magnetomotive force

Flux Density (kilogauss) B	Flux Φ_m (kilolines) $BA \times 6.45$	Magnetizing Force H: (amp-turns/in.)	Magnetomotive Force, F, or Mag. Potential difference U. (amp-turns) $H \times L_m$ $H \times 2.78"$
10.3	67.3	0	0
9.98	65.2	100	278
9.50	62.0	200	556
8.99	58.65	300	833
8.20	53.60	400	1113
7.05	46.00	500	1390
5.20	34.0	600	1669
3.75	24.5	650	1807
2.00	13.05	700	1945
0.0	0.0	750	2085

TABLE 1

FIGURE 1

Plot of the degradation curve of Alnico V in terms of
flux and magnetic force

Flux Density (kilogauss) B	Flux Φ (kilolines) $BA \times 10^{-6}$	Magnetizing Force H: (amp-turns/in.)	Magnetomotive Force, V, or Magnetizing Force, H: (amp-turns/in.)
10.7	67.5	0	0
9.68	60.8	100	25
8.58	58.0	200	50
8.22	56.05	300	75
8.00	55.00	400	100
7.68	48.00	500	125
7.50	48.0	600	150
7.40	47.5	650	162.5
7.00	45.00	700	175
6.5	42.0	750	187.5

DETAILS OF CALCULATED DATA (cont.)

Plot of magnetization curve of USS Electrical Steel in terms of flux and magnetic potential drop:

Flux density (Kilogauss) multiplied by effective cross section and a conversion factor 6.45 equals flux in kilolines:

$$\phi = B \times A \times 6.45 = B \times .156 \times 6.45 \quad (50)$$

Magnetizing force H (Oersteds) multiplied by the length of the magnetic path and the conversion factor 2.01 equals magnetic potential drop U in ampere turns:

$$U = H \times L \times 2.01 = H \times 2.25 \times 2.01 \quad (51)$$

TABLE II

26 Gauge USS Electrical

ϕ (kilolines)	U (amp-turns)
0	3.15
4.68	4.28
6.24	4.73
7.80	6.30
9.36	7.20
10.92	11.25
11.70	14.25
12.50	21.6
13.26	32.6
14.05	54.0
14.82	88.9
15.60	157.6
16.39	239
17.18	446
17.95	619

TABLE II

Plot of magnetization curves of USS Electrical Steel in terms

of flux and magnetic potential drop:

Flux density (kilogauss) multiplied by effective cross

section and a conversion factor 0.47 equals flux in

kilolines:

$$\Phi = B \times A \times 0.47 = B \times 1.56 \times 0.47 \quad (50)$$

Magnetizing force H (Oersteds) multiplied by the length of

the magnetic path and the conversion factor 0.01 equals

magnetic potential drop U in ampere turns:

$$U = H \times L \times 0.01 = H \times 2.50 \times 0.01 \quad (51)$$

TABLE II

50 Gauss USS Electrical

U (amp-turns)

B (kilolines)

0	0
4.66	4.66
6.64	6.64
7.80	7.80
9.40	9.40
10.90	10.90
11.70	11.70
12.40	12.40
13.40	13.40
14.00	14.00
14.50	14.50
14.80	14.80
15.00	15.00
15.20	15.20
15.40	15.40
15.60	15.60
15.80	15.80
16.00	16.00
16.20	16.20
16.40	16.40
16.60	16.60
16.80	16.80
17.00	17.00

DETAILS OF CALCULATED DATA (cont.)

TABLE III

Magnetic Circuit Dimensions

Area of magnet pole-face = 1.011 sq. in.

Minimum area of stator path = 0.156 sq. in.

Length of mean rotor flux path = 2.78 inches.

Length of air gap = 0.007 inches (at each pole face)

Total effective length of air gap = 0.0154 inches

Length of stator (saturable) path = 2.25 inches

DETAILS OF CALCULATED DATA (cont.)

TABLE III

Magnetic Circuit Dimensions

Area of magnet pole-face = 1.01 sq. in.
Minimum area of stator path = 0.135 sq. in.
Length of mean rotor flux path = 2.78 inches.
Length of air gap = 0.007 inches (at each pole face)
Total effective length of air gap = 0.0154 inches
Length of stator (assumed) path = 0.32 inches

DETAILS OF CALCULATED DATA (cont.)

TABLE IV

Plot of the magnetization curve of HIPERNIK in terms of
flux and magnetic potential drop

Conversion factors same as on previous page:

B (Kilogauss)	ϕ (kilolines)	H (Oersted)	U (amp-turns)
0	0	0	0
9.6	9.65	0.2	.911
10.6	10.65	0.4	1.82
11.2	11.25	0.6	2.73
11.6	11.68	0.8	3.64
11.9	11.98	1.0	4.55
12.1	12.18	1.2	5.56
15.2	15.29	20.0	91.1
15.75	15.85	40.0	182.0
15.85	15.95	60.0	273
15.9	16.0	80.0	364
16.0	16.09	100.0	455

DETAILS OF CALCULATED DATA (Cont.)

TABLE IV

Plot of the magnetization curves of HYPERMIX in terms of flux and magnetic potential drop

Conversion factors same as in previous pages

B (kilogauss)	H (kilolines)	H (oersteds)	B (gauss-cm)
0	0	0	0
9.8	98.9	0.3	110.
10.8	108.8	0.4	118.1
11.8	118.8	0.6	125.8
11.8	118.8	0.8	130.8
11.9	119.8	1.0	135.8
12.1	121.8	1.2	140.8
12.2	122.8	0.05	141.1
12.35	123.8	0.04	142.0
12.85	128.8	0.03	143
12.9	129.8	0.08	144
13.0	130.8	0.001	145

DATA

TABLE V

DETAILS OF STATORS

STATOR NO. 1:

Material: USS Electrical Grade Steel, 0.014" Laminations

Toroidal
Winding: 9 turns per slot, 162 total turns, #24 wire
0.96 ohms cold
4.4 millihenries

Three-phase
Winding: 40 turns per coil of #29 wire
Line to line Resistance: 23.4 ohms (cold)
Skewed one slot pitch

STATOR NO. 2:

Material: Hipernik, annealed in Hydrogen atmosphere

Toroidal
Winding: 11 turns per slot, 198 turns total, #24 wire
1.11 ohms (room temperature)
16 millihenries

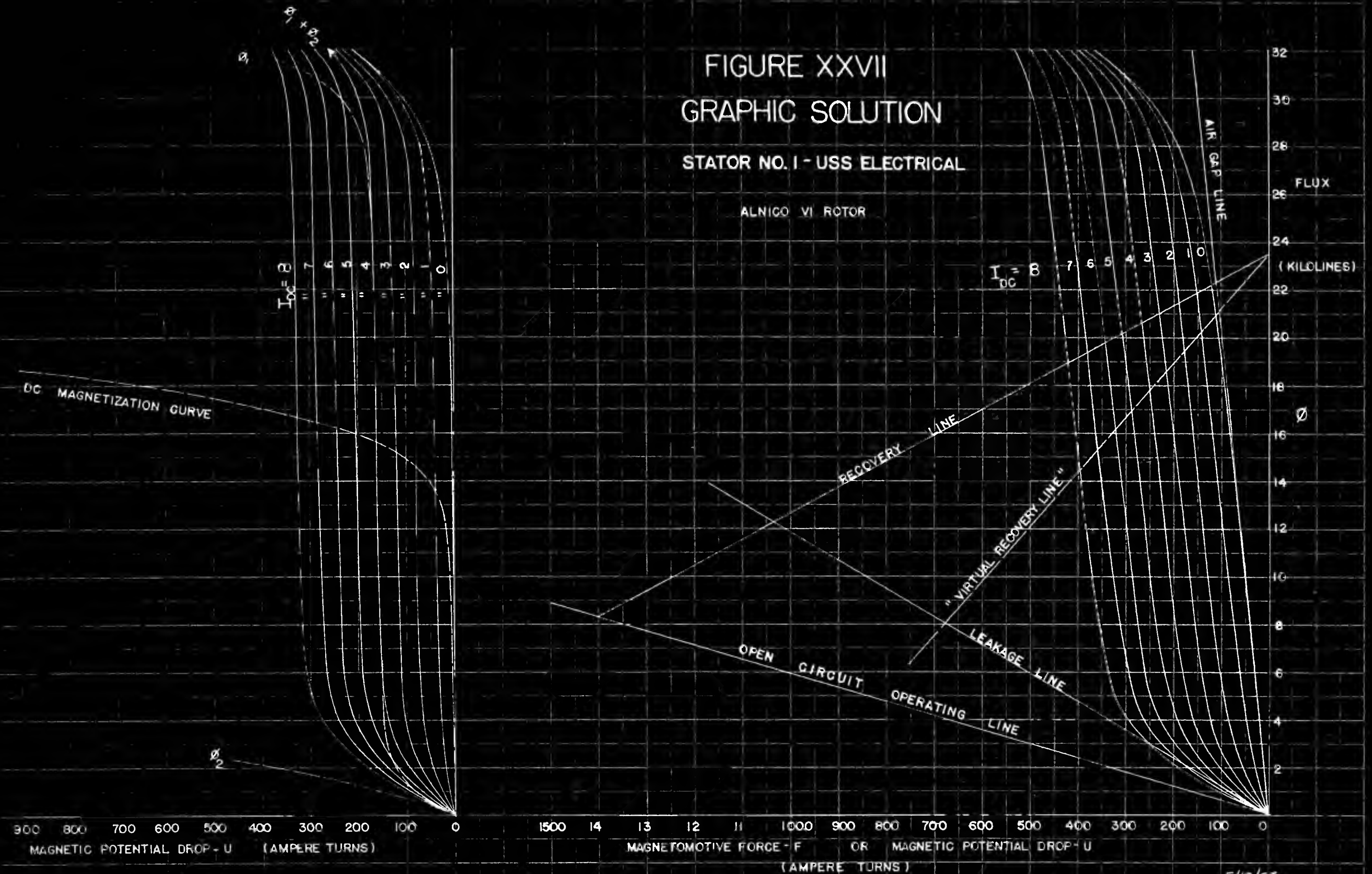
Three-phase
Winding: 40 turns per coil of #26 wire
Line to line resistance: 11 ohms (Rm. Temp)
9.5 millihenries
No skew

In both stators the length of the magnetic path was assumed to be 2.25 inches, and the cross sectional area 0.156 square inches.

FIGURE XXVII GRAPHIC SOLUTION

STATOR NO. 1 - USS ELECTRICAL

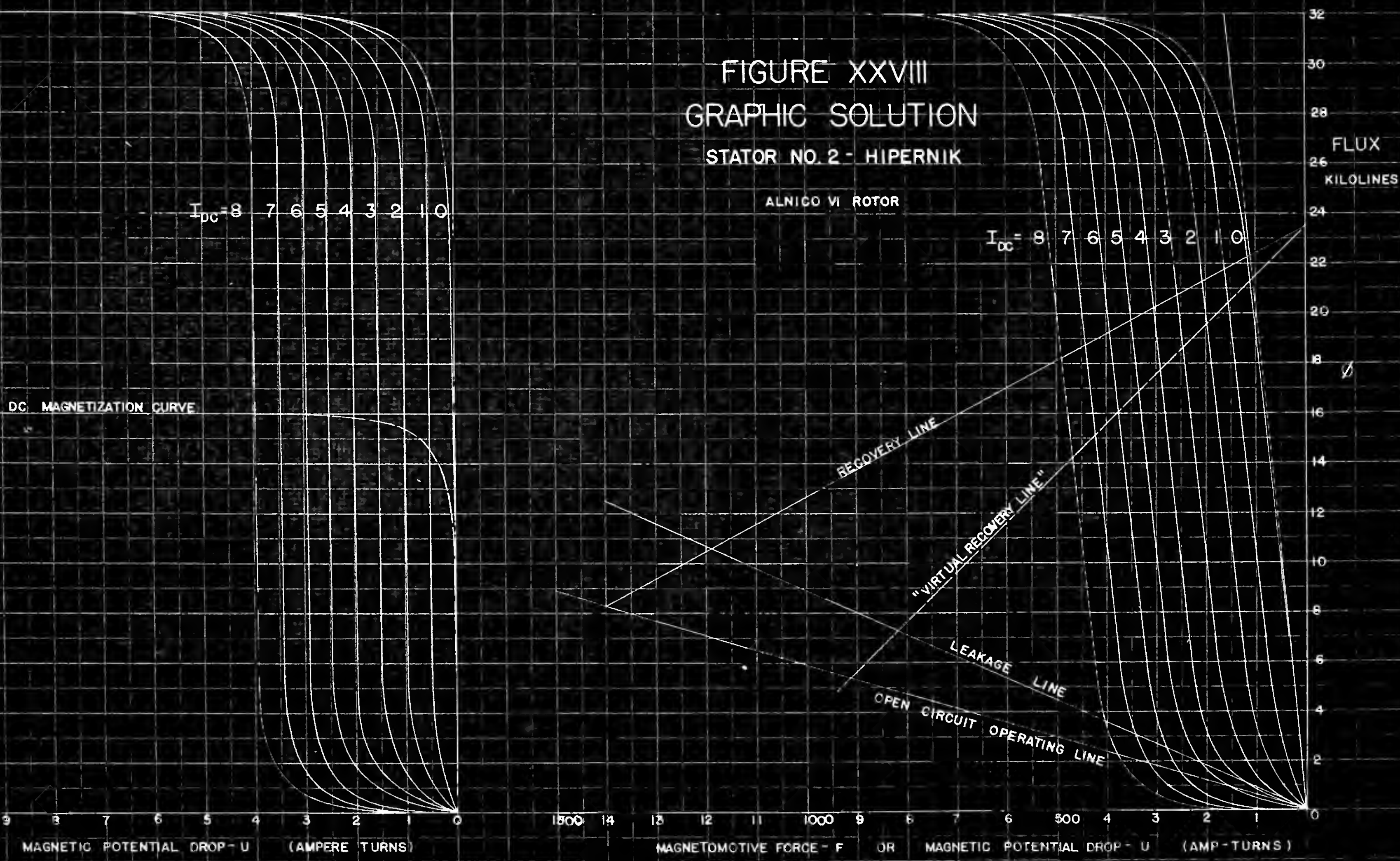
ALNICO VI ROTOR



5/18/53
JLA:WJA

FIGURE XXVIII
GRAPHIC SOLUTION
STATOR NO. 2 - HIPERNIK

ALNICO VI ROTOR



5/12/63
STA 214

VI. APPENDIX C

SUMMARY OF DATA AND CALCULATIONS

O KURUMETA . IV

DEL ITA. TO. CIA. ATAC. VO. YAMENE

SUMMARY OF DATA AND CALCULATIONS

The summary of data and calculations is presented in the graphs following.

Figure XXIX:

This figure shows the percentage of initial voltage of the alternator as obtained both by theoretical means and by experiment. The stator laminations are of USS Electrical Grade Steel, and the stack is skewed one slot pitch. The dotted line is the theoretical curve as calculated by the method explained in Section II, "PROCEDURE". Experimental values obtained under various conditions of loading are shown and explained on the figure.

Figure XXX:

This figure is a summary of raw data for the HIPERNIK stator.

Figure XXXI:

This figure is similar to Figure XXIX, except that it represents analysis and experiment on a stator whose laminations are of HIPERNIK and whose slots have no skew. The loads are also slightly different as explained on the figure.

Figure XXXII:

This figure shows the comparison of voltage behavior with and without additional leakage paths being added to the magnetic circuit.

SUMMARY OF DATA AND CALCULATIONS

The summary of data and calculations is presented in

the graphs following.

Figure XXIX:

This figure shows the percentage of initial voltage of the alternator as obtained both by theoretical means and by experiment. The stator laminations are of USS Electrical Grade Steel, and the stack is shown one slot pitch. The dotted line is the theoretical curve as calculated by the method explained in Section II, "PROCEDURE". Experimental values obtained under various conditions of loading are shown and explained on the figure.

Figure XXX:

This figure is a summary of raw data for the HIFERNIX

stator.

Figure XXXI:

This figure is similar to Figure XXIX, except that it represents analysis and experiment on a stator whose laminations are of HIFERNIX and whose slots have no skew. The loads are also slightly different as explained on the figure.

Figure XXXII:

This figure shows the comparison of voltage behavior with and without additional leakage paths being added to the magnetic circuit.

FIGURE XXIX

FIGURE XXIX

STATOR NO. 1 - USS ELECTRICAL

PERCENT OF INITIAL VOLTAGE VS. CONTROL MAGNETOMOTIVE FORCE

EXPERIMENTAL - 400 CPS - ALL LOADS
CALCULATED FROM FIG. XXVIII

PERCENT OF INITIAL VOLTAGE

NOTE: THIS STATOR CONTAINED MULTIPLE GROUNDS IN THE TOROIDAL WINDING, MAKING THE EXPERIMENTAL DATA QUANTITATIVELY UNRELIABLE. THEREFORE FURTHER CONCLUSIONS WERE BASED PRINCIPALLY ON THE REACTIONS OF STATOR NO. 2

CONTROL MAGNETOMOTIVE FORCE AMP TURNS

FIGURE XXX

STATOR NO.2 - HIPERNIK

TERMINAL VOLTAGE VS. CONTROL MMF
FOR VARIOUS LOADS

400 CPS

VOLTAGE

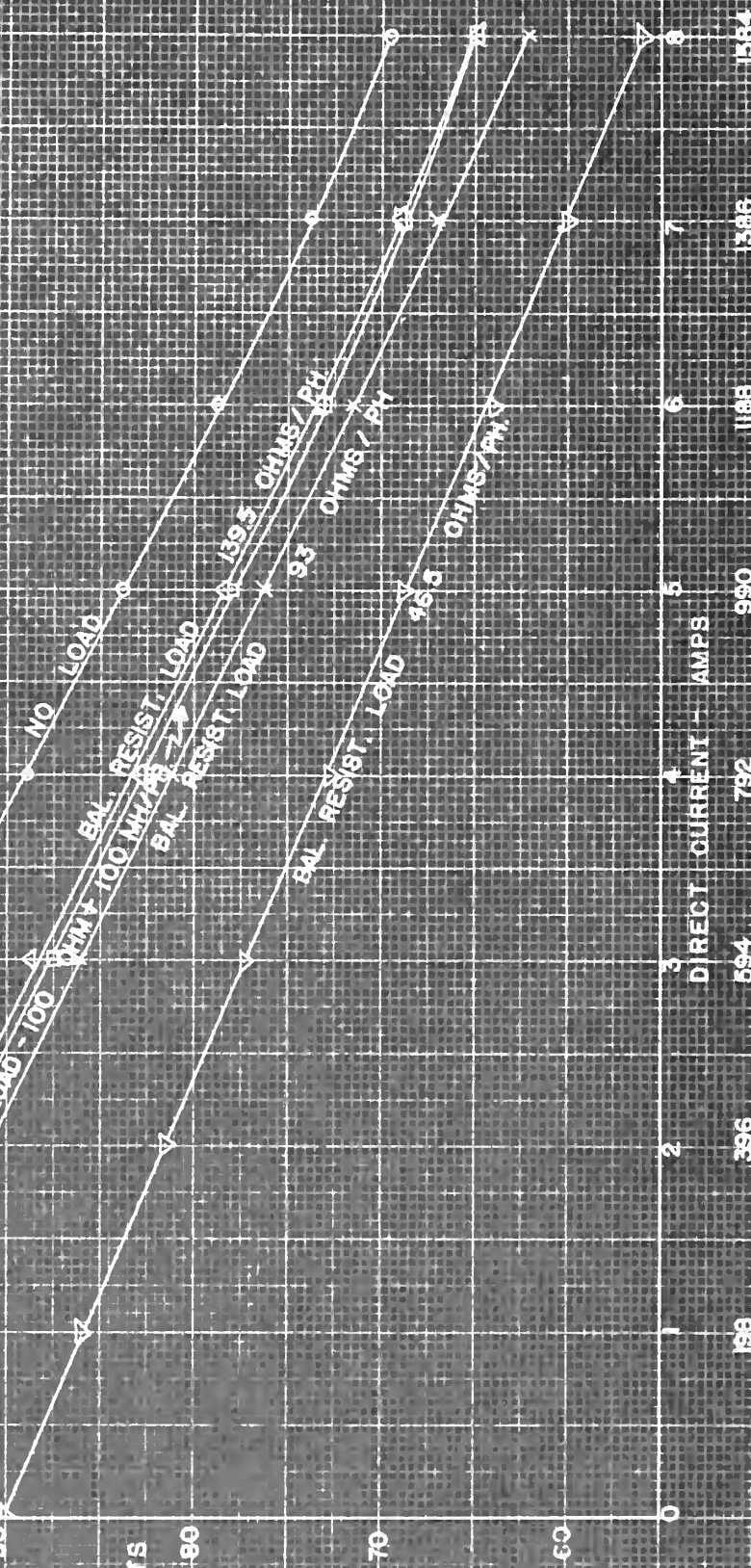
LINE TO LINE

VOLTS

DIRECT CURRENT - AMPS

MAGNETOMOTIVE FORCE - AMP TURNS

FIGURE XXX



5-18-53
FCA WLA

FIGURE XXXI

STATOR NO. 2 - HIPERNIK

PERCENT OF INITIAL VOLTAGE

VS.

CONTROL MAGNETOMOTIVE FORCE

CALCULATED
EXPERIMENTAL

FROM FIG. XXVIII

PERCENT
OF
INITIAL VOLTAGE

NOTE: THE DIFFERENCE BETWEEN CALCULATED AND EXPERIMENTAL RESULTS IS DUE TO THE DIFFERENCE BETWEEN ACTUAL LEAKAGE AND ESTIMATED LEAKAGE.

100

300

500

700

900

1100

1300

1500

1700

1900

2100

2300

2500

2700

2900

3100

70

80

90

100

110

120

1000

1200

1400

1600

1800

2000

2200

2400

2600

2800

3000

3200

3400

3600

3800

4000

4200

4400

4600

4800

5000

5200

5400

5600

5800

6000

6200

6400

6600

6800

FORCE (F) - AMP TURNS

MAGNETOMOTIVE

CONTROL

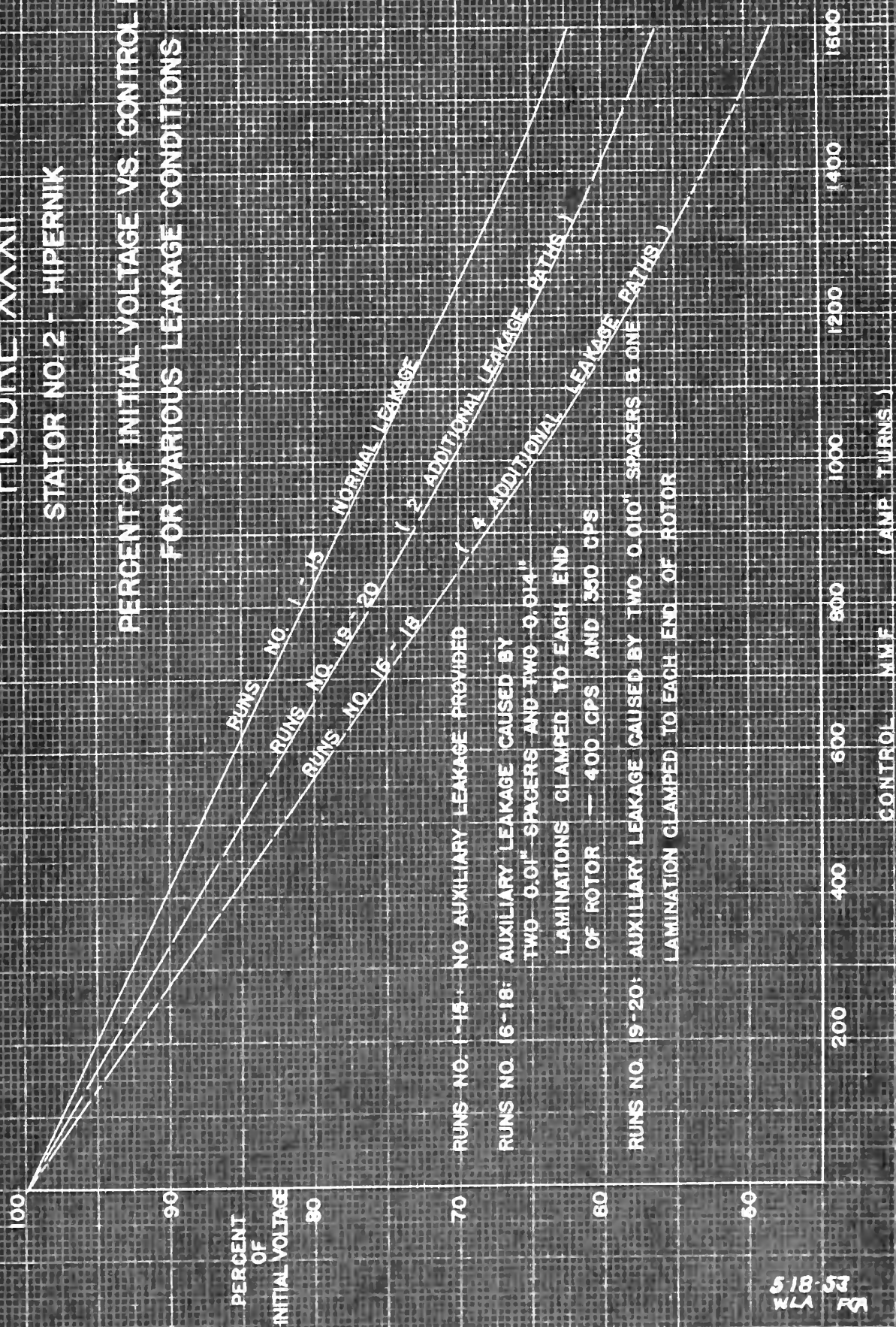
5-18-53
WLA RA

FIGURE XXXII

STATOR NO. 2 - HIPERNIK

PERCENT OF INITIAL VOLTAGE VS. CONTROL MMF
FOR VARIOUS LEAKAGE CONDITIONS

FIGURE XXXII



518-53
WLA FOR

SUMMARY OF DATA AND CALCULATIONS (cont.)

Figures XXXIII through XXXVIII:

These curves are all derived from the three curves mentioned on the previous page. They are presented as an aid in visualizing the behavior of the alternator under the specified conditions.

EXAMINATION OF DATA AND CALCULATIONS (cont.)

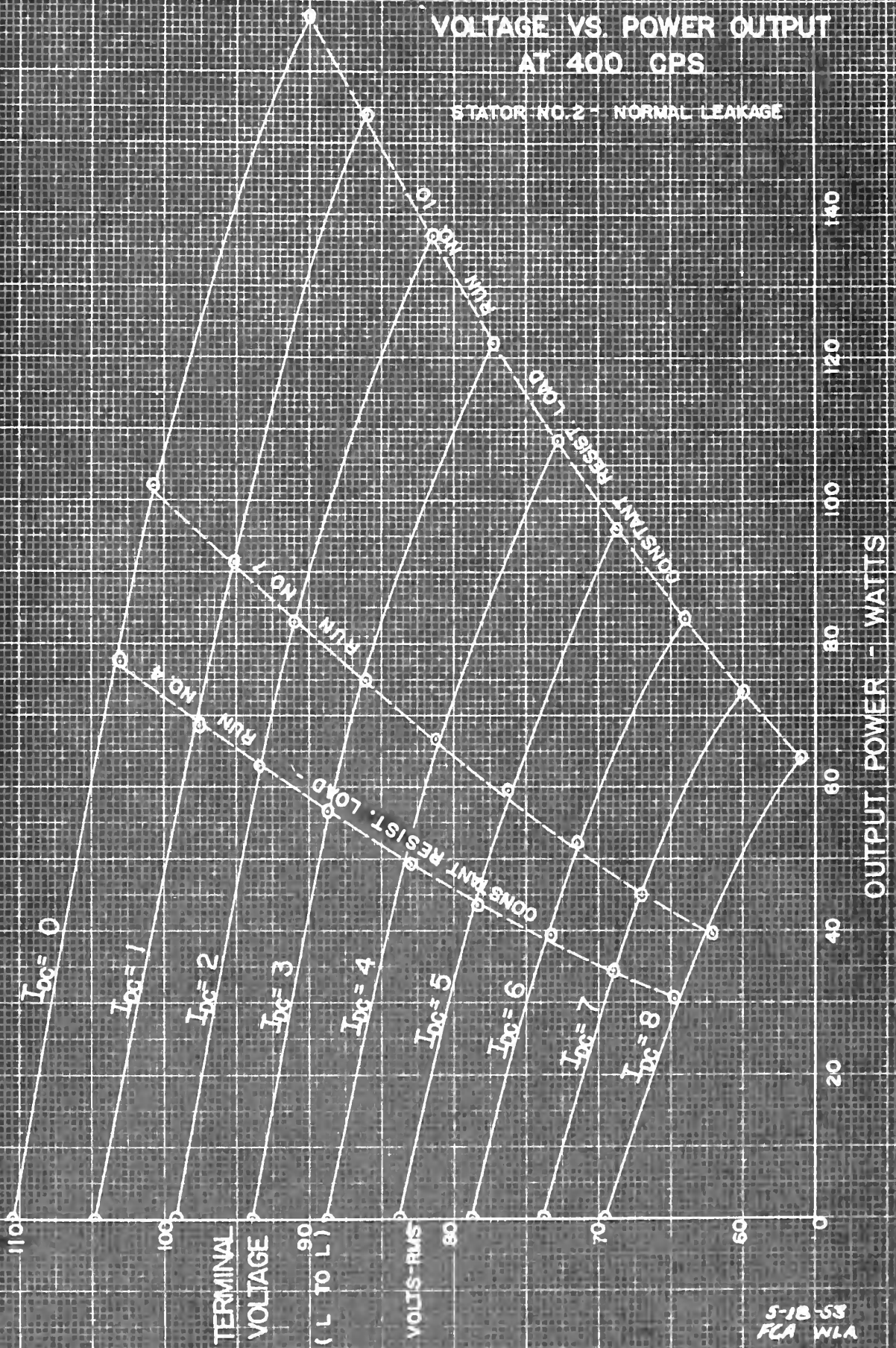
Figure XXXIII (cont.) XXXIV

These curves are all derived from the same curves mentioned on the previous page. They are presented as an aid in visualizing the behavior of the reactor under the specified conditions.

FIGURE XXXIII

VOLTAGE VS. POWER OUTPUT AT 400 CPS

STATOR NO. 2 - NORMAL LEAKAGE

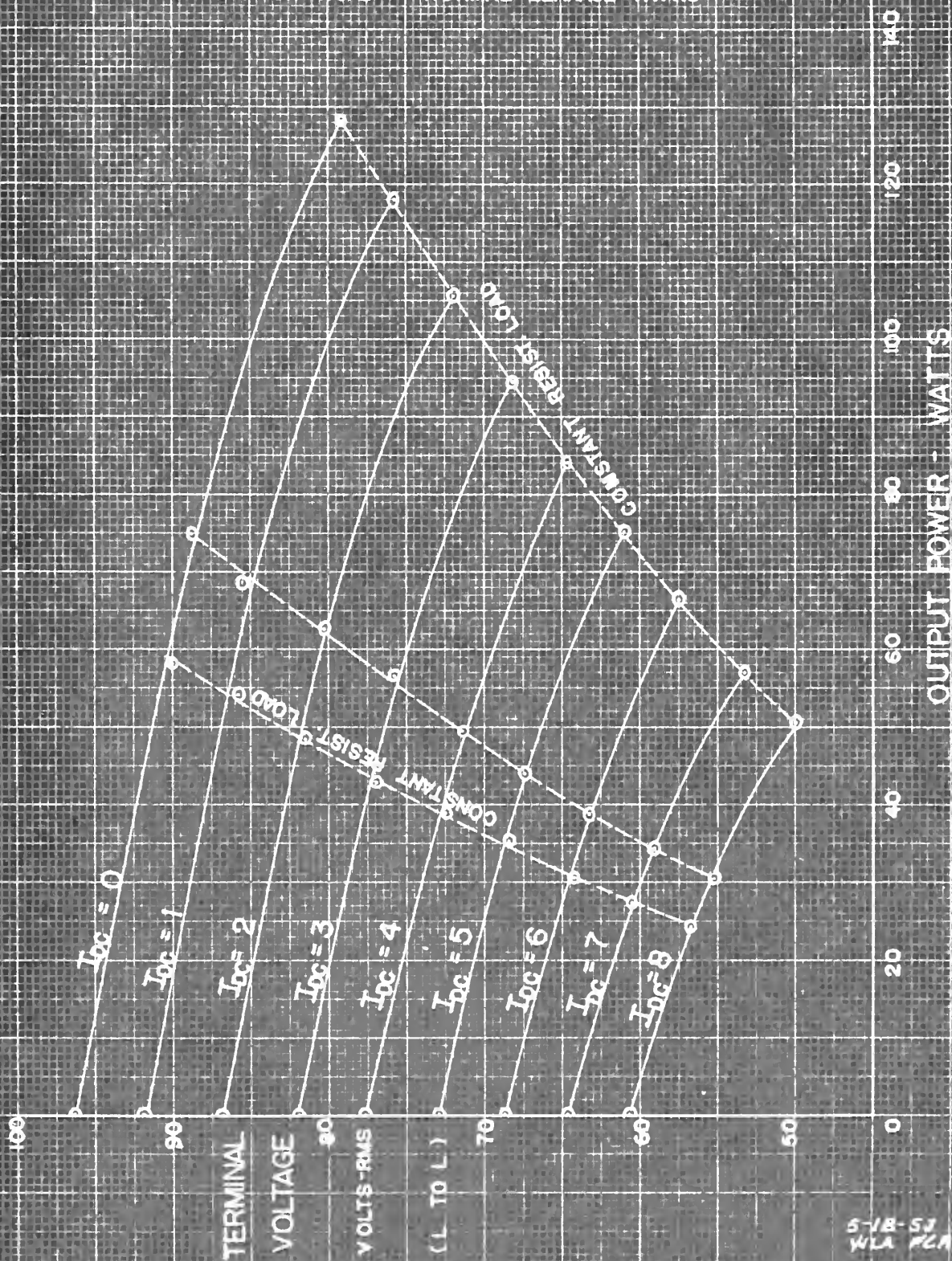


5-18-53
FLA WLA

FIGURE XXXIV

VOLTAGE VS. POWER OUTPUT
AT 350 CPS

STATOR NO. 2 NORMAL LEAKAGE PATHS

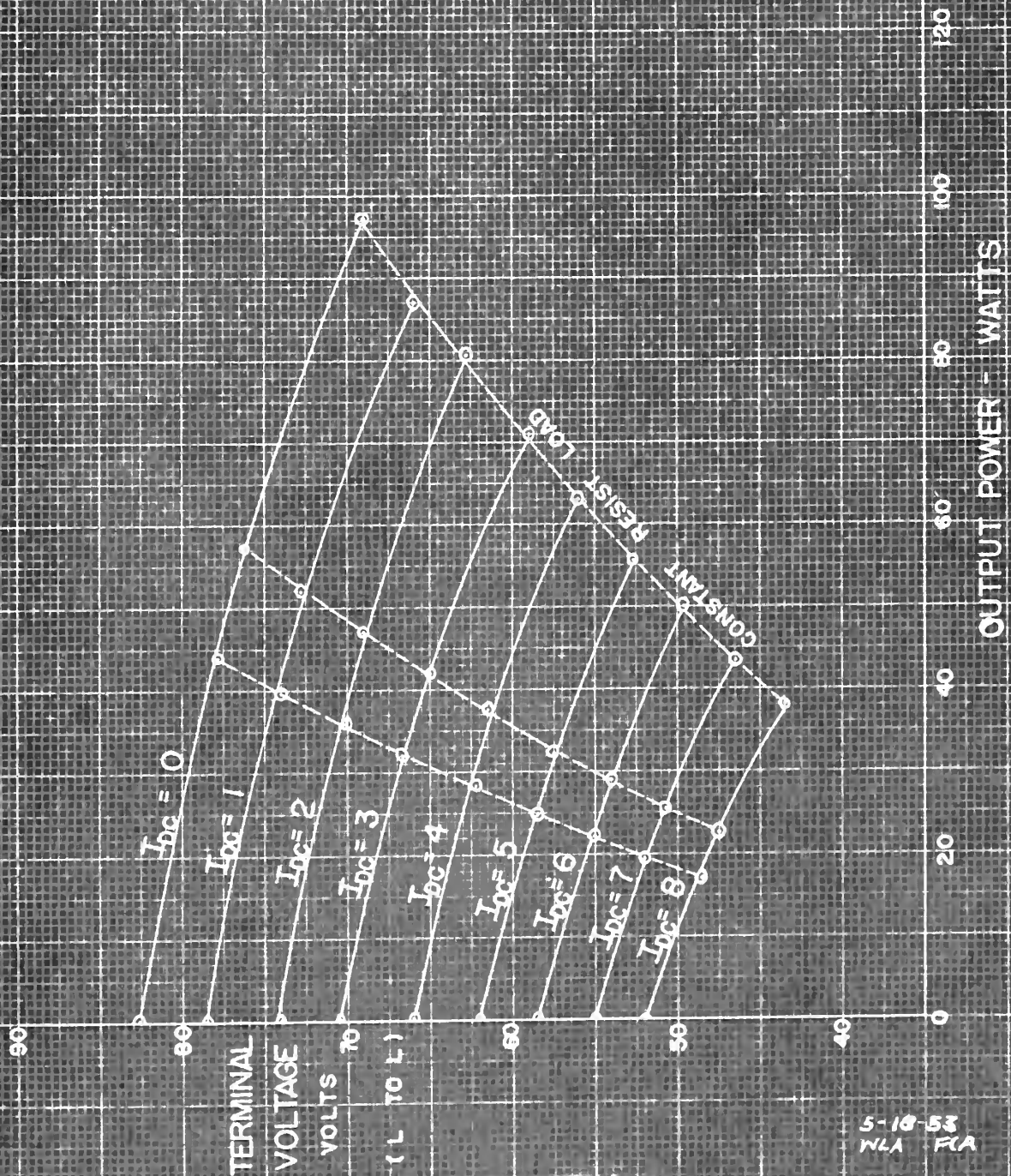


5-18-53
WLA WLA

FIGURE XXXV

VOLTAGE VS. POWER OUTPUT
- AT 300 CPS

STATOR NO. 2 - NORMAL LEAKAGE PATHS



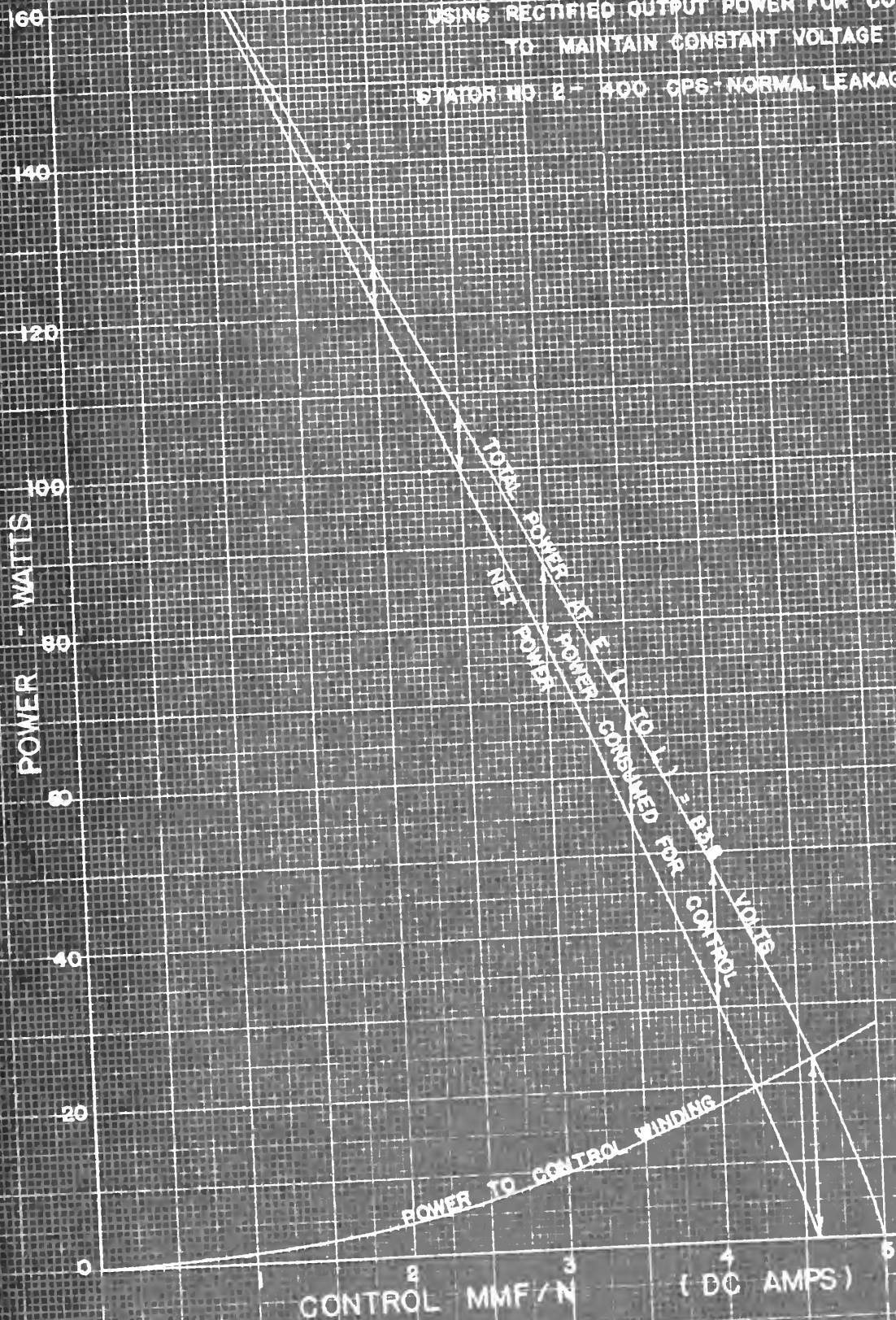
5-18-53
WLA FCA

FIGURE XXXVI

POWER ANALYSIS -

USING RECTIFIED OUTPUT POWER FOR CONTROL
TO MAINTAIN CONSTANT VOLTAGE

STATOR NO. 2 - 400 CPS - NORMAL LEAKAGE PATHS



3-18-52
WLA KLA

FIGURE XXXVII

CONSTANT POWER OUTPUT WITH VARIABLE ALTERNATOR SPEEDS BETWEEN 9000 AND 12000 REV. PER MIN.

STATOR NO. 2 - NORMAL LEAKAGE

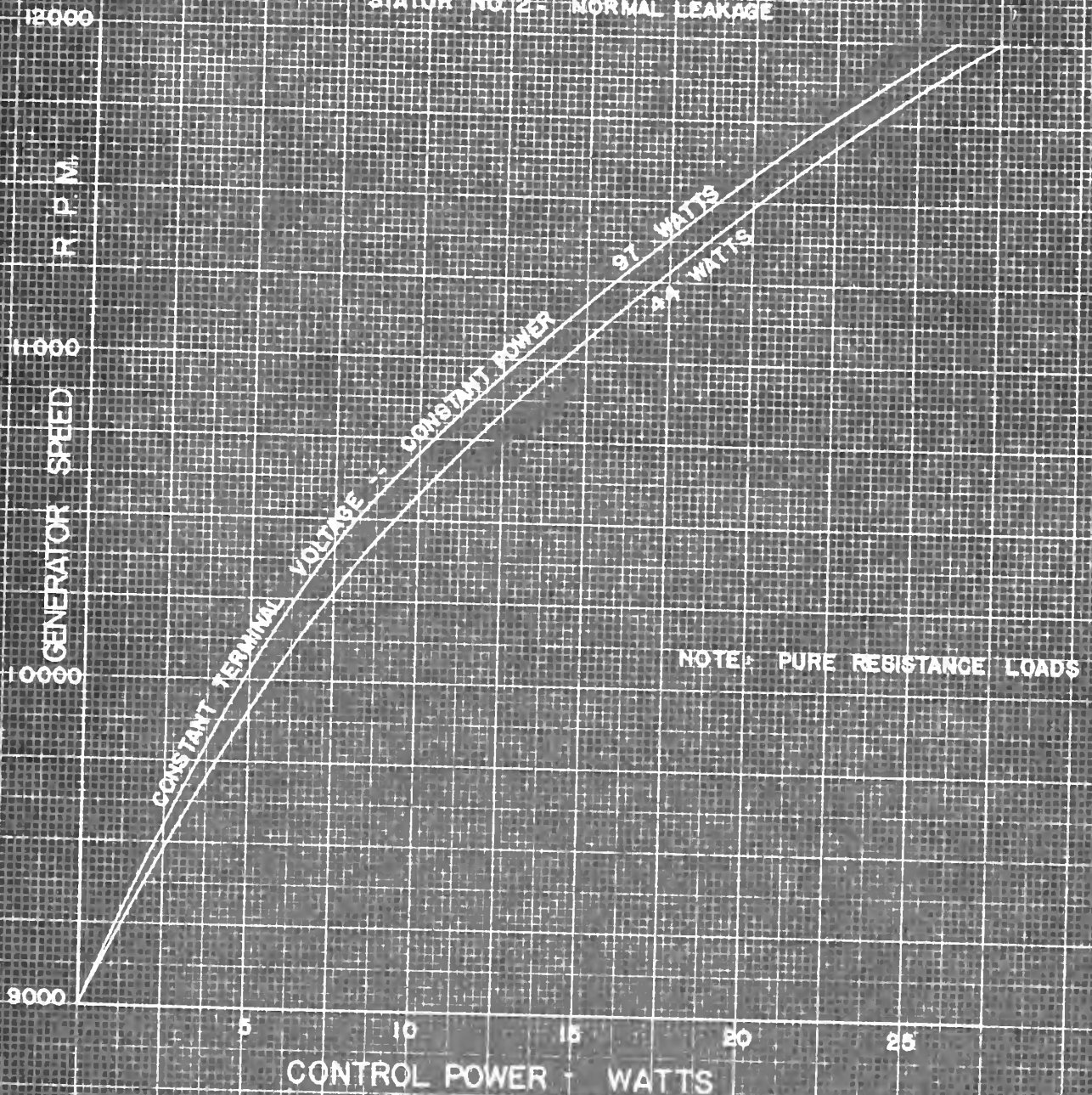
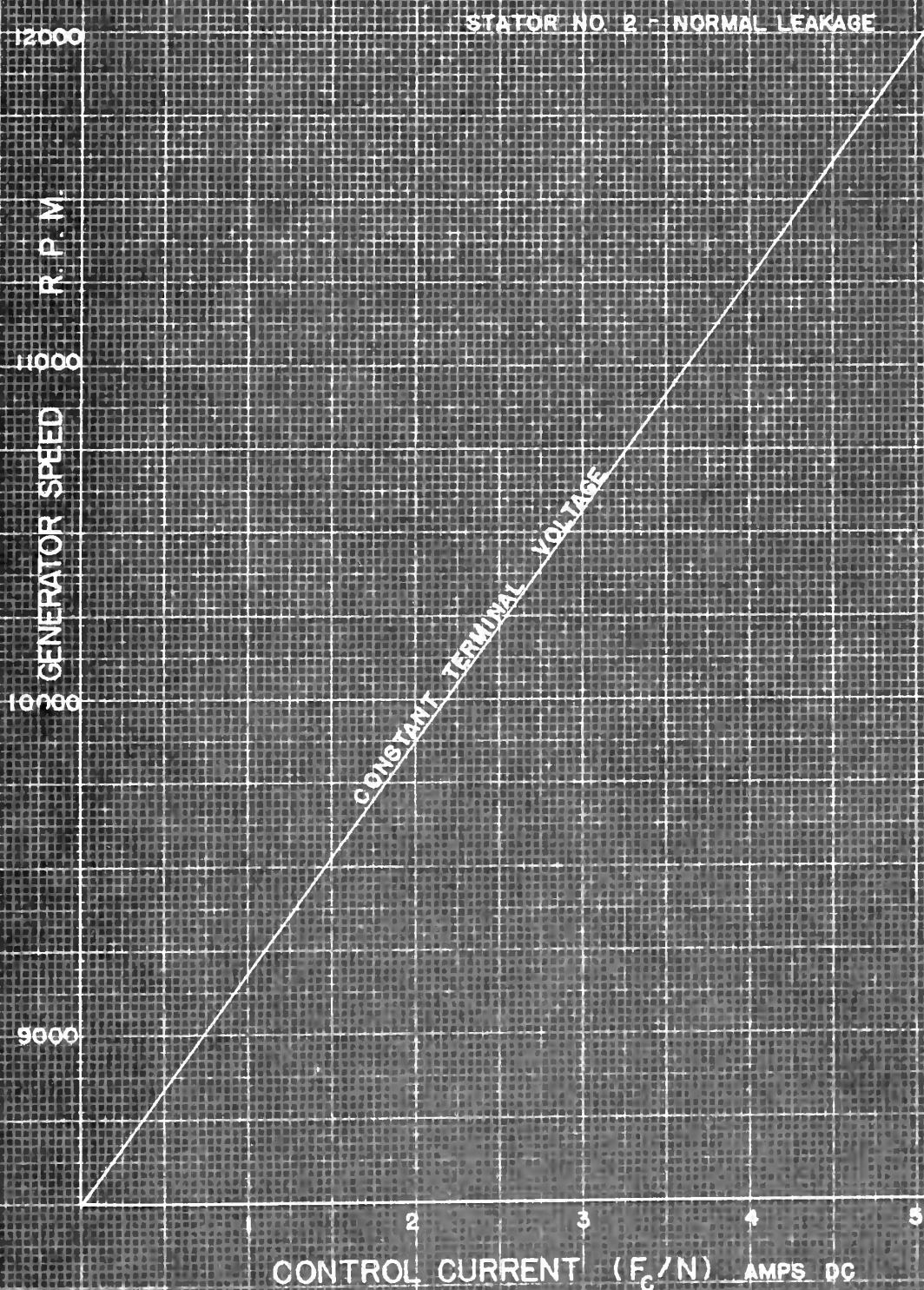


FIGURE XXXVIII

GENERATOR SPEED VS. CONTROL CURRENT
AT CONSTANT TERMINAL VOLTAGE



5-18-53
FLA WLA

VII. APPENDIX D

EXPERIMENTAL DATA

ALL. APPENDIX D

EXPERIMENTAL DATA

DATA

STATOR NO. 1
USS ELECTRICAL GRADE STEEL

RUN NO. 1
NO LOAD- CONSTANT FREQUENCY
400 cps

I_{dc}	F_c	$V_{L \text{ to } L}$	I_a	P_{dc}	P_{ac}	PERCENT INITIAL V
AMPS	AMP-TURNS	VOLTS	AMPS	WATTS	WATTS	%
0	0	101.5	0	0	No load	100
1	162	99.0	0	0.96	0	97.5
2	324	96.0	0	3.84	0	94.5
3	486	93.0	0	8.64	0	91.5
4	648	89.9	0	15.36	0	88.5
5	810	86.8	0	24.0	0	85.5
6	972	83.9	0	34.56	0	82.6
7	1134	81.0	0	47.04	0	79.7
8	1296	78.1	0	61.44	0	76.9

RMS

DATA

STATOR NO. 1
USS ELECTRICAL GRADE STEEL

RUN NO. 2
BALANCED RESISTIVE LOAD—200 OHMS PER PH.
CONSTANT FREQUENCY— 400 cps

I_{dc}	F_c	V_L to L	I_a	P_{dc}	P_{ac}	PERCENT INITIAL V
Amps	Amp-turns	Volts	amps	Watts	Watts	%
0	0	95.0	.2665	0	42.6	100
1	162	92.9	.260	0.96	40.6	97.6
2	324	90.1	.252	3.84	38.1	94.7
3	486	87.1	.244	8.64	35.7	91.6
4	648	83.9	.236	15.36	33.4	88.2
5	810	81.1	.228	24.0	31.2	85.3
6	972	78.1	.219	34.56	28.8	82.1
7	1134	75.4	.211	47.04	26.7	79.3
8	1296	73.0	.205	61.44	25.2	76.75

DATA

STATOR NO. 1
USS ELECTRICAL GRADE STEEL

RUN NO. 3

BALANCED RESISTIVE LOAD - 150 OHMS/PHASE
CONSTANT FREQUENCY - 400 cps

I_{dc}	F_c	$V_{L \text{ to } L}$	I_a	P_c	P_{ac}	PERCENT INITIAL V
Amps	Amp-turns	Volts	amps	watts	watts	%
0	0	92.6	.325	0	47.5	100
1	162	90.5	.317	0.96	45.3	97.6
2	324	87.9	.308	3.84	42.6	94.9
3	486	84.9	.298	8.64	40.0	91.6
4	648	82.0	.288	15.36	37.3	88.5
5	810	79.1	.279	24.0	35.0	85.4
6	972	76.5	.269	34.56	32.5	82.6
7	1134	73.6	.259	47.04	30.2	79.4
8	1296	71.0	.251	61.44	28.4	76.7

DATA

STATOR NO. 1
USS ELECTRICAL GRADE STEEL

RUN NO. 4

BALANCED RESISTIVE LOAD - 100 OHMS/PH
CONSTANT FREQUENCY - 400 cps

I_{dc}	F_c	V_L to L	I_a	P_{dc}	P_{ac}	PERCENT INITIAL V
Amps	Amp-turns	Volts	Amps	Watts	Watts	%
0	0	89.0	.454	0	61.9	100
1	162	87.1	.444	0.96	59.1	97.9
2	324	84.1	.429	3.84	55.3	94.5
3	486	81.1	.415	8.64	51.8	91.1
4	648	77.6	.398	15.36	47.5	87.2
5	810	74.4	.386	24.00	44.7	83.6
6	972	73.1	.376	34.56	42.4	82.1
7	1134	70.9	.363	47.04	39.5	79.7
8	1296	68.1	.350	61.44	36.8	76.6

DATA

STATOR NO. 1
USS ELECTRICAL GRADE STEEL

RUN NO. 5

BALANCED INDUCTIVE LOAD- 100 OHMS & 100 Mh/PH
CONSTANT FREQUENCY - 400 cps

I_{dc}	F_c	V_L to L	I_a	P_{dc}	P_{ac}	PERCENT INITIAL V
Amps	Amp-turns	Volts	Amps	Watts	Watts	%
0	0	93.5	.195	0	11.4	100
1	162	91.2	.191	0.96	10.95	97.5
2	324	88.8	.185	3.84	10.28	95.0
3	486	85.4	.179	8.64	9.62	91.4
4	648	82.8	.174	15.36	9.08	88.6
5	810	80.0	.1675	24.0	8.42	85.6
6	972	77.3	.161	34.56	7.78	82.7
7	1134	74.5	.156	47.04	7.30	79.6
8	1296	72.0	.150	61.44	6.75	77.0

DATA
 STATOR NO. 2
 HIPERNIK
 RUN NO. 1
 NO LOAD—CONSTANT FREQUENCY
 400 cps

I_{dc} Amps	F_c Amp-turns	V_L to L Volts	I_a amps	P_{dc} watts	P_{ac} watts	Percent Initial V %
0	0	110.5	0	0	0	100
1	198	104.5	0	1.1	0	94.8
2	396	99.3	0	4.4	0	89.8
3	594	94.0	0	10.0	0	85.0
4	792	88.9	0	17.8	0	80.4
5	990	83.8	0	27.7	0	75.8
6	1188	78.8	0	39.5	0	71.4
7	138.6	73.8	0	54.4	0	66.8
8	1584	69.6	0	71.1	0	63.0

RMS

DATA

STATOR NO. 2
HIPERNIK

RUN NO. 2

NO LOAD
CONSTANT FREQUENCY - 350 cps

I_{dc} Amps	F_c Amp-turns	$V_{L \text{ to } L}$ Volts	I_a Amps	P_{dc} Watts	P_{ac} Watts	PERCENT INITIAL V %
0	0	96.4	0	0	0	100
1	198	92.0	0	1.1	0	95.5
2	396	86.8	0	4.4	0	90.2
3	594	82.0	0	10.0	0	85.2
4	792	77.7	0	17.8	0	80.6
5	990	73.0	0	27.7	0	75.8
6	1188	68.8	0	39.5	0	71.4
7	1386	64.7	0	54.4	0	67.2
8	1584	60.7	0	71.1	0	63.0

DATA

STATOR NO. 2
HIPERNIK

RUN NO. 3

NO LOAD
CONSTANT FREQUENCY - 300 cps

I_{dc} Amps	F_c Amp-turns	$V_{L \text{ to } L}$ Volts	I_a Amps	P_{dc} Watts	P_{ac} Watts	PERCENT INITIAL V %
0	0	82.6	0	0	0	100
1	198	78.5	0	1.1	0	95.0
2	396	74.0	0	4.4	0	89.6
3	594	70.5	0	10.0	0	85.4
4	792	66.0	0	17.8	0	79.8
5	990	62.1	0	27.7	0	75.2
6	1188	58.5	0	39.5	0	70.8
7	1386	55.0	0	54.4	0	66.6
8	1584	52.0	0	71.1	0	63.0

DATA

STATOR NO. 2
HIPERNIK

RUN NO. 4

BALANCED RESISTIVE LOAD - 139.5 OHMS/PH
CONSTANT FREQUENCY - 400 cps

I_{dc} Amps	F_c Amp-turns	$V_{L \text{ to } L}$ Volts	I_a Amps	P_{dc} Watts	P_{ac} Watts	PERCENT INITIAL V %
0	0	103	.43	0	77.4	100
1	198	97.5	.405	1.1	68.6	94.6
2	396	93.5	.388	4.4	62.9	90.8
3	594	88.7	.368	10.0	56.6	86.1
4	792	82.9	.343	17.8	49.2	80.6
5	990	78.4	.322	27.7	43.4	76.1
6	1188	73.3	.307	39.5	39.4	71.2
7	1386	69.0	.287	54.4	34.4	67.0
8	1584	64.8	.270	71.1	30.5	62.9

DATA

STATOR NO. 2
HIPERNIK

RUN NO. 5

BALANCED RESISTANCE LOAD - 139.5 OHMS/PH
CONSTANT FREQUENCY - 350 cps

I_{dc}	F_c	$V_{L \text{ to } L}$	I_a	P_{dc}	P_{ac}	PERCENT INITIAL V
Amps	Amp-Turn	Volts	Amps	Watts	Watts	%
0	0	90.0	.372	0	57.9	100
1	198	85.8	.360	1.1	54.2	95.4
2	396	81.5	.340	4.4	48.4	90.6
3	594	77.0	.320	10.0	42.9	85.6
4	792	72.5	.305	17.8	39.0	80.6
5	990	68.5	.290	27.7	35.2	76.1
6	1188	64.3	.270	39.5	30.5	71.5
7	1386	60.5	.255	54.4	27.2	67.2
8	1584	56.8	.240	71.1	24.1	63.2

DATA

STATOR NO. 2
HIPERNIK

RUN NO. 6

BALANCED RESISTIVE LOAD - 139.5 OHMS/PH
CONSTANT FREQUENCY - 300 cps

I_{dc} Amps	F_c Amp-turns	$V_{L \text{ to } L}$ Volts	I_a Amps	P_{dc} Watts	P_{ac} Watts	PERCENT INITIAL V %
0	0	77.9	.324	0	43.9	100
1	198	74.0	.308	1.1	39.7	95.0
2	396	70.1	.293	4.4	35.9	90.0
3	594	66.7	.277	10.0	32.1	85.6
4	792	62.2	.260	17.8	28.3	79.8
5	990	58.5	.244	27.7	24.9	75.1
6	1188	55.0	.230	39.5	22.2	70.6
7	1386	52.0	.215	54.4	19.4	66.8
8	1584	48.5	.201	71.1	16.9	62.3

DATA

STATOR NO. 2
HIPERNIK

RUN NO. 7

BALANCED RESISTIVE LOAD - 93 OHMS/PH
CONSTANT FREQUENCY - 400 cps

I_{dc}	F_c	$V_{L \text{ to } L}$	I_a	P_{dc}	P_{ac}	PERCENT INITIAL V
Amps	Amp-turns	Volts	Amps	Watts	Watts	%
0	0	100.8	.605	0	102.1	100
1	198	95.1	.572	1.1	91.3	94.4
2	396	91.0	.545	4.4	82.9	90.3
3	594	86.1	.518	10.0	74.9	85.5
4	792	81.2	.489	17.8	66.7	80.5
5	990	76.2	.462	27.7	59.5	75.6
6	1188	71.5	.432	39.5	52.0	70.9
7	1386	67.0	.401	54.4	44.9	66.5
8	1584	62.1	.376	71.1	39.5	61.6

DATA

STATOR NO. 2
HIPERNIK

RUN NO. 8

BALANCED RESISTIVE LOAD - 93 OHMS/PH
CONSTANT FREQUENCY - 350 cps

I _{dc}	F _c	V _L to L	I _a	P _{dc}	P _{ac}	PERCENT INITIAL V
Amps	Amp-turns	Volts	Amps	Watts	Watts	%
0	0	88.8	.518	0	74.9	100
1	198	85.5	.496	1.1	68.6	96.2
2	396	80.2	.472	4.4	62.6	90.2
3	594	75.8	.450	10.0	56.5	85.3
4	792	71.4	.421	17.8	49.5	80.1
5	990	67.4	.397	27.7	43.9	75.8
6	1188	63.3	.373	39.5	38.8	71.3
7	1386	59.1	.350	54.4	34.2	66.5
8	1584	55.2	.330	71.1	30.4	62.1

DATA

STATOR NO. 2
HIPERNIK

RUN NO. 9

BALANCED RESISTIVE LOAD - 93 OHMS/PH
CONSTANT FREQUENCY - 300 cps

I_{dc} Amps	F_c Amp-turns	$V_{L \text{ to } L}$ Volts	I_a Amps	P_{dc} Watts	P_{ac} Watts	PERCENT INITIAL V %
0	0	76.2	.453	0	57.2	100
1	198	72.8	.432	1.1	52.0	95.8
2	396	69.0	.410	4.4	46.9	90.6
3	594	65.0	.388	10.0	42.0	85.4
4	792	61.5	.367	17.9	37.6	80.9
5	990	57.5	.340	27.7	32.2	75.6
6	1188	54.0	.322	39.5	28.9	70.9
7	1386	50.7	.302	54.4	25.4	66.6
8	1584	47.5	.285	71.1	22.6	62.4

DATA

STATOR NO. 2
HIPERNIK

RUN NO. 10

BALANCED RESISTIVE LOAD - 46.5 OHMS/PH
CONSTANT FREQUENCY - 400 cps

I_{dc}	F_c	V_L to L	I_a	P_{dc}	P_{ac}	PERCENT INITIAL V
Amps	Amp-turns	Volts	Amps	Watts	Watts	%
0	0	90.0	1.097	0	167.8	100
1	198	86.0	1.05	1.1	153.9	95.6
2	396	81.5	0.99*	4.4	136.9	90.6
3	594	77.3	0.935	10.0	122.0	85.9
4	792	72.8	0.882	17.8	108.5	81.0
5	990	68.8	0.830	27.7	96.1	76.5
6	1188	64.0	0.772	39.5	83.3	71.2
7	1386	60.0	0.725	54.4	73.4	66.7
8	1584	56.0	0.677	71.1	63.9	62.2

* CHANGE IN AMMETERS WAS REQUIRED

DATA

STATOR NO. 2
HIPERNIK

RUN NO. 11

BALANCED RESISTIVE LOAD - 46.5 OHMS/PH
CONSTANT FREQUENCY - 350 cps

I_{dc}	F_c	V_L to L	I_a	P_{dc}	P_{ac}	PERCENT INITIAL V
Amps	Amp-turns	Volts	Amps	Watts	Watts	%
0	0	79.1	.957	0	128.2	100
1	198	75.7	.920	1.1	118.1	95.6
2	396	72.0	.870	4.4	105.7	90.9
3	594	68.2	.824	10.0	94.6	86.1
4	792	64.4	.776	17.8	84.1	81.6
5	990	61.0	.734	27.7	75.1	77.1
6	1188	57.5	.690	39.5	66.4	72.6
7	1386	53.2	.640	54.4	57.1	67.2
8	1584	50.0	.601	71.1	50.4	63.1

DATA

STATOR NO. 2
HIPERNIK

RUN NO. 12

BALANCED RESISTIVE LOAD - 46.5 OHMS/PH
CONSTANT FREQUENCY - 300 cps

I_{dc} Amps	F_c Amp-turns	$V_{L \text{ to } L}$ Volts	I_a Amps	P_{dc} Watts	P_{ac} Watts	PERCENT INITIAL V %
0	0	69.1	.835	0	97.3	100
1	198	66.0	.79	1.1	87.0	95.5
2	396	62.8	.76	4.4	80.6	91.0
3	594	59.0	.713	10.0	70.9	85.4
4	792	56.0	.673	17.8	63.1	81.0
5	990	52.7	.632	27.7	55.7	76.2
6	1188	49.6	.598	39.5	49.9	71.8
7	1386	46.5	.558	54.4	43.4	67.3
8	1584	43.5	.521	71.1	37.9	62.9

DATA

STATOR NO. 2
HIPERNIK

RUN NO. 13

BALANCED INDUCTIVE LOAD- 100 OHMS & 100 MILLIHENRIES/PH
CONSTANT FREQUENCY - 400 cps

I_{dc} Amps	F_c Amp-turns	$V_{L \text{ to } L}$ Volts	I_a Amps	P_{dc} Watts	P_{ac} Watts	PERCENT INITIAL V %
0	0	102.5	.215	0	13.9	100
1	198	97.5	.204	1.1	12.5	95.1
2	396	92.5	.194	4.4	11.3	90.2
3	594	87.5	.183	10.0	10.0	85.3
4	792	82.5	.172	17.8	8.87	80.5
5	990	78.0	.163	27.7	8.02	76.1
6	1188	73.0	.153	39.5	7.03	71.2
7	1386	69.0	.144	54.4	62.1	67.3
8	1584	65.0	.135	71.1	5.47	63.4

DATA

STATOR NO. 2
HIPERNIK

RUN NO. 14

BALANCED INDUCTIVE LOAD - 100 OHMS & 100 MILLIHENRIES/PH
CONSTANT FREQUENCY - 350 cps

I_{dc} Amps	F_c Amp-turns	V_L to L Volts	I_a Amps	P_{dc} Watts	P_{ac} Watts	PERCENT INITIAL V %
0	0	89.0	.206	0	12.7	100
1	198	84.8	.196	1.1	11.5	95.3
2	396	80.5	.186	4.4	10.4	90.5
3	594	76.0	.176	10.0	9.29	85.4
4	792	71.8	.165	17.8	8.17	80.75
5	990	67.0	.156	27.7	7.30	75.3
6	1188	64.0	.147	39.5	6.49	71.9
7	1386	60.0	.136	54.4	5.55	67.4
8	1584	56.5	.130	71.1	5.08	63.5

DATA

STATOR NO. 2
HIPERNIK

RUN NO. 15

BALANCED INDUCTIVE LOAD - 100 OHMS & 100 MILLIHENRIES/PH
CONSTANT FREQUENCY - 300 cps

I_{dc}	F_c	V_L to L	I_a	P_{dc}	P_{ac}	PERCENT INITIAL V
Amps	Amp-turns	Volts	Amps	Watts	Watts	%
0	0	76.5	.201	0	12.1	100
1	198	72.7	.190	1.1	10.8	95.1
2	396	69.0	.181	4.4	9.83	90.3
3	594	65.1	.171	10.0	8.79	85.1
4	792	61.8	.161	17.8	7.77	80.9
5	990	58.0	.151	27.7	6.84	75.8
6	1188	54.8	.141	39.5	5.96	71.8
7	1386	51.5	.134	54.4	5.39	67.3
8	1584	48.8	.125	71.1	4.69	63.8

DATA

STATOR NO. 2
HIPERNIK

RUN NO. 16

EFFECTS OF INCREASED LEAKAGE:

TWO 0.010" TETLON SPACERS PLUS TWO 0.014"
HIPERNIK LAMINATIONS CLAMPED TO EACH END OF ROTOR

NO LOAD
CONSTANT FREQUENCY - 400 cps

I_{dc} Amps	F_c Amp-turns	$V_{L \text{ to } L}$ Volts	I_a Amps	P_{dc} Watts	P_{ac} Watts	PERCENT INITIAL V %
0	0	89.5	0	0	0	100
1	198	82.8	0	1.1	0	92.5
2	396	76.0	0	4.4	0	84.8
3	594	69.7	0	10.0	0	77.8
4	792	63.6	0	17.8	0	71.0
5	990	58.0	0	27.7	0	64.75
6	1188	52.7	0	39.5	0	58.8
7	1386	48.0	0	54.4	0	53.6
8	1584	43.5	0	71.1	0	48.6

DATA

STATOR NO. 2
HIPERNIK

RUN NO. 17

EFFECTS OF INCREASED LEAKAGE:

TWO 0.010" TEFLON SPACERS PLUS TWO 0.014" HIPERNIK
LAMINATIONS CLAMPED TO EACH END OF THE ROTOR

BALANCED RESISTIVE LOAD - 100 OHMS/PH
CONSTANT FREQUENCY - 400 cps

I_{dc}	F_c	$V_{L \text{ to } L}$	I_a	P_{dc}	P_{ac}	PERCENT INITIAL V
Amps	Amp-turns	Volts	Amps	Watts	Watts	%
0	0	80.5	.427	0	54.8	100
1	198	75.0	.400	1.1	48.0	93.2
2	396	69.1	.367	4.4	40.4	85.8
3	594	63.1	.332	10.0	33.1	78.4
4	792	57.8	.306	17.8	28.1	71.9
5	990	52.6	.280	27.7	23.6	65.3
6	1188	47.5	.254	39.5	19.4	59.0
7	1386	42.9	.228	54.4	15.6	53.3
8	1584	39.0	.206	71.1	12.7	48.4

DATA

STATOR NO. 2
HIPERNIK

RUN NO. 18

EFFECTS OF INCREASED LEAKAGE:

TWO 0.010" TEFLON SPACERS PLUS TWO 0.014" HIPERNIK
LAMINATIONS CLAMPED TO EACH END OF ROTOR

BALANCED RESISTIVE LOAD - 100 OHMS/PH
CONSTANT FREQUENCY - 350 cps

I_{dc} Amps	F_c Amp-turns	$V_{L \text{ to } L}$ Volts	I_a Amps	P_{dc} Watts	P_{ac} Watts	PERCENT INITIAL V %
0	0	70.0	.375	0	42.2	100
1	198	65.1	.351	1.1	37.0	93.1
2	396	59.8	.322	4.4	31.1	85.5
3	594	55.1	.296	10.0	26.3	78.8
4	792	50.2	.270	17.8	21.9	71.8
5	990	45.5	.246	27.7	18.2	65.0
6	1188	41.5	.223	39.5	14.9	59.4
7	1386	37.5	.200	54.4	12.0	53.6
8	1584	34.0	.180	71.1	9.73	48.6

DATA

STATOR NO. 2
HIPERNIK

RUN NO. 19

EFFECTS OF INCREASED LEAKAGE:

TWO 0.010" TEFLON SPACERS PLUS ONE 0.014" HIPERNIK
LAMINATION CLAMPED TO EACH END OF ROTOR

NO LOAD
CONSTANT FREQUENCY - 400 cps

I_{dc} Amps	F_c Amp-turns	$V_{L \text{ to } L}$ Volts	I_a Amps	P_{dc} Watts	P_{ac} Watts	PERCENT INITIAL V %
0	0	97	0	0	0	100
1	198	91.3	0	1.1	0	94.2
2	396	85.5	0	4.4	0	88.2
3	594	79.6	0	10.0	0	82.1
4	792	73.9	0	17.8	0	76.3
5	990	69.0	0	27.7	0	71.2
6	1188	63.8	0	39.5	0	65.8
7	1386	59.0	0	54.4	0	60.9
8	1584	54.9	0	71.1	0	56.6

DATA

STATOR NO. 2
HIPERNIK

RUN NO. 20

EFFECTS OF INCREASED LEAKAGE:

TWO 0.010" TEFLON SPACERS PLUS ONE 0.014" HIPERNIK
LAMINATION CLAMPED TO EACH END OF ROTOR

BALANCED RESISTIVE LOAD - 100 OHMS/PH
CONSTANT FREQUENCY - 400 cps

I_{dc}	F_c	V_L to L	I_a	P_{dc}	P_{ac}	PERCENT INITIAL V
Amps	Amp-turns	Volts	Amps	Watts	Watts	%
0	0	88.5	.468	0	65.8	100
1	198	83.2	.442	1.1	58.7	94.1
2	396	78.1	.415	4.4	51.8	88.3
3	594	72.8	.388	10.0	45.2	82.3
4	792	68.0	.362	17.8	39.4	76.9
5	990	63.1	.336	27.7	33.9	71.3
6	1188	58.4	.310	39.5	28.8	66.0
7	1386	53.8	.288	54.4	24.9	60.8
8	1584	50.0	.266	71.1	21.2	56.5



BIBLIOGRAPHY

- 1 H. C. Roters; "Electromagnetic Devices", John Wiley & Sons, 1951 pp. 84-115.
- 2 C. T. Thomas and J. R. Ireland; "The Design and Performance of Permanent Magnet Rotors" - Elec. Mfg. Aug. 1947, p. 110.
- 3 K. L. Scott; "Magnet Steels and Permanent Magnets", AIEE Trans., Vol. 51, 1932, p. 410.
- 4 Indiana Steel Co.; "Indiana Steel Permanent Magnet Manual No. 4".
- 5 EE Staff, M.I.T.; "Magnetic Circuits and Transformers", Technology Press, M.I.T., John Wiley & Sons, Inc. pp. 90-93.
- 6 E. H. Harris; EE Thesis, 1950, M.I.T., "Magnetic Amplifiers with AC Control".
- 7 O. T. Estes and W. J. Hussong, Nav. Arch. Thesis, 1951, M.I.T.; "Study of Capacitor-Excited Induction Generators; Parallel Operation and Transient Loading".
- 8 R. W. Goode, H. A. Hoffmann, and W. F. Searle, Jr.; Nav. Arch. Thesis, 1952, M.I.T.; "The Experimental Determination of the Performance of a Capacitor Excited Induction Generator with an Inductive Reactance in Series with the Load".
- 9 J. H. Kulhman; "Design of Electrical Apparatus". John Wiley & Sons, 1930, pp. 174-214.

BIBLIOGRAPHY

1. H. C. Roberts; "Electromagnetic Devices", John Wiley & Sons, 1931, pp. 84-115.
2. C. T. Thomas and J. E. Ireland; "The Design and Performance of Permanent Magnet Motors", AIEE Trans., Vol. 61, 1947, p. 110.
3. K. L. Scott; "Magnet Steels and Permanent Magnets", AIEE Trans., Vol. 51, 1935, p. 410.
4. Indiana Steel Co.; "Indiana Steel Permanent Magnets", Manual No. 4.
5. E. E. Gault, M.I.T.; "Magnetic Circuits and Transformers", Technology Press, M.I.T., John Wiley & Sons, Inc., pp. 90-95.
6. H. E. Harris; EE Thesis, 1930, M.I.T., "Magnetic Amplifiers with AC Control".
7. O. T. Kates and W. L. Haggard, Nav. Arch. Thesis, 1931, M.I.T.; "Study of Capacitor-Excited Induction Generators; Parallel Operation and Transient Loading".
8. W. W. Goode, H. A. Hoffmann, and W. L. Kates, Jr.; Nav. Arch. Thesis, 1932, M.I.T.; "The Experimental Determination of the Performance of a Capacitor-Excited Induction Generator with an Inductive Resistance in Series with the Load".
9. J. E. Knibben; "Design of Electrical Apparatus", John Wiley & Sons, 1930, pp. 174-210.

JUL 2
NOV 10
94 833 97

BINDERY
348
23190

Thesis

20531

A33 Aitkenhead

Permanent magnet alternator
control by means of magnetic
saturation.

★ NOV 12 '53
NOV 10
94 833 97

BINDERY
348
23190

31

a-

Thesis

A33

Aitkenhead

20531

Permanent magnet alternator con-
trol by means of magnetic satura-
tion.

Library
U. S. Naval Postgraduate School
Monterey, California



thesA33

Permanent magnet alternator control by m



3 2768 001 90949 2

DUDLEY KNOX LIBRARY